TTP18-011, PSI-PR-18-04

Lepton flavour violation in the MSSM: exact diagonalization vs mass expansion

Andreas Crivellin[1], Zofia Fabisiewicz[3], Weronika Materkowska[3], Ulrich Nierste[2], Stefan Pokorski[3], and Janusz Rosiek[3]

[1]*Paul Scherrer Institut, CH–5232 Villigen PSI, Switzerland*
[2]*Institut für Theoretische Teilchenphysik, Karlsruhe Institute of Technology, 76128 Karlsruhe, Germany*
[3]*Faculty of Physics, University of Warsaw, Pasteura 5, 02-093 Warsaw, Poland*

February 20, 2018

Abstract

The forthcoming precision data on lepton flavour violating (LFV) decays require precise and efficient calculations in New Physics models. In this article lepton flavour violating processes within the Minimal Supersymmetric Standard Model (MSSM) are calculated using the method based on the Flavour Expansion Theorem, a recently developed technique performing a purely algebraic mass-insertion expansion of the amplitudes. The expansion in both flavour-violating and flavour-conserving off-diagonal terms of sfermion and supersymmetric fermion mass matrices is considered. In this way the relevant processes are expressed directly in terms of the parameters of the MSSM Lagrangian. We also study the decoupling properties of the amplitudes. The results are compared to the corresponding calculations in the mass eigenbasis (i.e. using the exact diagonalization of the mass matrices). Using these methods, we consider the following processes: $\ell \to \ell'\gamma$, $\ell \to 3\ell'$, $\ell \to 2\ell'\ell''$, $h \to \ell\ell'$ as well as $\mu \to e$ conversion in nuclei. In the numerical analysis we update the bounds on the flavour changing parameters of the MSSM and examine the sensitivity to the forthcoming experimental results. We find that flavour violating muon decays provide the most stringent bounds on supersymmetric effects and will continue to do so in the future. Radiative $\ell \to \ell'\gamma$ decays and leptonic three-body decays $\ell \to 3\ell'$ show an interesting complementarity in eliminating "blind spots" in the parameter space. In our analysis we also include the effects of non-holomorphic A-terms which are important for the study of LFV Higgs decays.

Contents

1 Introduction

So far, the LHC did not observe any particles beyond those of the Standard Model (SM). Complementary to direct high energy searches at the LHC, there is a continuous effort in indirect searches for new physics (NP). In this respect, a promising approach is the search for processes which are absent – or extremely suppressed – in the SM such as lepton flavour violation (LFV) which is forbidden in the SM in the limit of vanishing neutrino masses. The experimental sensitivity for rare LFV processes such as $\ell \to \ell'\gamma$, $\mu \to e$ conversion in nuclei and $\ell \to \ell'\mu^+\mu^-$ or $\ell \to \ell' e^+ e^-$ will improve significantly in the near future, probing scales well beyond those accessible at foreseeable colliders. Furthermore, the discovery of the 125 GeV Higgs boson h [1,2] has triggered an enormous experimental effort in measuring its properties, including studies of its LFV decays. The most recent experimental limits on the LFV processes are given in Table 2 in Sec. 5.

Many studies of LFV processes within the MSSM (and possible extensions of it) exist (see e.g. Refs. [3–27] and Ref. [28] for a recent review). In this article we revisit this subject in the light of the new calculational methods which have been recently developed [29, 30]. These methods allow for a systematic expansion of the amplitudes of the LFV processes in terms of mass insertions (MI), i.e. in terms of off-diagonal elements of the mass matrices. We show that a transparent qualitative behaviour of the amplitudes of the LFV processes is obtained by expanding them not only in the flavour-violating off-diagonal terms in the sfermion mass matrices but also in the flavour conserving but chirality violating entries related to the tri-linear A-terms as well as in the off-diagonal terms of the gaugino and higgsino mass matrices. This procedure is useful because in the MI approximation we work directly with the parameters of the Lagrangian and can therefore easily put experimental bounds on them. We compare the results of the calculations performed in the mass eigenbasis (i.e. using a numerical diagonalization of the slepton mass matrices) with those obtained at leading non-vanishing order of the MI approximation, in different regions of the supersymmetric parameter space and considering various decoupling limits. Of course, the MI approximation [31, 32] has already been explored for many years as a very useful tool in flavour physics. However, a detailed comparison between the full calculation and the MI approximation is still lacking, partly because a fully systematic discussion of the MI approximation [29] to any order and the technical tools facilitating it [30] have not been available until recently.

Concerning the phenomenology, we summarise and update the bounds on the flavour violating SUSY parameters, show their complementarity and examine the impact of the anticipated increase in the experimental sensitivity. We investigate in detail the decay $h \to \mu\tau$ showing the results in various decoupling limits and analyse the role of the so-called non-holomorphic A-terms [33, 34], which are usually neglected in literature. As another novel feature, we avoid simplifying assumptions on the sparticle spectrum and assume neither degeneracies nor hierarchies among the supersymmetric particles.

This article is structured as follows: in Sec. 2 we establish our conventions and present the results for the 2-point, 3-point, and 4-point functions related to flavour violating charged lepton interactions in the mass eigenbasis, i.e. expressed in terms of rotation matrices and physical masses. Sec. 3 contains the formula for the decay rates of the processes under investigation. In Sec. 4 we discuss the MI expansion and summarise important properties of the decoupling limits $M_{\rm SUSY} \to \infty$ and $M_A \to \infty$. In Sec. 5 we

present the numerical bounds on LFV parameters obtained from current experimental measurements and discuss the dependence of the results on the SUSY spectrum. We also discuss the correlations between the radiative decays and the 3-body decays of charged lepton as well as the non-decoupling effects in LFV neutral Higgs decays. Finally we conclude in Sec. 6. All required Feynman rules used in our calculations are collected in appendix A. The definitions of loop integrals can be found in appendix B. In appendix C we explain the notation for the "divided differences" of the loop functions used in the expanded form of the amplitudes. The expression for the 4-lepton box diagrams and for the MI-expanded expression of the amplitudes are given in the appendices D and E, respectively.

2 Effective LFV interactions

In this Section we collect the analytical formula in the mass eigenbasis for flavour violating interactions generated at the one-loop level[1]. We use the notation and conventions for the MSSM as given in Ref. [33, 34][2].

In our analysis, we include the so-called non-holomorphic trilinear soft SUSY breaking terms:

$$L_{nh} = \sum_{I,J=1}^{3} \sum_{i=1}^{2} \left(A_l'^{IJ} H_i^{2\star} L_i^I R^J + A_d'^{IJ} H_i^{2\star} Q_i^I D^J + A_u'^{IJ} H_i^{1\star} Q_i^I U^J + \text{H.c.} \right) , \tag{2.1}$$

which couple up(down)-sfermions to the down(up)-type Higgs doublets. Here, as throughout the rest of the paper, capital letters $I, J = 1, 2, 3$ denote flavour indices and the small letters $i = 1, 2$ are $SU(2)_L$ indices.

2.1 $\gamma - \ell - \ell'$ interactions

We define the effective Lagrangian for flavour violating couplings of leptons to on-shell photons as

$$L_{\ell\gamma} = -e \sum_{I,J} \left(F_\gamma^{JI} \bar{\ell}^J \sigma_{\mu\nu} P_L \ell^I + F_\gamma^{IJ*} \bar{\ell}^J \sigma_{\mu\nu} P_R \ell^I \right) F^{\mu\nu} , \tag{2.2}$$

The SM contribution to F_γ^{JI} is suppressed by powers of m_ν^2/M_W^2 and thus completely negligible. In the mass eigenbasis the supersymmetric contributions to F_γ^{JI} come from the diagrams displayed in Fig. 1. Let us decompose F_γ in the following way

$$F_\gamma^{JI} = F_{\gamma A}^{JI} - m_J F_{\gamma LB}^{JI} - m_I F_{\gamma RB}^{JI} , \tag{2.3}$$

[1]Note that these expressions are not valid in the flavour conserving case where additional terms should be included and renormalization is required.

[2]The conventions of [33, 34] are very similar to the later introduced and now widely accepted SLHA2 [35] notation, up to the minor differences summarised in the Appendix A.

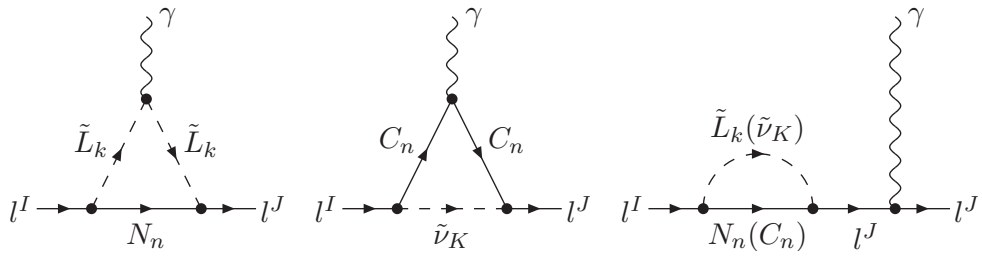

Figure 1: One-loop supersymmetric contributions to the LF violating effective lepton-photon interaction (mirror-reflected self-energy diagram not shown).

with

$$\begin{aligned}
(4\pi)^2 F_{\gamma A}^{JI} &= \sum_{K=1}^{3}\sum_{n=1}^{2} V_{\ell\tilde{\nu}C,R}^{JKn*} V_{\ell\tilde{\nu}C,L}^{IKn}\; m_{C_n} C_{11}(m_{C_n}, m_{\tilde{\nu}_K}) \\
&- \frac{1}{2}\sum_{k=1}^{6}\sum_{n=1}^{4} V_{\ell\tilde{L}N,R}^{Jkn*} V_{\ell\tilde{L}N,L}^{Ikn}\; m_{N_n} C_{12}(m_{\tilde{L}_k}, m_{N_n})\,, \\
(4\pi)^2 F_{\gamma LB}^{JI} &= -\sum_{K=1}^{3}\sum_{n=1}^{2} V_{\ell\tilde{\nu}C,L}^{JKn*} V_{\ell\tilde{\nu}C,L}^{IKn}\; C_{23}(m_{C_n}, m_{\tilde{\nu}_K}) \\
&+ \frac{1}{2}\sum_{k=1}^{6}\sum_{n=1}^{4} V_{\ell\tilde{L}N,L}^{Jkn*} V_{\ell\tilde{L}N,L}^{Ikn} C_{23}(m_{\tilde{L}_k}, m_{N_n})\,. \qquad (2.4)
\end{aligned}$$

Here, V abbreviates the tree-level lepton-slepton-neutrino and lepton-sneutrino-chargino vertices, i.e. the subscripts of V stand for the interacting particles and the chirality of the lepton involved. The super-scripts refer to the lepton or slepton flavour as well as to the chargino and neutralino involved. The specific form of the chargino and neutralino vertices $V_{L(R)}$ is defined in Appendix A and the 3-point loop functions C_{ij} are given in Appendix B. $F_{\gamma A}\,(F_{\gamma LB})$ denotes the parts of the amplitude which is (not) proportional to the masses of fermions exchanged in the loop. $F_{\gamma RB}$ can be obtained from $F_{\gamma LB}$ by exchanging $L \leftrightarrow R$ on the RHS of Eq. (2.4).

Gauge invariance requires that LFV (axial) vectorial photon couplings vanish for on-shell external particles. However, off-shell photon contributions are necessary to calculate three body decays of charged leptons. The vectorial part of the amplitude for the $\gamma\ell\ell'$ vertex can be written as

$$iA_\gamma^{JI\,\mu} = ieq^2\bar{u}_J(p_J)\left(\Gamma_{\gamma L}^{JI} P_L + \Gamma_{\gamma R}^{JI} P_R\right)\gamma^\mu u_I(p_I)\,, \qquad (2.5)$$

where $q = p_I - p_J$ and $\Gamma_{\gamma L}^{JI}$ is at the leading order in $p^2/M_{\rm SUSY}^2$ momentum independent and reads

$$\begin{aligned}
\Gamma_{\gamma L}^{JI} &= \sum_{K=1}^{3}\sum_{n=1}^{2} V_{\ell\tilde{\nu}C,L}^{JKn*} V_{\ell\tilde{\nu}C,L}^{IKn}\; C_{01}(m_{C_n}, m_{\tilde{\nu}_K}) \\
&- \sum_{k=1}^{6}\sum_{n=1}^{4} V_{\ell\tilde{L}N,L}^{Jkn*} V_{\ell\tilde{L}N,L}^{Ikn}\; C_{02}(m_{N_n}, m_{\tilde{L}_k})\,. \qquad (2.6)
\end{aligned}$$

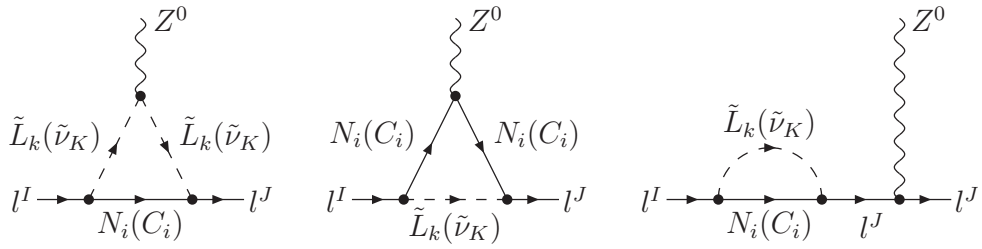

Figure 2: One-loop supersymmetric contributions to the LFV effective lepton-Z^0 interaction (the mirror-reflected self-energy diagram not shown).

$\Gamma^{JI}_{\gamma R}$ can be obtained by replacing $L \leftrightarrow R$. Again, the loop functions C_{01}, C_{02} are defined in Appendix B.

Finally, one should note that for heavy MSSM spectrum the 2-loop Barr-Zee diagrams [36] involving the non-decoupling LFV Higgs interactions (see Sec. 5.4) are important and have to be included [37–42].

2.2 $Z - \ell - \ell'$ interactions

In order to calculate the three body decays of charged leptons as to be considered in Sec. 3.3 it is sufficient to calculate the effective $Z - \ell - \ell'$ interactions in the limit of vanishing external momenta. The Wilson coefficients of the effective Lagrangian for the Z coupling to charged leptons are generated at one-loop level by the diagrams shown in Fig. 2 and can be written as

$$L^{JI}_{\ell Z} = \left(F^{JI}_{ZL}\bar{\ell}^J\gamma_\mu P_L\ell^I + F^{JI}_{ZR}\bar{\ell}^J\gamma_\mu P_R\ell^I\right) Z^\mu \,, \tag{2.7}$$

with

$$\begin{aligned} F^{JI}_{ZL} &= \Gamma^{JI}_{ZL} - \frac{e(1-2s^2_W)}{2s_W c_W}\,\Sigma^{JI}_{VL}(0)\,, \\ F^{JI}_{ZR} &= \Gamma^{JI}_{ZR} + \frac{es_W}{c_W}\,\Sigma^{JI}_{VR}(0)\,. \end{aligned} \tag{2.8}$$

Here, $\Gamma_{ZL(R)}$ denote the contribution originating from the one-particle irreducible (1PI) vertex diagram and $\Sigma_{VL(R)}$ is the left-(right-)handed part of the lepton self-energy defined as

$$\Sigma^{JI}(p^2) = \Sigma^{JI}_{VL}(p^2)\,\not{p}\,P_L + \Sigma^{JI}_{VR}(p^2)\,\not{p}\,P_R + \Sigma^{JI}_{mL}(p^2)\,P_L + \Sigma^{JI}_{mR}(p^2)\,P_R\,. \tag{2.9}$$

Contrary to the left- and right-handed magnetic photon-lepton couplings, which change chirality, the $Z\bar{\ell}^I\ell^J$ coupling is chirality conserving. Therefore, the Wilson coefficients of the left-handed and right-handed couplings are not related to each other but rather satisfy $F^{IJ}_{ZL(R)} = F^{JI*}_{ZL(R)}$. In the mass eigenbasis the vectorial part of the lepton self-energy and

the 1PI triangle diagrams are given by (see Appendix A for definitions of vertices V)

$$\begin{aligned}(4\pi)^2\Sigma_{VL}^{JI}(p^2) &= \sum_{i=1}^{2}\sum_{K=1}^{3} V_{\ell\tilde{\nu}C,L}^{IKi} V_{\ell\tilde{\nu}C,L}^{JKi*} B_1(p, m_{\tilde{\nu}_K}, m_{C_i}) \\ &+ \sum_{i=1}^{4}\sum_{j=1}^{6} V_{\ell\tilde{L}N,L}^{Iji} V_{\ell\tilde{L}N,L}^{Jji*} B_1(p, m_{L_j}, m_{N_i})\,, \end{aligned} \tag{2.10}$$

$$\begin{aligned}(4\pi)^2\Gamma_{ZL}^{JI} &= \frac{1}{2}\sum_{i,j=1}^{2}\sum_{K=1}^{3} V_{\ell\tilde{\nu}C,L}^{IKi} V_{\ell\tilde{\nu}C,L}^{JKj*} \left(V_{CCZ,L}^{ij} C_2(m_{\tilde{\nu}_K}, m_{C_i}, m_{C_j})\right. \\ &- \left. 2V_{CCZ,R}^{ij} m_{C_i} m_{C_j} C_0(m_{\tilde{\nu}_K}, m_{C_i}, m_{C_j})\right) \\ &+ \frac{e}{4 s_W c_W}\sum_{i=1}^{2}\sum_{K=1}^{3} V_{\ell\tilde{\nu}C,L}^{IKi} V_{\ell\tilde{\nu}C,L}^{JKi*} C_2(m_{\tilde{\nu}_K}, m_{\tilde{\nu}_K}, m_{C_i}) \\ &+ \frac{1}{2}\sum_{j=1}^{6}\sum_{i,k=1}^{4} V_{\ell\tilde{L}N,L}^{Iji} V_{\ell\tilde{L}N,L}^{Jjk*} \left(V_{NNZ,L}^{ik} C_2(m_{L_j}, m_{N_i}, m_{N_k})\right. \\ &- \left. 2V_{NNZ,R}^{ik} m_{N_i} m_{N_k} C_0(m_{L_j}, m_{N_i}, m_{N_k})\right) \\ &- \frac{1}{2}\sum_{j,k=1}^{6}\sum_{i=1}^{4} V_{\ell\tilde{L}N,L}^{Iji} V_{\ell\tilde{L}N,L}^{Jki*} V_{LLZ}^{jk} C_2(m_{L_j}, m_{L_k}, m_{N_i})\,, \end{aligned} \tag{2.11}$$

at vanishing external momenta with obvious replacements $L \leftrightarrow R$ for Σ_{VR}^{JI}, Γ_{ZR}^{JI}.

2.3 LFV Higgs interactions

To compactify the notation, we denote the CP-even Higgs boson decays by $H_0^K \to \bar{\ell}^I \ell^J$, where, following again the notation of [33, 34], $H \equiv H_0^1, h \equiv H_0^2$. As usual, we denote CP-odd neutral Higgs boson by A_0.

In order to study $h \to \ell\ell'$ decays precisely, we keep the terms depending on the external Higgs mass. Therefore, we assume the following effective action governing the LFV Higgs-lepton interaction:

$$\begin{aligned}A_{H\text{eff}}^{\ell} &= \bar{\ell}^J(k_J)(F_{h\ell}^{JIK}(k_J,k_I)P_L + F_{h\ell}^{IJK*}(k_J,k_I)P_R)\ell^I(k_I)H_0^K(k_I-k_J) \\ &+ \bar{\ell}^J(k_J)(F_{A\ell}^{JI}(k_J,k_I)P_L + F_{A\ell}^{IJ*}(k_J,k_I)P_R)\ell^I(k_I)A_0(k_I-k_J)\,. \end{aligned} \tag{2.12}$$

In addition, to calculate the $\mu \to e$ conversion rate one needs to include the effective Higgs-quark couplings. For this purpose, one can set all external momenta to zero and consider the effective Lagrangian

$$L_{H\text{eff}}^{q} = \bar{u}^J(F_{hu}^{JIK}P_L + F_{hu}^{IJK*}P_R)u^I H_0^K + \bar{d}^J(F_{hd}^{JIK}P_L + F_{hd}^{IJK*}P_R)d^I H_0^K\,. \tag{2.13}$$

However, in this article we consider only the lepton sector and therefore do not give the explicit forms of Higgs quark couplings. The relevant 1-loop expressions in the same notation as used in the current paper are given in Ref. [43] and the formulae that take into

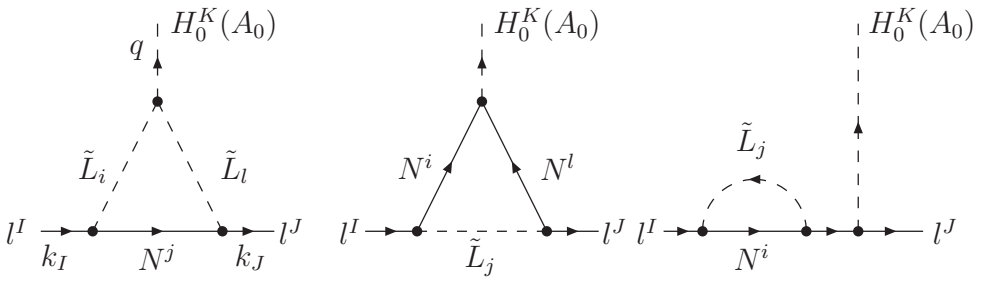

Figure 3: Slepton-neutralino diagrams contributing to the $H_0^K \to \ell^I \bar{\ell}^J$ and $A_0 \to \ell^I \bar{\ell}^J$ decays in the MSSM (the mirror-reflected self-energy diagram is omitted).

account also non-decoupling chirally enhanced corrections and 2-loop QCD corrections in the general MSSM can be found in Refs. [44–46][3].

At the 1-loop level there are eight diagrams contributing to the effective lepton Yukawa couplings. The ones with slepton and neutralino exchange are displayed in Fig. 3, while diagrams with the chargino exchange can be obtained by the obvious replacements $N \to C, L \to \tilde{\nu}$.

The expressions for F_h are obtained from 1PI triangle diagrams and the scalar part of lepton self-energies (see Eq. (2.9)) while the chirality conserving parts of the self-energies are absorbed by a field rotation required to go to the physical basis with a diagonal lepton mass matrix. Therefore,

$$\begin{aligned} F_h^{JIK}(k_J, k_I) &= \Gamma_h^{JIK}(k_J, k_I) - \frac{Z_R^{1K}}{v_1}\,\Sigma_{mL}^{JI}(0)\,, \\ F_A^{JI}(k_J, k_I) &= \Gamma_A^{JI}(k_J, k_I) - \frac{i\sin\beta}{v_1}\,\Sigma_{mL}^{JI}(0)\,, \end{aligned} \tag{2.14}$$

where the Z_R denotes the CP-even Higgs mixing matrix (see Appendix A) and the scalar self-energy contributions are evaluated at zero momentum transfer and given by:

$$\begin{aligned} (4\pi)^2\Sigma_{mL}^{JI}(0) &= \sum_{i=1}^{2}\sum_{L=1}^{3} m_{C_i} V_{\ell\tilde{\nu}C,L}^{ILi} V_{\ell\tilde{\nu}C,R}^{JLi\,*}\; B_0\,(0, m_{\tilde{\nu}_L}, m_{C_i}) \\ &+ \sum_{i=1}^{4}\sum_{j=1}^{6} m_{N_i} V_{\ell\tilde{L}N,L}^{Iji} V_{\ell\tilde{L}N,R}^{Jji\,*}\; B_0\,(0, m_{L_j}, m_{N_i}) \end{aligned} \tag{2.15}$$

The neutralino-slepton contributions to the 1PI vertex diagrams can be written as (the

[3]Earlier accounts on chiral resummation can be found in Refs. [47–55]

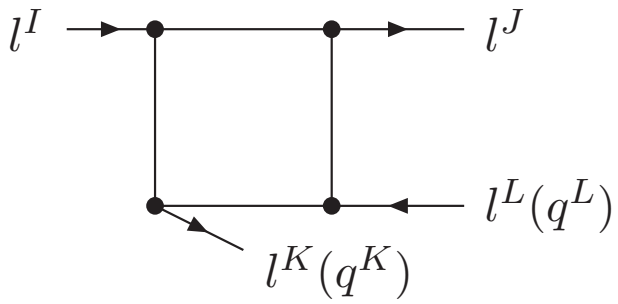

Figure 4: Box diagrams with external charged leptons or quarks

symbols in square brackets denote common arguments of the 3-point functions)[4]

$$
\begin{aligned}
(4\pi)^2\Gamma_h^{JIK}(k_J,k_I) &= -\sum_{n=1}^{4}\sum_{l,m=1}^{6} V^{Jmn*}_{\ell\tilde{L}N,L}V^{Iln}_{\ell\tilde{L}N,L}V^{Klm}_{H\tilde{L}\tilde{L}}m_{N_n}C_0[k_J,k_I-k_J,m_{N_n},m_{\tilde{L}_m},m_{\tilde{L}_l}] \\
&-\sum_{l,n=1}^{4}\sum_{m=1}^{6} V^{Jnm*}_{\ell\tilde{L}N,R}V^{Inl}_{\ell\tilde{L}N,L}(V^{lKm}_{NHN,R}C_2+V^{lKm}_{NHN,L}m_{N_l}m_{N_m}C_0)[k_J,k_I-k_J,m_{\tilde{L}_n},m_{N_m},m_{N_l}]\,, \\
(4\pi)^2\Gamma_A^{JI}(k_J,k_I) &= -\sum_{n=1}^{4}\sum_{l,m=1}^{6} V^{Jmn*}_{\ell\tilde{L}N,L}V^{Iln}_{\ell\tilde{L}N,L}V^{1lm}_{A\tilde{L}\tilde{L}}m_{N_n}C_0[k_J,k_I-k_J,m_{N_n},m_{\tilde{L}_m},m_{\tilde{L}_l}] \\
&-\sum_{l,n=1}^{4}\sum_{m=1}^{6} V^{Jnm*}_{\ell\tilde{L}N,R}V^{Inl}_{\ell\tilde{L}N,L}(V^{l1m}_{NAN,R}C_2+V^{l1m}_{NAN,L}m_{N_l}m_{N_m}C_0)[k_J,k_I-k_J,m_{\tilde{L}_n},m_{N_m},m_{N_l}]\,,
\end{aligned}
\tag{2.16}
$$

while the chargino-sneutrino triangle diagram is obtained by replacing $\tilde{L}\to\tilde{\nu}, N\to C$ and adjusting the summation limits appropriately in vertex factors $V^{\cdots}_{\cdots}$ (see Appendix A).

2.4 Box contributions

4-fermion interactions are also generated by box diagrams. The corresponding conventions for incoming and outgoing particles are shown in Fig. 4. We calculate all box diagrams in the approximation of vanishing external momenta. The effective Lagrangian for the 4-lepton interactions involves the quadrilinear operators

$$
\begin{aligned}
O^{JIKL}_{VXY} &= (\bar{\ell}^J\gamma^\mu P_X\ell^I)\times(\bar{\ell}^K\gamma_\mu P_Y\ell^L)\,, \\
O^{JIKL}_{SXY} &= (\bar{\ell}^J P_X\ell^I)\times(\bar{\ell}^K P_Y\ell^L)\,, \\
O^{JIKL}_{TX} &= (\bar{\ell}^J\sigma^{\mu\nu}\ell^I)\times(\bar{\ell}^K\sigma_{\mu\nu}P_X\ell^L)\,,
\end{aligned}
\tag{2.17}
$$

[4]As we shall see later using MI expanded formulae (see Appendix E.3), due to strong cancellations the leading order terms in Eqs. (2.15, 2.16) are suppressed by the ratios of m_ℓ/M_W or A'_l/M_{SUSY}. Additional terms linear in m_ℓ/M_W, not included in Eq. (2.16), appear in 1PI vertex diagrams when external lepton masses are not neglected. We calculated such terms and proved explicitly that after performing the MI expansion they are suppressed by additional powers of v^2/M^2_{SUSY} and therefore, *a posteriori*, negligible. Thus, we do not display such terms in Eq. (2.16).

where X, Y stands for the chirality L or R[5]. The Wilson coefficients of these operators are calculated from the box diagrams in Fig. 4 and are denoted by B_{NXY}^{JIKL} with $N = V$,S, or B_{TX}^{JIKL}.

The operator basis in Eq. (2.17) is redundant. First, we note that

$$\begin{aligned} O_{NXY}^{JIKL} &= O_{NYX}^{KLJI} \quad \text{for } N = V, S, \\ O_{TX}^{JIKL} &= O_{TX}^{KLJI}. \end{aligned} \tag{2.18}$$

Second, there are Fierz relations among different operators:

$$\begin{aligned} O_{VXX}^{JIKL} &= O_{VXX}^{KIJL}, \\ O_{VXY}^{JIKL} &= -\,2\,O_{SXY}^{KIJL} \quad \text{for } X \neq Y, \\ O_{TX}^{JIKL} &= \frac{1}{2} O_{TX}^{KIJL} - 6\,O_{SXX}^{KIJL}, \\ O_{SXX}^{JIKL} &= -\frac{1}{2} O_{SXX}^{KIJL} - \frac{1}{8} O_{TX}^{KIJL}. \end{aligned} \tag{2.19}$$

Furthermore, we have

$$\begin{aligned} O_{VXY}^{JIKL\dagger} &= O_{VXY}^{IJLK}, & O_{SLL}^{JIKL\dagger} &= O_{SRR}^{IJLK}, \\ O_{SLR}^{JIKL\dagger} &= O_{SRL}^{IJLK}, & O_{TL}^{JIKL\dagger} &= O_{TR}^{JILK}. \end{aligned} \tag{2.20}$$

Eqs. (2.18) to (2.20) must be taken into account when deriving the effective Lagrangian.

2.4.1 Leptonic operators with J ≠ K and I ≠ L

The case with both $J \neq K$ and $I \neq L$ covers the decays $\tau^{\mp} \to \mu^{\mp} e^{\mp} \ell^{\pm}$ with $\ell = e$ or μ, but does not appear in $\mu^{\mp}$ decays. We can therefore specify to $I = 3$ for the effective Lagrangian. Furthermore, we can choose either $(J, K) = (1, 2)$ or $(J, K) = (2, 1)$ without the need to sum over both cases: The Fierz identities in Eq. (2.19) permit to bring all operators into the form $(\overline{e} \ldots \tau) \times (\overline{\mu} \ldots \ell)$ (corresponding to the case $(J, K) = (1, 2)$) or into an alternative form with e interchanged with μ. Thus we have

$$L_{4\ell}^{J3KL} = \sum_{L=1,2} \left[\sum_{\substack{N=V,S \\ X,Y=L,R}} B_{NXY}^{J3KL} O_{NXY}^{J3KL} + \sum_{X=L,R} B_{TX}^{J3KL} O_{TX}^{J3KL} \right] + \text{h.c.} \qquad \text{with } J \neq K \text{ and } J, K, L \leq 2, \tag{2.21}$$

as the four-lepton interaction in the Lagrangian. Note that the "+h.c." piece of $L_{4\ell}^{JK}$ describes τ^+ decays.

The Wilson coefficients B_{NXY}^{J3KL} and B_{TX}^{J3KL} in Eq. (2.21) are simply identical to the results of the sum of all contributing box diagrams to the decay amplitude. The latter is given in Eq. (3.7) with the coefficients of the spinor structure in the right column of Tab. 1. The relation to the analytic expressions in Eqs. (D.3) to (D.6) is

$$B_{NXY}^{JIKL} = B_{A\,NXY}^{JIKL} + B_{B\,NXY}^{JIKL} + B_{C\,NXY}^{JIKL} + B_{D\,NXY}^{JIKL}, \qquad \text{for } N = V, S \tag{2.22}$$

and an analogous expression for B_{TX}^{JIKL}.

[5] Recall that $(\bar{\ell}^J \sigma^{\mu\nu} P_L \ell^I) \times (\bar{\ell}^K \sigma_{\mu\nu} P_R \ell^L) = 0$.

2.4.2 Leptonic operators with J = K and I ≠ L

The case $J = K$ occurs for the decays $\mu^\pm \to e^\pm e^\pm e^\mp$ and $\tau^\pm \to \ell^\pm \ell^\pm \ell^{\mp\prime}$ with $\ell, \ell' = e, \mu$. Thanks to the Fierz identities in Eq. (2.19) we may restrict the operator basis to

$$O^{JIJL}_{VXX}, \qquad O^{JIJL}_{VXY} \;=\; -2O^{JIJL}_{SXY}, \qquad O^{JIJL}_{SXX} \;=\; -\frac{1}{12}O^{JIJL}_{TX}, \qquad \text{with } X, Y = L, R \text{ and } X \neq Y. \quad (2.23)$$

The four-lepton piece of the effective Lagrangian for the decay $\ell^{I\mp} \to \ell^{J\mp}\ell^{J\mp}\ell^{L\pm}$ reads:

$$L^{JIJL}_{4\ell} \;=\; \sum_{L=1,2}\left[\sum_{X,Y=L,R}\widetilde{C}^{JIJL}_{VXY}O^{JIJL}_{VXY} + \sum_{X=L,R}\widetilde{C}^{JIJL}_{SXX}O^{JIJL}_{SXX}\right] \;+\; \text{h.c.} \qquad \text{with } L, J < I. \quad (2.24)$$

For the matching calculation it is useful to quote the tree-level matrix elements of the operators:

$$\begin{aligned}
&\langle l^{J-}(p_J,s_J)l^{J-}(p'_J,s'_J)l^{L+}(p_L,s_J)|O^{JIJL}_{VXX}|l^{I-}(p_I,s_I)\rangle \\
&\qquad = \quad [\bar u(p_J,s_J)\gamma_\mu P_X u(p_I,s_I)][\bar u(p'_J,s'_J)\gamma^\mu P_X v(p_L,s_L)] \\
&\qquad\quad - [\bar u(p'_J,s'_J)\gamma_\mu P_X u(p_I,s_I)][\bar u(p_J,s_J)\gamma^\mu P_X v(p_L,s_L)] \\
&\qquad = \quad 2\,[\bar u(p_J,s_J)\gamma_\mu P_X u(p_I,s_I)][\bar u(p'_J,s'_J)\gamma^\mu P_X v(p_L,s_L)] \\
&\langle l^{J-}(p_J,s_J)l^{J-}(p'_J,s'_J)l^{L+}(p_L,s_J)|O^{JIJL}_{VXY}|l^{I-}(p_I,s_I)\rangle \\
&\qquad = \quad [\bar u(p_J,s_J)\gamma_\mu P_X u(p_I,s_I)][\bar u(p'_J,s'_J)\gamma^\mu P_Y v(p_L,s_L)] \\
&\qquad\quad - [\bar u(p'_J,s'_J)\gamma_\mu P_X u(p_I,s_I)][\bar u(p_J,s_J)\gamma^\mu P_Y v(p_L,s_L)] \\
&\qquad = \quad [\bar u(p_J,s_J)\gamma_\mu P_X u(p_I,s_I)][\bar u(p'_J,s'_J)\gamma^\mu P_Y v(p_L,s_L)] \\
&\qquad\quad - 2\,[\bar u(p_J,s_J)P_X u(p_I,s_I)][\bar u(p'_J,s'_J)P_Y v(p_L,s_L)], \qquad \text{for } X \neq Y, \\
&\langle l^{J-}(p_J,s_J)l^{J-}(p'_J,s'_J)l^{L+}(p_L,s_J)|O^{JIJL}_{SXX}|l^{I-}(p_I,s_I)\rangle \\
&\qquad = \quad [\bar u(p_J,s_J)P_X u(p_I,s_I)][\bar u(p'_J,s'_J)P_X v(p_L,s_L)] \\
&\qquad\quad - [\bar u(p'_J,s'_J)P_X u(p_I,s_I)][\bar u(p_J,s_J)P_X v(p_L,s_L)] \\
&\qquad = \quad \frac{1}{2}[\bar u(p_J,s_J)P_X u(p_I,s_I)][\bar u(p'_J,s'_J)P_X v(p_L,s_L)] \\
&\qquad\quad - \frac{1}{8}\,[\bar u(p_J,s_J)\sigma_{\mu\nu}P_X u(p_I,s_I)][\bar u(p'_J,s'_J)\sigma^{\mu\nu}P_X v(p_L,s_L)]
\end{aligned} \quad (2.25)$$

Here we have used the Fierz transform to group the spinors into the canonical order $[\bar u(p_J,...)...u(p_I,...)][\bar u(p'_J,...)...v(p_L,...)]$. This allows us to use the same formula for spin-summed squared matrix elements as in the case of $J \neq K$ of Sec. 2.4.1.

To quote the Wilson coefficients $\widetilde{C}^{JIJL}_{NXY}$, $N = V, S$ in terms of the box diagrams B^{JIJL}_{NXY} in Eq. (2.22) we must compare the results of the MSSM decay amplitude in Eq. (3.6) with the matrix elements in Eq. (2.25) and read off coefficients of the various Dirac structures. The result is

$$\begin{aligned}
\widetilde{C}^{JIJL}_{VXX} &= \frac{1}{2}B^{JIJL}_{VXX}, \\
\widetilde{C}^{JIJL}_{VXY} &= B^{JIJL}_{VXY} \qquad \text{for } X \neq Y, \\
\widetilde{C}^{JIJL}_{SXX} &= 2\,B^{JIJL}_{SXX}.
\end{aligned} \quad (2.26)$$

The Fierz identities further imply the equalities

$$\begin{aligned} B_{SXY}^{JIJL} &= -2B_{VXY}^{JIJL} \qquad \text{for } X \neq Y, \\ B_{TX}^{JIJL} &= -\frac{1}{4}B_{SXX}^{JIJL}\,. \end{aligned} \tag{2.27}$$

2.4.3 Leptonic operators with J = K and I = L

These operators do not appear in lepton decays, but trigger muonium-antimuonium transitions and describe muon or tau pair production in e^-–e^- collisions at energies far below M_{SUSY}. Their Wilson coefficients are tiny in the MSSM.

2.4.4 Operators with two leptons and two quarks

The analogous Lagrangian for the 2-lepton–2-quark interactions reads

$$L_{2\ell 2q}^{IJKL} = \sum_{N,X,Y} B_{q\,NXY}^{IJKL} O_{q\,NXY}^{JIKL} \tag{2.28}$$

where

$$\begin{aligned} O_{qVXY}^{IJKL} &= (\bar{\ell}_I \gamma^\mu P_X \ell_J) \times (\bar{q}_K \gamma_\mu P_Y q_L)\,, \\ O_{q\,SXY}^{IJKL} &= (\bar{\ell}_I P_X \ell_J) \times (\bar{q}_L P_Y q_K)\,, \\ O_{qTX}^{IJKL} &= (\bar{\ell}_I \sigma^{\mu\nu} \ell_J) \times (\bar{q}_K \sigma_{\mu\nu} P_X q_L)\,. \end{aligned} \tag{2.29}$$

Again, we consider only purely leptonic contributions here in detail but do not give explicit expressions for the 2-lepton–2-quark box diagrams. The relevant expressions in the mass eigenbasis can be found using formulae of Appendix D and inserting proper quark vertices from Refs. [33, 34] into these.

3 Observables

In this Section we collect the formulae for the LFV observables in terms of the effective interactions defined in Sec. 2. All the processes listed here will be included in the future version of the SUSY_FLAVOR numerical library calculating an extensive set of flavour and CP-violating observables both in the quark and leptonic sectors [56–58].

3.1 Radiative lepton decays: $\ell^I \to \ell^J \gamma$

The branching ratios for the radiative lepton decays $\ell^I \to \ell^J \gamma$ are given by

$$\mathrm{Br}(\ell^I \to \ell^J \gamma) = \frac{48\pi^2 e^2}{m_I^2 G_F^2} \left(|F_\gamma^{JI}|^2 + |F_\gamma^{IJ}|^2 \right) \mathrm{Br}(\ell^I \to e\nu\nu)\,. \tag{3.1}$$

Here we used $\Gamma(\ell^I \to e\nu\nu) \approx G_F^2 m_I^5/(192\pi^3)$ for the tree-level leptonic decay width and the factors $\mathrm{Br}(\mu \to e\nu\nu) \approx 1$, $\mathrm{Br}(\tau \to e\nu\nu) = 0.1785 \pm 0.0005$ [59] are introduced to account for the hadronic decay modes of the τ lepton.

Even though in our numerical analyses we restrict ourselves to LFV processes, we remind the reader that the expressions for the anomalous magnetic moments and electric dipole moments of the charged leptons can be also calculated in term of the quantities defined in Eq. (2.4) and read:

$$\begin{aligned} \Delta a_I &= -4m_I \,\mathrm{Re}\left[F_{\gamma A}^{II} - m_I\left(F_{\gamma LB}^{II} + F_{\gamma RB}^{II}\right)\right], & (3.2)\\ d_l^I &= -2e\,\mathrm{Im}\,F_{\gamma A}^{II} & (3.3)\end{aligned}$$

3.2 $h(H) \to \bar{\ell}^I \ell^J$ decays

The decay branching ratios for the CP-even and CP-odd Higgs bosons read:

$$\begin{aligned} Br(H_0^K \to \ell^{I+}\ell^{J-}) &= \frac{m_{H_0^K}}{16\pi\Gamma_{H_0^K}}\left(\left|F_h^{IJK}\right|^2 + \left|F_h^{JIK}\right|^2\right)\\ Br(A_0 \to \ell^{I+}\ell^{J-}) &= \frac{m_A}{16\pi\Gamma_A}\left(\left|F_A^{IJ}\right|^2 + \left|F_A^{JI}\right|^2\right) \end{aligned} \quad (3.4)$$

with F_h^{IJK}, F_A^{IJ} defined in Eq. (2.14). Note that summing over lepton charges in the final state, $\ell^{I+}\ell^{J-}$ and $\ell^{J+}\ell^{I-}$, would produce an additional factor of 2.

3.3 $\ell^I \to \ell^J\ell^K\bar{\ell}^L$ decays

The LFV decays of charged lepton into three lighter ones can be divided into 3 classes, depending on the flavours in the final state:

(A) $\ell \to \ell'\ell'\ell'$: Three leptons of the same flavour, i.e. $\mu^\pm \to e^\pm e^+ e^-$, $\tau^\pm \to e^\pm e^+ e^-$ and $\tau^\pm \to \mu^\pm\mu^+\mu^-$, with a pair of opposite charged leptons.

(B) $\ell^\pm \to \ell'^\pm \ell''^+ \ell''^-$: Three distinguishable leptons with ℓ' carrying the same charge as ℓ, i.e. $\tau^\pm \to e^\pm\mu^+\mu^-$ and $\tau^\pm \to \mu^\pm e^+ e^-$.

(C) $\ell^\pm \to \ell'^\mp \ell''^+ \ell''^-$: Three distinguishable leptons with ℓ' carrying the opposite charge as ℓ, i.e. $\tau^\pm \to e^\mp\mu^\pm\mu^\pm$ and $\tau^\pm \to \mu^\mp e^\pm e^\pm$.

Class (C), representing a $\Delta L = 2$ processes, is tiny within the MSSM: it could only be generated at 1-loop level by box diagrams suppressed by double flavour changes, or at the 2-loop level by double penguin diagrams involving two LFV vertices. Therefore, we will not consider these process in our numerical analysis.
In order to calculate $\mathrm{Br}(\ell^I \to \ell^J\ell^K\bar{\ell}^L)$ we decompose the corresponding amplitude A as

$$A = A_0 + A_\gamma\,, \quad (3.5)$$

The relevant diagrams are displayed in Fig. 5. A_0 contains contributions from 4-lepton box diagrams and from penguin diagrams (including vector-like off-shell photon couplings, see Eq. (2.5)) which in the limit of vanishing external momenta can be represented as the 4-fermion contact interactions. A_γ is the on-shell photon contribution originating from the magnetic operator (see Eq. (2.2)) which has to be treated separately with more care as the photon propagator becomes singular in the limit of vanishing external momenta.

Figure 5: Diagrams contributing to $\ell^I \to \ell^J \ell^K \bar{\ell}^L$ decay. I): 1PI irreducible box diagrams; II): penguin diagrams with $V = Z, \gamma, h, H$ or A. For $K = J$ crossed diagrams must be also included.

We further decompose A_0 for the two cases (A) and (B) according to its Lorentz structure:

$$A_0^{(A)} = \sum_{Q=V,S,T} C_{Q,XY}^{(A)} [\bar{u}(p_J)\Gamma'_Q P_X u(p_I)][\bar{u}(p'_J)\Gamma_Q P_Y v(p_L)]] \,, \tag{3.6}$$

$$A_0^{(B)} = \sum_{Q=V,S,T} C_{Q,XY}^{(B)} [\bar{u}(p_J)\Gamma'_Q P_X u(p_I)][\bar{u}(p_K)\Gamma_Q P_Y v(p_L)]] \,. \tag{3.7}$$

with $X, Y = L, R$. Note that the amplitude $A_0^{(A)}$ in general contains a second term which is obtained from the one given in Eq. (3.6) by replacing $(p_J \leftrightarrow p'_J)$. However, one can use Fierz identities to reduce it to the structure given in Eq. (3.6). The basis of Dirac quadrilinears Γ_Q is the same as the one used to decompose 4-lepton box diagrams in Eq. (2.17):

$$\Gamma_S = 1 \,, \qquad \Gamma_V = \gamma^\mu \,, \qquad \Gamma_T = \sigma_{\mu\nu} \,, \tag{3.8}$$

and Γ'_Q is obtained from Γ_Q by lowering the Lorentz indices.

The amplitudes originating from on-shell photon exchange are given by

$$\begin{aligned} A_\gamma^{(A)} &= \frac{e}{(p_I - p_J)^2} [\bar{u}(p_J) i\sigma^{\mu\nu} (C_{\gamma L} P_L + C_{\gamma R} P_R)(p_I - p_J)_\nu u(p_I)][\bar{u}(p'_J)\gamma_\mu v(p_L)] \\ &\quad -(p_J \leftrightarrow p'_J) \\ A_\gamma^{(B)} &= \frac{e}{(p_I - p_J)^2} [\bar{u}(p_J) i\sigma^{\mu\nu} (C_{\gamma L} P_L + C_{\gamma R} P_R)(p_I - p_J)_\nu u(p_I)][\bar{u}(p_K)\gamma_\mu v(p_L)]. \end{aligned} \tag{3.9}$$

The full form of the coefficients $C_N^{(A,B)}$, C_γ is displayed in Table 1, where we compactified the expressions by using the following abbreviations for the Higgs penguin contributions[6]:

$$V_H^{JI} = \sum_{N=1}^{2} \frac{Z_R^{1N}}{m^2_{H_0^N}} F_h^{JIN} \,, \qquad V_A^{JI} = \frac{i \sin\beta}{m^2_{A_0}} F_A^{JI} \,. \tag{3.10}$$

Note that in Eq. (3.7) and Eq. (3.9) we do not explicitly display flavour indices, but they are specified in Table 1.

[6]Note that we define lepton Yukawa coupling appearing in Table 1 to be negative, $Y_l^I = -\sqrt{2} m_l^I / v_1$

	Decay (A)	Decay (B)
C_{VLL}	$B_{VLL}^{JIJJ} - \frac{e(1-2s_W^2)}{s_W c_W M_Z^2} F_{ZL}^{JI} + 2e^2 V_{\gamma L}^{JI}$	$B_{VLL}^{JIKK} - \frac{e(1-2s_W^2)}{2s_W c_W M_Z^2} F_{ZL}^{JI} + e^2 V_{\gamma L}^{JI}$
C_{VRR}	$B_{VRR}^{JIJJ} + \frac{2es_W}{c_W M_Z^2} F_{ZR}^{JI} + 2e^2 V_{\gamma R}^{JI}$	$B_{VRR}^{JIKK} + \frac{es_W}{c_W M_Z^2} F_{ZR}^{JI} + e^2 V_{\gamma R}^{JI}$
C_{VLR}	$B_{VLR}^{JIJJ} + \frac{es_W}{c_W M_Z^2} F_{ZL}^{JI} + e^2 V_{\gamma L}^{JI} + \frac{1}{2} Y_l^J (V_H^{IJ*} - V_A^{IJ*})$	$B_{VLR}^{JIKK} + \frac{es_W}{c_W M_Z^2} F_{ZL}^{JI} + e^2 V_{\gamma L}^{JI}$
C_{VRL}	$B_{VRL}^{JIJJ} - \frac{e(1-2s_W^2)}{2s_W c_W M_Z^2} F_{ZR}^{JI} + e^2 V_{\gamma R}^{JI} + \frac{1}{2} Y_l^J (V_H^{JI} - V_A^{JI})$	$B_{VRL}^{JIKK} - \frac{e(1-2s_W^2)}{2s_W c_W M_Z^2} F_{ZR}^{JI} + e^2 V_{\gamma R}^{JI}$
C_{SLL}	$B_{SLL}^{JIJJ} + \frac{3}{2} Y_l^J (V_H^{JI} + V_A^{JI})$	$B_{SLL}^{JIKK} + Y_l^K (V_H^{JI} + V_A^{JI})$
C_{SRR}	$B_{SRR}^{JIJJ} + \frac{3}{2} Y_l^J (V_H^{IJ*} + V_A^{IJ*})$	$B_{VRR}^{JIKK} + Y_l^K (V_H^{IJ*} + V_A^{IJ*})$
C_{SLR}	$-2B_{VLR}^{JIJJ} - \frac{2es_W}{c_W M_Z^2} F_{ZL}^{JI} - 2e^2 V_{\gamma L}^{JI} + Y_l^J (V_H^{JI} - V_A^{JI})$	$B_{SLR}^{JIKK} + Y_l^K (V_H^{JI} - V_A^{JI})$
C_{SRL}	$-2B_{SRL}^{JIJJ} + \frac{e(1-2s_W^2)}{s_W c_W M_Z^2} F_{ZR}^{JI} - 2e^2 V_{\gamma R}^{JI} + Y_l^J (V_H^{IJ*} - V_A^{IJ*})$	$B_{SRL}^{JIKK} + Y_l^K (V_H^{IJ*} - V_A^{IJ*})$
C_{TL}	$-\frac{1}{4} B_{SLL}^{JIJJ} + \frac{1}{8} Y_l^J (V_H^{JI} + V_A^{JI})$	B_{TL}^{JIKK}
C_{TR}	$-\frac{1}{4} B_{SRR}^{JIJJ} + \frac{1}{8} Y_l^J (V_H^{IJ*} + V_A^{IJ*})$	B_{TR}^{JIKK}
$C_{\gamma L}$	$-2eF_\gamma^{JI}$	$-2eF_\gamma^{JI}$
$C_{\gamma R}$	$-2eF_\gamma^{IJ*}$	$-2eF_\gamma^{IJ*}$

Table 1: Coefficients C_N, C_γ of Eq. (3.7) and Eq. (3.9) for decay types (A) and (B). B_{QXY},B_{TX} denote the irreducible box diagram contributions (see Eq. (2.21)), the terms with F_Z stem from the Z penguin Lagrangian (Eq. (2.7)), V_γ is the sum of the vector-like photon contributions (Eq. (2.5)), Higgs contributions are defined in Eq. (3.10) and the coefficients F_γ of the magnetic operator are defined in Eq. (2.2).

Neglecting the lighter lepton masses whenever possible, the expression for the branching ratios can be written down as (for comparison see [23]):

$$\begin{aligned}
\mathrm{Br}(\ell^I \to \ell^J \ell^K \bar{\ell}^L) &= \frac{N_c \mathrm{Br}(\ell^I \to e\nu\nu)}{32 G_F^2} \left(4 \left(|C_{VLL}|^2 + |C_{VRR}|^2 + |C_{VLR}|^2 + |C_{VRL}|^2\right)\right. \\
&+ |C_{SLL}|^2 + |C_{SRR}|^2 + |C_{SLR}|^2 + |C_{SRL}|^2 \\
&+ \left. 48 \left(|C_{TL}|^2 + |C_{TR}|^2\right) + X_\gamma\right) \qquad (3.11)
\end{aligned}$$

where $N_c = 1/2$ if two of the final state leptons are identical (decays (A)), $N_c = 1$ for decays (B) and X_γ denotes the contribution to matrix element from the photon penguin A_γ, including also its interference with the A_0 part of the amplitude (m denotes the mass of the heaviest final state lepton)

$$\begin{aligned}
X_\gamma^{(A)} &= -\frac{16e}{m_{\ell^I}} \mathrm{Re}\left[\left(2C_{VLL} + C_{VLR} - \frac{1}{2} C_{SLR}\right) C_{\gamma R}^\star + \left(2C_{VRR} + C_{VRL} - \frac{1}{2} C_{SRL}\right) C_{\gamma L}^\star\right] \\
&+ \frac{64e^2}{m_{\ell^I}^2} \left(\log \frac{m_{\ell^I}^2}{m^2} - \frac{11}{4}\right) \left(|C_{\gamma L}|^2 + |C_{\gamma R}|^2\right) \\
X_\gamma^{(B)} &= -\frac{16e}{m_{\ell^I}} \mathrm{Re}\left[\left(C_{VLL} + C_{VLR}\right) C_{\gamma R}^\star + \left(C_{VRR} + C_{VRL}\right) C_{\gamma L}^\star\right] \\
&+ \frac{32e^2}{m_{\ell^I}^2} \left(\log \frac{m_{\ell^I}^2}{m^2} - 3\right) \left(|C_{\gamma L}|^2 + |C_{\gamma R}|^2\right) . \qquad (3.12)
\end{aligned}$$

3.4 $\mu \to e$ conversion in Nuclei

The full 1-loop expressions for the $\mu \to e$ conversion in Nuclei depend on both the squark and slepton SUSY breaking terms. Thus, in principle the resulting upper bounds on the slepton mass insertions depend to some extent on the squark masses. Therefore, we do not include $\mu \to e$ conversion in nuclei in our numerical analysis[7]. However, for completeness we collect here the complete set of formulae required to calculate the rate of this process.

$\mu \to e$ conversion in nuclei is produced by the dipole, the vector, and the scalar operators already at the tree level [61]. Following the discussion of Ref. [62] we use the effective Lagrangian

$$L_{\mu\to e} = \sum_{N,X,Y} C^{N\,XY}_{q_I q_I} O^{q_I q_I}_{N\,XY} + C^{gg}_X O^{gg}_X \tag{3.13}$$

where $N = V, S$ and $X, Y = L, R$ with the operators defined as

$$\begin{aligned} O^{q_I q_I}_{V\,XY} &= (\bar{e}\gamma^\mu P_X \mu)\,(\bar{q}_I \gamma_\mu P_Y q_I) \\ O^{q_I q_I}_{S\,XY} &= (\bar{e} P_X \mu)\,(\bar{q}_I P_Y q_I) \\ O^{gg}_X &= \alpha_s m_\mu G_F\,(\bar{e} P_X \mu)\, G^a_{\mu\nu} G^{\mu\nu}_a \end{aligned} \tag{3.14}$$

Using the notation introduced in previous Sections, the corresponding Wilson coefficients can be expressed as

$$\begin{aligned} C^{d_I d_I}_{V\,XL} &= C^{12II}_{d\ell VXL} - \frac{1}{m_Z^2}\frac{e}{2 s_W c_W}\left(1 - \frac{2}{3}s_W^2\right) F^{12}_{ZX} - \frac{1}{3} e^2 V^{JI}_{\gamma X} \\ C^{d_I d_I}_{V\,XR} &= C^{12II}_{d\ell VXR} + \frac{1}{m_Z^2}\frac{e}{3 s_W c_W} s_W^2 F^{12}_{ZX} - \frac{1}{3} e^2 V^{JI}_{\gamma X} \\ C^{u_I u_I}_{V\,XL} &= C^{12II}_{u\ell VXL} + \frac{1}{m_Z^2}\frac{e}{2 s_W c_W}\left(1 - \frac{4}{3}s_W^2\right) F^{12}_{ZX} + \frac{2}{3} e^2 V^{JI}_{\gamma X} \\ C^{u_I u_I}_{V\,XR} &= C^{12II}_{u\ell VXR} - \frac{1}{m_Z^2}\frac{e}{s_W c_W}\frac{2}{3} s_W^2 F^{12}_{ZX} + \frac{2}{3} e^2 V^{JI}_{\gamma X} \\ C^{d_I d_I}_{S\,LX} &= C^{12II}_{d\ell SLX} + \frac{1}{(m_0^K)^2} F^{12K}_h F^{IIK}_{hd} \\ C^{u_I u_I}_{S\,LX} &= C^{12II}_{u\ell SLX} + \frac{1}{(m_0^K)^2} F^{12K}_h F^{IIK}_{hu} \\ C^{d_I d_I}_{S\,RX} &= C^{12II}_{d\ell SRX} + \frac{1}{(m_0^K)^2} F^{21K*}_h F^{IIK}_{hd} \\ C^{u_I u_I}_{S\,RX} &= C^{12II}_{u\ell SRX} + \frac{1}{(m_0^K)^2} F^{21K*}_h F^{IIK}_{hu} \end{aligned} \tag{3.15}$$

For this process, a Lagrangian involving only quark, lepton and photon fields is not sufficient. Instead, an effective Lagrangian at the nucleon level containing proton and neutron fields is required. It can be obtained in two steps. First, heavy quarks are

[7] Recent discussion of interplay between the bounds on MI's in the slepton and squark sectors can be found in Ref. [60].

integrated out. This results in a redefinition of the Wilson coefficient of the gluonic operator [63]

$$C_L^{gg} \;\to\; \tilde{C}_L^{gg} = C_L^{gg} - \frac{1}{12\pi}\sum_{q=c,b}\frac{C_{S\,LL}^{qq}+C_{S\,LR}^{qq}}{G_F\, m_\mu m_q} \tag{3.16}$$

with an analogous equation for C_{gg}^R. Second, the resulting Lagrangian is matched at the scale of $\mu_n = 1$ GeV to an effective Lagrangian at the nucleon level. Following [64] the transition rate $\Gamma_{\mu\to e}^N = \Gamma(\mu^- N \to e^- N)$ can then be written as

$$\begin{aligned}\Gamma_{\mu\to e}^N &= \frac{m_\mu^5}{4}\left|-e\,C_L^D\;F_\gamma^{12}/m_\mu + 4\left(G_F m_\mu m_p \tilde{C}_{SL}^{(p)} S_N^{(p)} + \tilde{C}_{VR}^{(p)}\,V_N^{(p)} + (p\to n)\right)\right|^2 \\ &+ (L\leftrightarrow R),\end{aligned} \tag{3.17}$$

where p and n denote the proton and the neutron, respectively. The effective couplings in Eq. (3.17) can be expressed in terms of our Wilson coefficients as

$$\tilde{C}_{VR}^{(p/n)} = \sum_{q=u,d,s}\left(C_{V\,RL}^{qq} + C_{V\,RR}^{qq}\right)\; f_{Vp/n}^{(q)}\,, \tag{3.18}$$

$$\tilde{C}_{SL}^{(p/n)} = \sum_{q=u,d,s}\frac{\left(C_{S\,LL}^{qq}+C_{S\,LR}^{qq}\right)}{m_\mu m_q G_F}\; f_{Sp/n}^{(q)} \;+\; \tilde{C}_L^{gg}\, f_{Gp/n} \tag{3.19}$$

with analogous relations for $L \leftrightarrow R$. The Wilson coefficients in Eqs. (3.18) and (3.19) are to be evaluated at the scale μ_n.

The nucleon form factors for vector operators are fixed by vector-current conservation, i.e. $f_{Vp}^{(u)} = 2$, $f_{Vn}^{(u)} = 1$, $f_{Vp}^{(d)} = 1$, $f_{Vn}^{(d)} = 2$, $f_{Vp}^{(s)} = 0$, $f_{Vn}^{(s)} = 0$. Hence, the sum in Eq. (3.18) is in fact only over $q = u, d$. The calculation of the scalar form factors is more involved. The values of the up- and down-quark scalar couplings $f_{Sp/n}^{(u/d)}$ (based on the two-flavour chiral perturbation theory framework of [65]) can be found in Refs. [66, 67], while the values of the s-quark scalar couplings $f_{Sp/n}^{(s)}$ can be borrowed from a lattice calculation [68]. In summary, one has

$$\begin{aligned} f_{Sp}^{(u)} &= (20.8 \pm 1.5)\times 10^{-3}, \qquad f_{Sn}^{(u)} = (18.9 \pm 1.4)\times 10^{-3}, \\ f_{Sp}^{(d)} &= (41.1 \pm 2.8)\times 10^{-3}, \qquad f_{Sn}^{(d)} = (45.1 \pm 2.7)\times 10^{-3}, \\ f_{Sp}^{(s)} &= f_{Sn}^{(s)} = (53 \pm 27)\times 10^{-3}. \end{aligned} \tag{3.20}$$

The form factor for the gluonic operator can be obtained from a sum rule. In our normalisation

$$f_{Gp/n} = -\frac{8\pi}{9}\left(1 - \sum_{q=u,d,s} f_{Sp/n}^{(q)}\right). \tag{3.21}$$

The quantities D_N, $S_N^{(p/n)}$, and $V_N^{(p/n)}$ in Eq. (3.17) are related to the overlap integrals [69] between the lepton wave functions and the nucleon densities. They depend on the nature of the target N. Their numerical values can be found in Ref. [61]:

$$\begin{aligned} &D_{\rm Au} = 0.189, \quad S_{\rm Au}^{(p)} = 0.0614, \quad V_{\rm Au}^{(p)} = 0.0974, \quad S_{\rm Au}^{(n)} = 0.0918, \quad V_{\rm Au}^{(n)} = 0.146; \\ &D_{\rm Al} = 0.0362, \quad S_{\rm Al}^{(p)} = 0.0155, \quad V_{\rm Al}^{(p)} = 0.0161, \quad S_{\rm Al}^{(n)} = 0.0167, \quad V_{\rm Al}^{(n)} = 0.0173; \end{aligned} \tag{3.22}$$

for gold and aluminum, respectively.

Finally, the branching ratio is defined as the transition rate, (see Eq. (3.17)), divided by the capture rate, the latter given in Ref. [70]:

$$\Gamma^{\rm capt}_{\rm Au} = 8.7 \times 10^{-15}\ {\rm MeV}, \qquad \Gamma^{\rm capt}_{\rm Al} = 4.6 \times 10^{-16}\ {\rm MeV}\,. \tag{3.23}$$

4 Mass eigenstates vs. mass insertions calculations

For each process, we have given the exact one-loop expressions calculated in the mass eigenbasis (ME). These formulae are compact and well suited for numerical computations, however, do not allow for an easy understanding of the qualitative behaviour of the LFV amplitudes for various choices of the MSSM parameters. Therefore, in this Section we expand the Wilson coefficients in terms of the "mass insertions", defined as the off-diagonal elements (both flavour violating and flavour conserving) of the mass matrices. Such an expansion allows us to:

- Recover the direct analytical dependence of the results on the MSSM Lagrangian parameters.
- Prove analytically the expected decoupling features of the amplitudes in the limit of a heavy SUSY spectrum. In the case of Higgs boson decays, we also identify explicitly the terms decoupling only with the heavy CP-odd Higgs mass M_A (which also determines the heavy CP even and the charged Higgs masses). The decoupling properties serve also as an important cross-check of the correctness of our calculations.
- Test the dependence of the results on the pattern of the MSSM spectrum and the size of the mass splitting between SUSY particles. Such analyses are missing in most of the existing literature on the subject.
- Better understand the possible cancellations between various types of contributions and correlations between different LFV processes.

The mass insertion expansion in flavour off-diagonal terms has been used for a long time in numerous articles on the subject. However, always some simplifying assumptions have been made, i.e. some terms have been neglected and a fully general non-degenerate slepton spectrum was never considered. This is understandable as a consistent MI expansion of the amplitudes for the LFV processes in the MSSM, mediated by the virtual chargino and neutralino exchanges, is technically challenging. The standard approach used in literature is to calculate diagrammatically the LFV amplitudes with the "mass insertions" treated as the new interaction vertices. We follow the common practice and normalise such slepton mass insertions to dimensionless "Δ-parameters"[8]:

$$\Delta^{IJ}_{LL} = \frac{(M^2_{LL})^{IJ}}{\sqrt{(M^2_{LL})^{II}(M^2_{LL})^{JJ}}}\,, \qquad \Delta^{IJ}_{RR} = \frac{(M^2_{RR})^{IJ}}{\sqrt{(M^2_{RR})^{II}(M^2_{RR})^{JJ}}}\,,$$
$$\Delta^{IJ}_{LR} = \frac{A^{IJ}_l}{((M^2_{LL})^{II}(M^2_{RR})^{JJ})^{1/4}}\,, \qquad \Delta'^{IJ}_{LR} = \frac{A'^{IJ}_l}{((M^2_{LL})^{II}(M^2_{RR})^{JJ})^{1/4}}\,, \tag{4.1}$$

[8] We assume that trilinear A_l, A'_l terms scale linearly with the slepton mass scale.

where $M^2_{LL}, M^2_{RR}, A_l, A'_l$ are the slepton soft mass matrices and trilinear terms.

As lepton flavour violation is already strongly constrained experimentally, it is sufficient to expand the amplitudes up to the first order in flavour-violating Δ's. For instance, the effective vertices listed in Sec. 3 take the schematic form:

$$\begin{aligned} F^{IJ} &= \frac{1}{(4\pi)^2}\left(F^{IJ}_{LL}\Delta^{IJ}_{LL} + F^{IJ}_{RR}\Delta^{JI}_{RR}\right. \\ &+ \left. F^{IJ}_{ALR}\Delta^{JI}_{LR} + F^{IJ}_{BLR}\Delta^{IJ*}_{LR} + F'^{IJ}_{ALR}\Delta'^{JI}_{LR} + F'^{IJ}_{BLR}\Delta'^{IJ*}_{LR}\right) . \end{aligned} \tag{4.2}$$

The MSSM contributions to $F_{LL}, \ldots, F'_{BLR}$ can be classified according to their decoupling behaviour, distinguishing the following types (M denotes the average SUSY mass scale):

1. Effects related to the diagonal trilinear slepton soft terms or to the off-diagonal elements of supersymmetric fermion mass matrices, decoupling as v^2/M^2.

2. Effects related to the external momenta of the (on-shell) Higgs or Z^0 bosons, decoupling as M_h^2/M^2 or M_Z^2/M^2 (we did not include the M_Z dependence as it is not necessary for the considered processes).

3. Non-decoupling effects related to the 2HDM structure of the MSSM. Such effects are constant in the limit of heavy M but decouple as v^2/M_A^2. They are proportional either to the lepton Yukawa couplings or to the non-holomorphic A'_l terms.

The structure of the box diagrams is more complicated as they carry 4 flavour indices. Their MI expansion is given in Appendix E.5. All box diagram contributions decouple at least as v^2/M^2.

Calculating consistently the quantities $F_{LL}, \ldots, F'_{BLR}$ to the order v^2/M^2 is not trivial for chargino and neutralino contributions. If the MI expansion is used only for the sfermion mass matrices but the calculations for the supersymmetric fermions are done in the mass eigenbasis, the direct dependence on the Lagrangian parameters is hidden and the decoupling properties of the amplitude cannot be seen directly. However, one can also treat the off-diagonal entries of the chargino and neutralino mass matrices as "mass insertions". With such an approach, the final result is expressed explicitly in terms of Lagrangian parameters, but the computations can get very complicated. At the order v^2/M^2 one needs to include diagrams with all combinations of two fermionic mass insertions (each providing one power of v/M_1, v/M_2 or v/μ) or flavour diagonal slepton terms originating from trilinear A-terms (providing powers of vA_l/M^2, vA'_l/M^2). Thus, to obtain an expansion of the F's in Eq. (4.2), one needs to formally go to the 3rd order of MI expansion, adding all diagrams with up to two flavour conserving and one flavour violating mass insertion. Therefore, the number of diagrams grows quickly with the order of the expansion and such a method is tedious and prone to calculational mistakes.

In our paper, we employ a recently developed technique using a purely algebraic MI expansion of the ME amplitudes listed in Sec. 3, without the need for direct diagrammatic MI calculations ("FET theorem") [29], automatised in the specialised `MassToMI` *Mathematica* package [30, 71]. The use of this package and full automation of the calculations allows us to perform the required 3rd order MI expansion for a completely general SUSY mass spectrum, without making any simplifying assumptions. Such a result would be very difficult to obtain diagrammatically, as in the intermediate steps of the calculations

(before accounting for the cancellations and simplifications between various contributions) the expressions may contain up to tens of thousand terms, even if the final results collected in Appendix E are again relatively compact. In detail:

- We perform the expansion always up to the lowest non-vanishing order in the slepton LFV terms, taking into account the possible cancellations. Compared to previous analyses, we consider the non-holomorphic trilinear soft terms as well.

- In the MI expanded expressions we include all terms decreasing with the SUSY mass scale as v^2/M_{SUSY}^2 (or slower), where M_{SUSY} denotes any of the relevant mass parameters in the MSSM Lagrangian (apart from the soft Higgs mass terms): diagonal soft slepton masses, gaugino masses M_1, M_2 or the μ parameter.

- Contrary to previous analyses, we do not assume degeneracy or any specific hierarchy for the sleptons, sneutrinos or supersymmetric fermion masses.

- In calculating the LFV Higgs decays we keep the leading terms in the external Higgs boson mass ($m_{h(H)}^2/M_{SUSY}^2$).

The full set of the expanded expressions in the MI approximation for the photon, Z^0 and CP-even Higgs leptonic penguins and for the 4-lepton box diagrams is collected in Appendix E.

We illustrate the accuracy of the derived MI formulae in Fig. 6. The plots show the ratio of the MI expanded couplings over the ones obtained in the mass eigenbasis with exact diagonalization. For this purpose, we start from the following setup where all mass parameters are given in GeV:

$$\begin{array}{lll} \tan\beta = 5 & m_{\tilde{\mu}_L} = 300 & A_{\mu\mu} = A'_{\mu\mu} = 0.1\sqrt{m_{\tilde{\mu}_L} m_{\tilde{\mu}_R}} \\ \mu = 200 + 100i & m_{\tilde{\tau}_L} = 330 & \\ M_1 = 150 & m_{\tilde{\mu}_R} = 300 & A_{\tau\tau} = A'_{\tau\tau} = 0.1\sqrt{m_{\tilde{\tau}_L} m_{\tilde{\tau}_R}} \\ M_2 = 300 & m_{\tilde{\tau}_R} = 350 & \end{array} \tag{4.3}$$

Next, to see the decoupling effects we scale this spectrum uniformly up to slepton masses of 2 TeV. For each of the six penguin Wilson coefficients describing the transition between 2nd and 3rd generation, $F^{23}_{\gamma L(R)}$ (Eq. (2.2)), $F^{23}_{ZL(R)}$ (Eq. (2.7)) and $F^{23}_{hL} \equiv F^{232}_{h}$, $F^{23}_{hR} \equiv F^{322}_{h}$ (Eq. (2.13)) we plot the quantity

$$\Delta F = \left| \frac{F_{\rm MI}}{F_{\rm ME}} \right| - 1 \,, \tag{4.4}$$

as a function of the average slepton mass. The accuracy of left-handed (right-handed) Wilson coefficients is illustrated with red(blue) lines. As can be seen from Fig. 6, the accuracy of MI expanded amplitudes is very good even for light SUSY particles and for $M_{SUSY} > 500$ GeV always better than 95%.

Most analyses published to date for simplicity did not include the complete set of the contributions scaling like v/M order and/or assumed a partially or fully degenerate SUSY spectrum. This procedure is inconsistent with non-zero off-diagonal elements of mass matrices, because the latter enforce unequal eigenvalues of the corresponding mass matrix. To illustrate the numerical effects arising from the incorrect neglect of SUSY

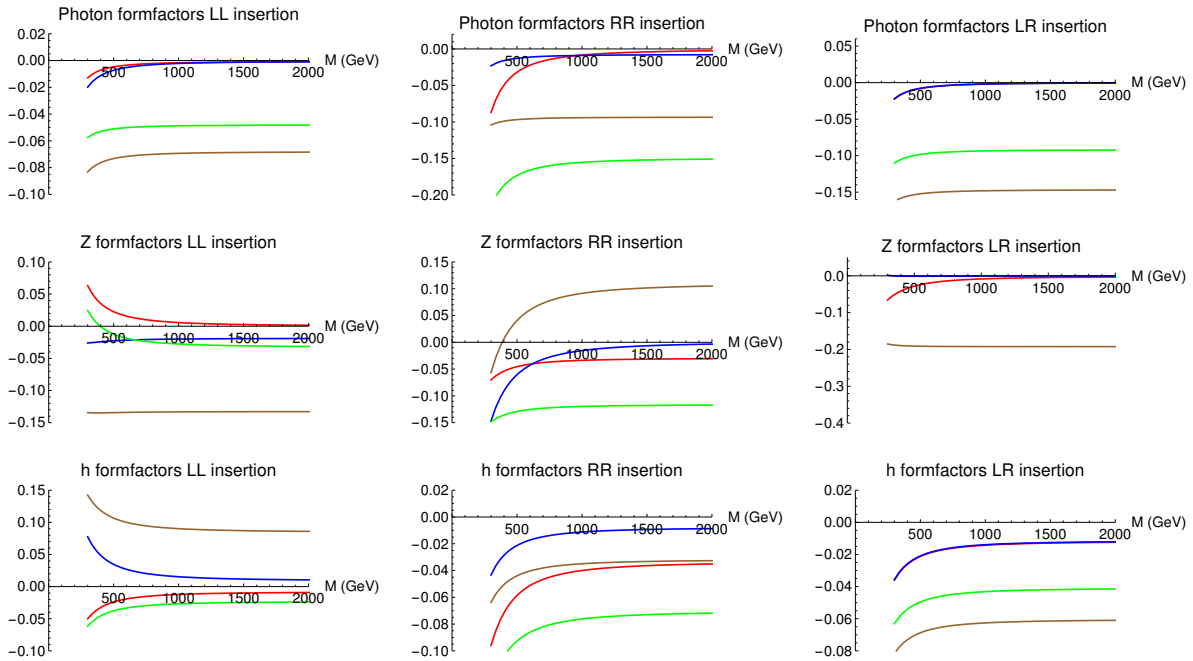

Figure 6: Accuracy of MI expansion for the penguin amplitudes. The curves show the ratio defined in Eq. (4.4). Red and blue lines: ΔF for left and right couplings assuming a spectrum of Eq. (4.3) for both the MI and ME expressions. Brown and green lines: ΔF (again for left and right couplings, respectively) assuming spectrum (4.3) for ME expressions but an universal degenerate sfermion mass in MI expressions. This assumption is inconsistent with non-zero off-diagonal elements of the mass matrices, which imply non-degenerate mass eigenstates. The plots show that the associated error can be numerically sizeable. The average SUSY mass scale M (assumed to be equal to $M_2 = m_{\tilde{\mu}_L} = m_{\tilde{\mu}_R}$) is shown on the horizontal axis.

mass splitting we plot the ratio of our expressions in the MI approximation for penguin Wilson coefficients calculated for degenerate slepton masses (equal to 300 GeV rescaled by a common factor; other parameters as in Eq. (4.3)) and the exact mass eigenbasis formulae (calculated with non-degenerate sfermion spectrum of Eq. (4.3)) in Fig. 6. The accuracy of left-handed (right-handed) MI expanded Wilson coefficients with degenerate slepton spectrum is shown in green(brown). In this case discrepancy is much larger, of the order of 10%-40%, and does not disappear when increasing the total SUSY scale.

5 Phenomenological analysis

5.1 Generic bounds on LFV parameters

As outlined in the introduction, flavour violation in the charged lepton sector is strongly constrained experimentally. In Table 2 we collect the current and expected future experimental bounds on the processes discussed so far.

Assuming the absence of fine-tuned cancellations between different flavour violating parameters, the order of magnitude of the bounds on a given flavour violating entry Δ

	Experimental upper bound	CL	Future sensitivity	CL
$\tau \to e\gamma$	3.3×10^{-8} [72]	90%	10^{-9} [73]	90%
$\tau \to \mu\gamma$	4.4×10^{-8} [72, 74]	90%	10^{-9} [73]	90%
$\mu \to e\gamma$	5.7×10^{-13} [75]	90%	6×10^{-14} [76]	90%
$Z \to \mu e$	7.5×10^{-7} [77]	95%		
$Z \to \mu\tau$	1.2×10^{-5} [78]	95%		
$Z \to \tau e$	9.8×10^{-6} [78]	95%		
$\mu \to e^-e^+e^-$	1.0×10^{-12} [79]	90%	10^{-16} [80, 81]	90%
$\tau \to e^-e^+e^-$	2.7×10^{-8} [82]	90%		
$\tau \to \mu^-\mu^+\mu^-$	2.1×10^{-8} [82]	90%		
$\tau \to e^-\mu^+\mu^-$	2.7×10^{-8} [82]	90%		
$\tau \to e^+\mu^-\mu^-$	1.7×10^{-8} [82]	90%		
$\tau \to \mu^-e^+e^-$	1.8×10^{-8} [82]	90%		
$\tau \to \mu^+e^-e^-$	1.5×10^{-8} [82]	90%		
$h \to e\tau$	6.1×10^{-3} [83]	90%		
$h \to \mu\tau$	2.5×10^{-3} [83]	90%		
$h \to \mu e$	3.6×10^{-4} [84]	90%		
$(\mu \to e)_{Au}$	7.0×10^{-13} [85]	90%		
$(\mu \to e)_{Al}$			10^{-16} [86]	90%

Table 2: Upper bounds on LFV decays of charged leptons. h denotes the SM-like Higgs boson

can be obtained by assuming that it is the only source of flavour violation. At the lowest order in the MI expansion, any LFV observable X scales like Δ^2:

$$X \approx f(m_1, \ldots, m_n)|\Delta|^2 \,, \tag{5.1}$$

where f is a known (non-negative) function of diagonal mass parameters - for any given process it can be extracted from the expanded expressions listed in Appendix E. Thus, the experimental bound on Δ from a given measurement can be written as:

$$|\Delta| \leq \sqrt{\frac{X^{\rm exp}}{f(m_1, \ldots, m_n)}} \sqrt{\frac{X^{\rm future}}{X^{\rm exp}}} \equiv \Delta(m_1, \ldots, m_n) \sqrt{\frac{X^{\rm future}}{X^{\rm exp}}} \tag{5.2}$$

where by $X^{\rm exp}$ we denote one of the current experimental bounds listed in Sec. 5.1 and $X^{\rm future}$ is the expected future sensitivity.

To estimate the order of magnitude of the bounds on all types of mass insertions, we assume a common mass scale M for all flavour diagonal SUSY parameters:

$$\begin{aligned} &m_{\tilde{e}_{LI}} = m_{\tilde{e}_{RI}} = M_1 = M_2 = \mu = M_A = M \,, \\ &A_\ell^{II} = A_\ell'^{II} = Y_\ell^I \, M \,. \end{aligned} \tag{5.3}$$

Currently, the strongest bounds on the dimensionless LFV parameters Δ defined in Eq. (4.2) originate from the radiative lepton decays $\ell \to \ell'\gamma$. We list such bounds for the parameter setup defined in Eq. (5.3) and for the SUSY scale of $M = 400$ GeV in Table 3.

The 3-body decays of charged lepton lead to bounds which are approximately one order of magnitude weaker. In Table 4 we display the relative strength of such bounds comparing

Process	(I,J)	Δ^{IJ}_{LL}	Δ^{IJ}_{RR}	Δ^{IJ}_{LR}	Δ^{IJ}_{RL}	Δ'^{IJ}_{LR}	Δ'^{IJ}_{RL}
$\tan\beta = 2$							
$\mu \to e\gamma$	$(2,1)$	$8.4 \cdot 10^{-4}$	$5.0 \cdot 10^{-3}$	$8.4 \cdot 10^{-6}$	$8.3 \cdot 10^{-6}$	$4.1 \cdot 10^{-6}$	$4.1 \cdot 10^{-6}$
$\tau \to \mu\gamma$	$(3,2)$	$5.3 \cdot 10^{-1}$	$\mathcal{O}(1)$	$9.1 \cdot 10^{-2}$	$9.1 \cdot 10^{-2}$	$4.5 \cdot 10^{-2}$	$4.5 \cdot 10^{-2}$
$\tau \to e\gamma$	$(3,1)$	$4.6 \cdot 10^{-1}$	$\mathcal{O}(1)$	$7.8 \cdot 10^{-2}$	$7.8 \cdot 10^{-2}$	$3.9 \cdot 10^{-2}$	$3.8 \cdot 10^{-2}$
$\tan\beta = 20$							
$\mu \to e\gamma$	$(2,1)$	$1.0 \cdot 10^{-4}$	$4.5 \cdot 10^{-4}$	$7.5 \cdot 10^{-5}$	$7.4 \cdot 10^{-5}$	$3.7 \cdot 10^{-6}$	$3.7 \cdot 10^{-6}$
$\tau \to \mu\gamma$	$(3,2)$	$6.5 \cdot 10^{-2}$	$2.9 \cdot 10^{-1}$	$8.2 \cdot 10^{-1}$	$8.2 \cdot 10^{-1}$	$4.0 \cdot 10^{-2}$	$4.0 \cdot 10^{-2}$
$\tau \to e\gamma$	$(3,1)$	$5.7 \cdot 10^{-2}$	$2.5 \cdot 10^{-1}$	$7.0 \cdot 10^{-1}$	$7.0 \cdot 10^{-1}$	$3.4 \cdot 10^{-2}$	$3.4 \cdot 10^{-2}$

Table 3: Upper bounds on the LFV parameters Δ from radiative charged lepton decays for the MSSM spectrum defined in Eq. (5.3) and a SUSY scale of $M = 400$ GeV. All bounds scale (i.e. weaken) like M^2.

Process	(I,J)	Δ^{IJ}_{LL}	Δ^{IJ}_{RR}	Δ^{IJ}_{LR}	Δ^{IJ}_{RL}	Δ'^{IJ}_{LR}	Δ'^{IJ}_{RL}
$\tan\beta = 2$							
$\mu \to eee$	$(2,1)$	$1.7 \cdot 10^{+1}$	$1.5 \cdot 10^{+1}$	$1.6 \cdot 10^{+1}$	$1.6 \cdot 10^{+1}$	$1.6 \cdot 10^{+1}$	$1.6 \cdot 10^{+1}$
$\tau \to \mu\mu\mu$	$(3,2)$	$1.5 \cdot 10^{+1}$	$1.2 \cdot 10^{+1}$	$1.4 \cdot 10^{+1}$	$1.4 \cdot 10^{+1}$	$1.4 \cdot 10^{+1}$	$1.4 \cdot 10^{+1}$
$\tau \to \mu e^+ e^-$	$(3,2)$	$1.3 \cdot 10^{+1}$	$1.1 \cdot 10^{+1}$	$1.2 \cdot 10^{+1}$	$1.2 \cdot 10^{+1}$	$1.2 \cdot 10^{+1}$	$1.2 \cdot 10^{+1}$
$\tau \to eee$	$(3,1)$	$8.6 \cdot 10^{+0}$	$8.2 \cdot 10^{+0}$	$8.5 \cdot 10^{+0}$	$8.5 \cdot 10^{+0}$	$8.5 \cdot 10^{+0}$	$8.5 \cdot 10^{+0}$
$\tau \to e\mu^+\mu^-$	$(3,1)$	$6.9 \cdot 10^{+0}$	$6.7 \cdot 10^{+0}$	$6.8 \cdot 10^{+0}$	$6.8 \cdot 10^{+0}$	$6.8 \cdot 10^{+0}$	$6.8 \cdot 10^{+0}$
$\tan\beta = 20$							
$\mu \to eee$	$(2,1)$	$1.6 \cdot 10^{+1}$	$1.6 \cdot 10^{+1}$	$1.6 \cdot 10^{+1}$	$1.6 \cdot 10^{+1}$	$1.6 \cdot 10^{+1}$	$1.6 \cdot 10^{+1}$
$\tau \to \mu\mu\mu$	$(3,2)$	$1.4 \cdot 10^{+1}$	$1.4 \cdot 10^{+1}$	$1.4 \cdot 10^{+1}$	$1.4 \cdot 10^{+1}$	$1.4 \cdot 10^{+1}$	$1.4 \cdot 10^{+1}$
$\tau \to \mu e^+ e^-$	$(3,2)$	$1.3 \cdot 10^{+1}$	$1.2 \cdot 10^{+1}$	$1.2 \cdot 10^{+1}$	$1.2 \cdot 10^{+1}$	$1.2 \cdot 10^{+1}$	$1.2 \cdot 10^{+1}$
$\tau \to eee$	$(3,1)$	$8.5 \cdot 10^{+0}$	$8.5 \cdot 10^{+0}$	$8.5 \cdot 10^{+0}$	$8.5 \cdot 10^{+0}$	$8.5 \cdot 10^{+0}$	$8.5 \cdot 10^{+0}$
$\tau \to e\mu^+\mu^-$	$(3,1)$	$6.8 \cdot 10^{+0}$	$6.8 \cdot 10^{+0}$	$6.8 \cdot 10^{+0}$	$6.8 \cdot 10^{+0}$	$6.8 \cdot 10^{+0}$	$6.8 \cdot 10^{+0}$

Table 4: Ratios of upper bounds on the LFV parameters Δ from the searches for 3-body and radiative decays of charged leptons. The MSSM spectrum is defined in Eq. (5.3).

them to the ones obtained from the radiative lepton decays, i.e. the ratios of bounds from radiative decays over the ones from 3-body decays. Such ratios remain constant with increasing M up to the scale where the non-decoupling Higgs penguin contributions start to contribute. However, such effects occurs for $M \gtrsim 30$ TeV for $\tau^\pm \to \mu^\pm\mu^\pm\mu^\mp$ and $\tau^\pm \to e^\pm\mu^\pm\mu^\mp$ decays and for even higher M for the decays with electron pair in the final state. For such a large M the branching ratios for all 3-body decays are, anyway, below the current experimental sensitivities even for $\mathcal{O}(\Delta^{IJ}) \sim 1$.

We do not display the bounds from LFV violating Z^0 decays as they are much weaker (3 to 8 orders of magnitude depending on which parameter Δ is chosen). This can be attributed to the large Z boson width – for comparable $\Gamma(Z \to \ell\ell')$ and $\Gamma(\ell \to \ell'\gamma)$ partial decay widths the difference in total widths leads to $\mathrm{Br}(\ell \to \ell'\gamma) \gg \mathrm{Br}(Z \to \ell\ell')$. Thus, bounds from $\mathrm{Br}(Z \to \ell\ell')$ are not competitive (nor they will be in the foreseeable future) compared to these from other observables.

Process	(I,J)	Δ^{IJ}_{LL}	Δ^{IJ}_{RR}	Δ^{IJ}_{LR}	Δ^{IJ}_{RL}	Δ'^{IJ}_{LR}	Δ'^{IJ}_{RL}
$\tan\beta = 2$							
$h \to \mu e$	$(2,1)$	$1.8 \cdot 10^{+7}$	$1.7 \cdot 10^{+6}$	$2.6 \cdot 10^{+7}$	$2.6 \cdot 10^{+7}$	$1.0 \cdot 10^{+7}$	$1.0 \cdot 10^{+7}$
$h \to \tau \mu$	$(3,2)$	$4.4 \cdot 10^{+3}$	$3.8 \cdot 10^{+2}$	$6.3 \cdot 10^{+3}$	$6.3 \cdot 10^{+3}$	$2.5 \cdot 10^{+3}$	$2.5 \cdot 10^{+3}$
$h \to \tau e$	$(3,1)$	$8.0 \cdot 10^{+3}$	$7.5 \cdot 10^{+2}$	$1.1 \cdot 10^{+4}$	$1.1 \cdot 10^{+4}$	$4.9 \cdot 10^{+3}$	$4.9 \cdot 10^{+3}$
$\tan\beta = 20$							
$h \to \mu e$	$(2,1)$	$3.9 \cdot 10^{+6}$	$8.3 \cdot 10^{+6}$	$5.1 \cdot 10^{+7}$	$5.1 \cdot 10^{+7}$	$1.2 \cdot 10^{+6}$	$1.2 \cdot 10^{+6}$
$h \to \tau \mu$	$(3,2)$	$9.5 \cdot 10^{+2}$	$1.9 \cdot 10^{+3}$	$1.3 \cdot 10^{+4}$	$1.2 \cdot 10^{+4}$	$2.9 \cdot 10^{+2}$	$2.9 \cdot 10^{+2}$
$h \to \tau e$	$(3,1)$	$1.7 \cdot 10^{+3}$	$3.5 \cdot 10^{+3}$	$2.3 \cdot 10^{+4}$	$2.2 \cdot 10^{+4}$	$5.3 \cdot 10^{+2}$	$5.4 \cdot 10^{+2}$

Table 5: Ratios of upper bounds on the LFV Δ parameters from leptonic Higgs boson decays and from radiative decays of charged leptons. The MSSM spectrum is defined in Eq. (5.3) (with the exception of setting $A_l'^{II} = 0$) and a SUSY scale of $M = 400$ GeV. The ratios for Δ^{IJ}_{LL}, Δ^{IJ}_{RR}, Δ'^{IJ}_{LR}, Δ'^{IJ}_{RL} decrease with M^2, assuming fixed masses and mixing angles in the Higgs sector.

As can be seen in Table 5, the bounds on Δ parameters from LFV flavour Higgs boson decay searches are much weaker than those from the radiative charged lepton decays. However, in the Higgs sector some effects proportional to lepton Yukawa couplings or to the non-holomorphic terms are non-decoupling and are not weakened by increasing M like other contributions, for fixed Higgs sector parameters. In Table 5 we assume

$$\alpha - \beta = \frac{\pi}{2} - \gamma \,, \tag{5.4}$$

with $\gamma = \pi/100$. Using the tree-level relations of the MSSM Higgs sector in the limit of $\tan\beta > 1$ and small values of γ one has

$$M_A = M_Z \sqrt{\frac{\sin 2(\alpha+\beta)}{\sin 2(\alpha-\beta)}} \approx M_Z \sqrt{\frac{-\sin 4\beta}{2\gamma}} \,, \tag{5.5}$$

this corresponds to $M_A \sim 350$ GeV for $\tan\beta = 2$ and $M_A \sim 190$ GeV for $\tan\beta = 20$ (the exact value including loop corrections may vary, depending on the squark parameters which we do not specify here).

The bounds on $\Delta^{IJ}_{LL}, \Delta^{IJ}_{RR}, \Delta'^{IJ}_{LR}, \Delta'^{IJ}_{RL}$ from the leptonic Higgs boson decay would decouple only if also M_A is scaled up simultaneously with SUSY particle masses (thus assuring that the Higgs decay rates do not violate the Appelquist-Carrazone theorem [87]). This interesting feature is discussed in more details in Sec. 5.4.

5.2 Dependence on the mass splitting

The formulae derived in the previous Sections allow to analyse how the bounds on LFV mass insertions depend on the splitting between different SUSY masses. However, any process involving transition between the generations I and J depends in general, even at lowest order in the flavour violating MI's, on many mass parameters: μ, gaugino masses M_1, M_2, left and right diagonal slepton soft masses $m_{\tilde{e}_{LI}}, m_{\tilde{e}_{LJ}}, m_{\tilde{e}_{RI}}, m_{\tilde{e}_{RJ}}$, and for the Higgs decays also on M_A or on α angle. To simplify the discussion, we only take into account the bounds from $\ell \to \ell'\gamma$ decays, which are currently most constraining.

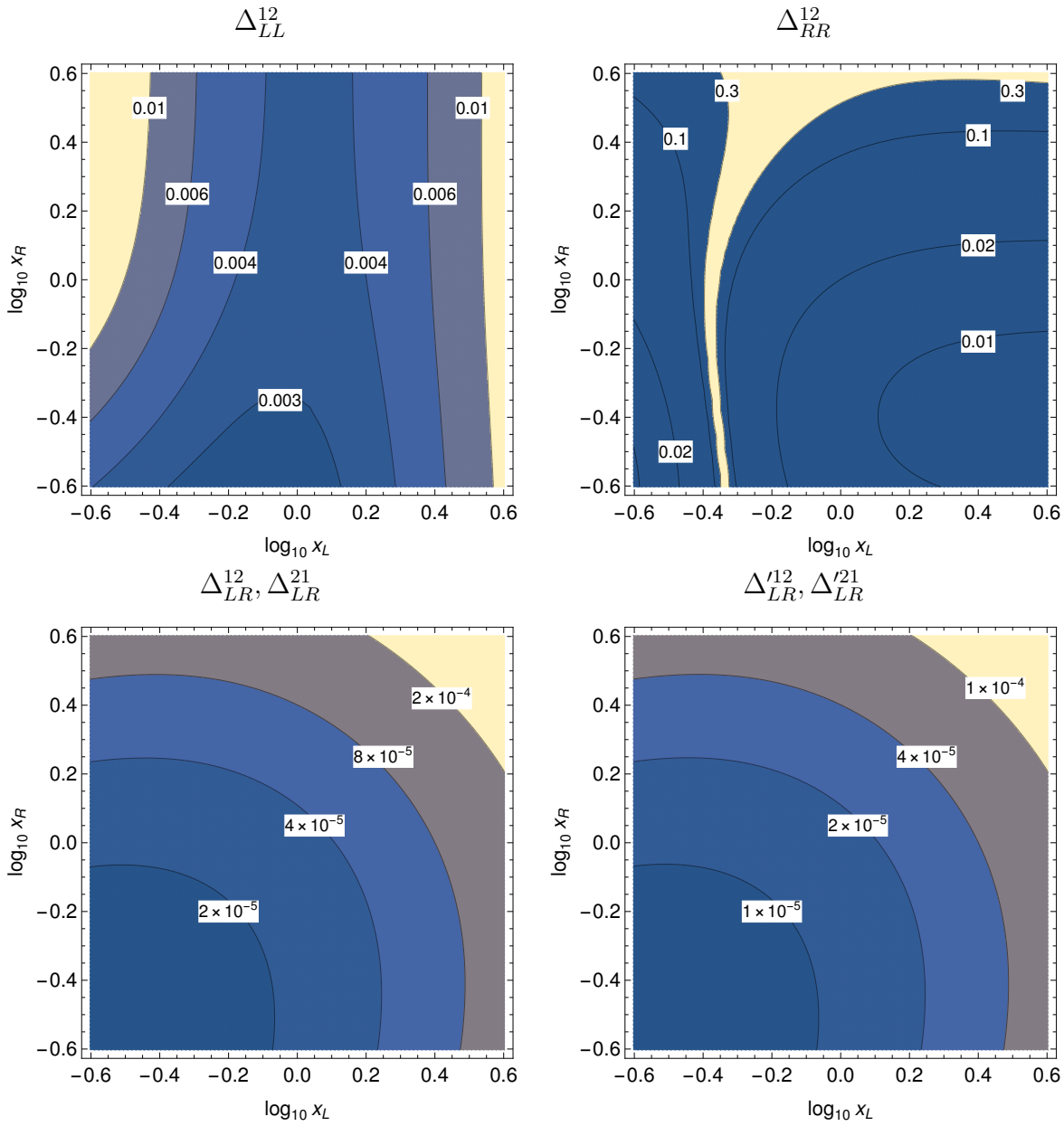

Figure 7: Upper bounds on the flavour violating parameters from $\mu \to e\gamma$ for $\tan\beta = 2$ and $M = 800$ GeV as a function of the splitting between the masses of gaugino and sleptons of different chiralities. The normalised slepton masses $x_{L(R)} = m_{L(R)}/M$ are plotted on the axes.

In Fig. 7 we illustrate the dependence of the upper bounds on the Δ parameters originating from $\mu \to e\gamma$ on the mass splitting between left and right-handed sleptons for

$$\begin{aligned} \tan\beta = 2\,, \qquad & \mu = M_1 = M_2 \equiv M = 800 \text{ GeV} \\ m_{\tilde{e}_L} = m_{\tilde{\mu}_L} = m_L\,, \qquad & m_{\tilde{e}_R} = m_{\tilde{\mu}_R} = m_R\,, \\ A_\ell^{ee} = A_\ell^{\prime ee} = Y_e\,\sqrt{m_L m_R}\,, \qquad & A_\ell^{\mu\mu} = A_\ell^{\prime \mu\mu} = Y_\mu\,\sqrt{m_L m_R}\,. \end{aligned}$$

We have chosen here an average SUSY mass scale of $M = 800$ GeV, higher than $M = 400$ GeV used in Tables 3-5, to avoid the experimental bounds on slepton masses even in the case of a large splitting between the left and right-handed masses.

The features of plots in Fig. 7 can be understood using the expanded expressions for effective photon couplings collected in Appendix E.1. As an example, let us consider the interesting cancellation between different contributions in the case of Δ^{12}_{RR} (right upper panel of Fig. 7). For our parameter setup, the coefficient $X^{e\mu}_{\gamma N2}$ multiplying the RR parameter (see Eq. (E.4)) can be reduced to the form

$$X^{e\mu}_{\gamma N2} = \frac{v_1 Y_\mu}{M^2}\, f(x_L, x_R)\,, \tag{5.6}$$

where $f(x_L, x_R)$ is a known, although complicated, dimensionless, rational and logarithmic function of mass ratios whose analytical form can be obtained using Eq. (E.4), the loop integrals collected in Appendix B and the definitions of divided differences from Appendix C. The properties of this function can be examined analytically and numerically. One finds

- For x_R in the wide range $0.1 - 4$ the function f vanishes for $x_L \sim 0.45$ (the exact value depends only weakly on x_R). As a result, the bounds on Δ^{12}_{RR} disappear completely for $m_L \sim 0.45M$.

- For large values of $x_R \gtrsim 5$ the position where the function f becomes zero shifts towards bigger values of x_L. In addition, in this limit f is suppressed by an overall factor $1/x_R$, thus the bounds on Δ^{12}_{RR} become weaker for a larger values of x_R.

- For large values of x_L the function f depends on x_R only. Therefore, the contour lines become horizontal.

- For small values of x_L the function f behaves like $1/x_L$. Thus, the bounds on Δ^{12}_{RR} become stronger.

A similar analysis can be done for the bounds on Δ^{12}_{LL}. However, the coefficient multiplying Δ^{12}_{LL} contains contributions from both chargino and neutralino loops and does not vanish for any mass pattern. Therefore, there is no cancellation area in the upper left panel of Fig. 7. In this case, the bound on Δ^{12}_{LL} is strongest for $m_L \sim M$ and $m_R \lesssim M$. For the case in which the left slepton masses are much lighter or much heavier than the masses of the SUSY fermion, the bounds become weaker.

Bounds on LR parameters, both holomorphic and non-holomorphic, are typically 1-2 orders of magnitude stronger than for LL and RR ones. In this case, the coefficient $X^{e\mu}_{\gamma N1}$ multiplying the LR terms has a much simpler functional form. Therefore, it never vanishes and in addition is explicitly symmetric (as follows from the properties of divided

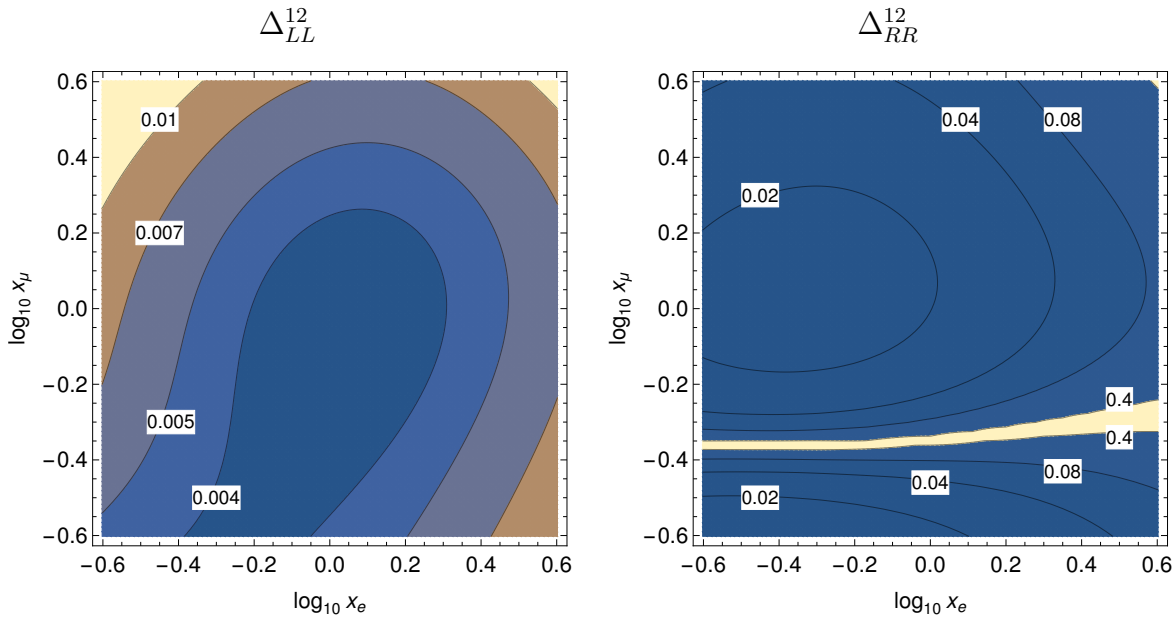

Figure 8: Upper bounds on the flavour violating LL and RR parameters using the current experimental limit on $\mathrm{Br}(\mu \to e\gamma)$ for $\tan\beta = 2$ and $M = 800$ GeV as a function of splitting between the masses of gaugino and sleptons of various flavours. The normalised selectron and smuon masses, $x_{e(\mu)} = m_{\tilde{e}(\tilde{\mu})}/M$ are plotted on the axes.

differences) under the exchange of slepton mass arguments, as visible in both lower panels of Fig. 7. Furthermore, one can see that bounds on LR parameters are strongest for $m_L, m_R \lesssim M$ and become weaker when the slepton masses are much heavier than the chargino and neutralino masses. More quantitatively, $X^{e\mu}_{\gamma N1}$ is proportional to the divided difference of the function C_{12}, which for $x \equiv x_L = x_R$ (corresponding to the diagonal of lower plots in Fig. 7) has the simple asymptotic behaviour

$$C_{12}(\{m_L, m_R\}, M) = \begin{cases} -\frac{5}{2M^2} & x \ll 1 \\ \frac{1}{2M^2 x^2} & x \gg 1 \end{cases} . \tag{5.7}$$

From the form of Eq. (5.7) it is immediately visible that the bounds become constant for small x and fall like $1/x^2$ for large x, as illustrated in the plots.

Using the formulae collected in Appendix E, a similar discussion can be, if necessary, performed to explain the features or cancellation areas of other plots presented in this Section. However, as the general analytical formulae in the MI approximation are rather complicated, we illustrate here other scenarios with numerical plots only.

Fig. 8 shows similar bounds assuming identical left-and right-handed slepton masses which however differ among the generations, so that we choose

$$\begin{aligned} \tan\beta = 2\,, \qquad & \mu = M_1 = M_2 \equiv M = 800 \text{ GeV}\,, \\ m_{\tilde{e}_L} = m_{\tilde{e}_R} = m_{\tilde{e}} \qquad & m_{\tilde{\mu}_L} = m_{\tilde{\mu}_R} = m_{\tilde{\mu}}\,, \\ A^{ee}_\ell = A'^{ee}_\ell = Y_e\, m_{\tilde{e}}\,, \qquad & A^{\mu\mu}_\ell = A'^{\mu\mu}_\ell = Y_\mu\, m_{\tilde{\mu}}\,, \end{aligned}$$

and plot the results in terms of $x_e = m_{\tilde{e}}/M$ and $x_\mu = m_{\tilde{\mu}}/M$. Again, a cancellation only exists for the bounds on Δ^{12}_{RR}, for an almost constant ratio $m_{\tilde{\mu}} \sim 2.5M$. In this case,

the bounds on Δ^{12}_{LL} are strongest for small splitting between slepton and SUSY fermion masses, while the bounds on Δ^{12}_{RR} are, apart from the cancellation region, stronger for $m_{\tilde{\mu}} \lesssim M$. It is obvious from the form of $X^{e\mu}_{\gamma N1}$ in Eq. (E.4) that the bounds on the LR parameters, both holomorphic and non-holomorphic, have an identical behaviour as in the case of the $m_L - m_R$ splitting plotted in Fig. 7, with the replacements $x_L \leftrightarrow x_e$, $x_R \leftrightarrow x_\mu$.

Finally in Fig. 9 we assume an identical mass of $m = 400$ GeV for all sleptons but vary $M_1 = M_2$ and μ. The results are displayed as a function of $x_2 = M_2/M$, $x_\mu = \mu/M$ (we do not plot small values of $|\mu| < 100$ GeV which are excluded by the direct searches for charginos and neutralinos). The structure of cancellation areas is more complicated, but again the "blind spots", where the bounds on MI's disappear, exist only for Δ^{12}_{RR}. As expected from the form of $X^{e\mu}_{\gamma N1}$ in Eq. (E.4), the bounds on Δ^{12}_{LR}, Δ'^{12}_{LR} are at leading order independent of the μ parameter. They are also correlated with the bounds displayed in lower plots of Fig. 7, as for a fixed slepton mass and varied M_2 the coefficient $X^{e\mu}_{\gamma N1}$ is now proportional to

$$C_{12}(\{m,m\},M_2) = \begin{cases} \frac{1}{2m^2} & x \ll 1 \\ -\frac{5}{2m^2 x_2^2} & x \gg 1 \end{cases} \tag{5.8}$$

so that again the bounds saturate for small x_2 and fall like $1/x_2^2$ in the opposite limit.

Similar plots constraining 13 and 23 mass insertions have almost identical shape; the bounds are just rescaled by constant factors. The bounds on Δ^{13}_{LL} and Δ^{13}_{RR} (Δ^{23}_{LL} and Δ^{23}_{RR}) are approximately 550 (650) times weaker than the bounds on Δ^{12}_{LL} and Δ^{12}_{RR}, respectively. The bounds on $\Delta^{13(31)}_{LR}$ and $\Delta'^{13(31)}_{LR}$ ($\Delta^{23(32)}_{LR}$ and $\Delta'^{23(32)}_{LR}$) are respectively 9000 (11000) times weaker than the bounds on $\Delta^{12(21)}_{LR}$ and $\Delta'^{12(21)}_{LR}$.

5.3 Correlations between LFV processes

The correlations between various leptonic decays, in particular radiative and 3-body charged lepton decays, are important for designing new experiments searching for the LFV phenomena. In the photon penguin domination scenario the ratio of decay rates for both processes is given by the simple formula:

$$\frac{\mathrm{Br}(\ell \to 3\ell')}{\mathrm{Br}(\ell \to \ell'\gamma)} \approx \frac{\alpha_{em}}{3\pi}\left(\log\frac{m_\ell^2}{m_{\ell'}^2} - \frac{11}{4}\right). \tag{5.9}$$

In this case the decision which measurement is more promising depends purely on experimental accuracy achievable for each of them. However, other type of contributions, like Z-penguin and box diagrams, can modify the ratio (5.9). Such contributions may be particularly important for a "blind spot" scenario, like the weakened limit on Δ_{RR} for some ratios of slepton and gaugino masses.

In Fig. 10 we plot the quantity $R_{\ell\ell'}$ defined as

$$R_{\ell\ell'} = \frac{\alpha_{em}}{3\pi}\left(\log\frac{m_\ell^2}{m_{\ell'}^2} - \frac{11}{4}\right)\frac{\mathrm{Br}(\ell \to \ell'\gamma)}{\mathrm{Br}(\ell \to 3\ell')}, \tag{5.10}$$

as a function of the SUSY mass splittings, in the same scenarios as described in Fig. 7 and Fig. 8. We assume non-vanishing Δ^{12}_{LL} and Δ^{12}_{RR} terms. For LR terms, both holomorphic

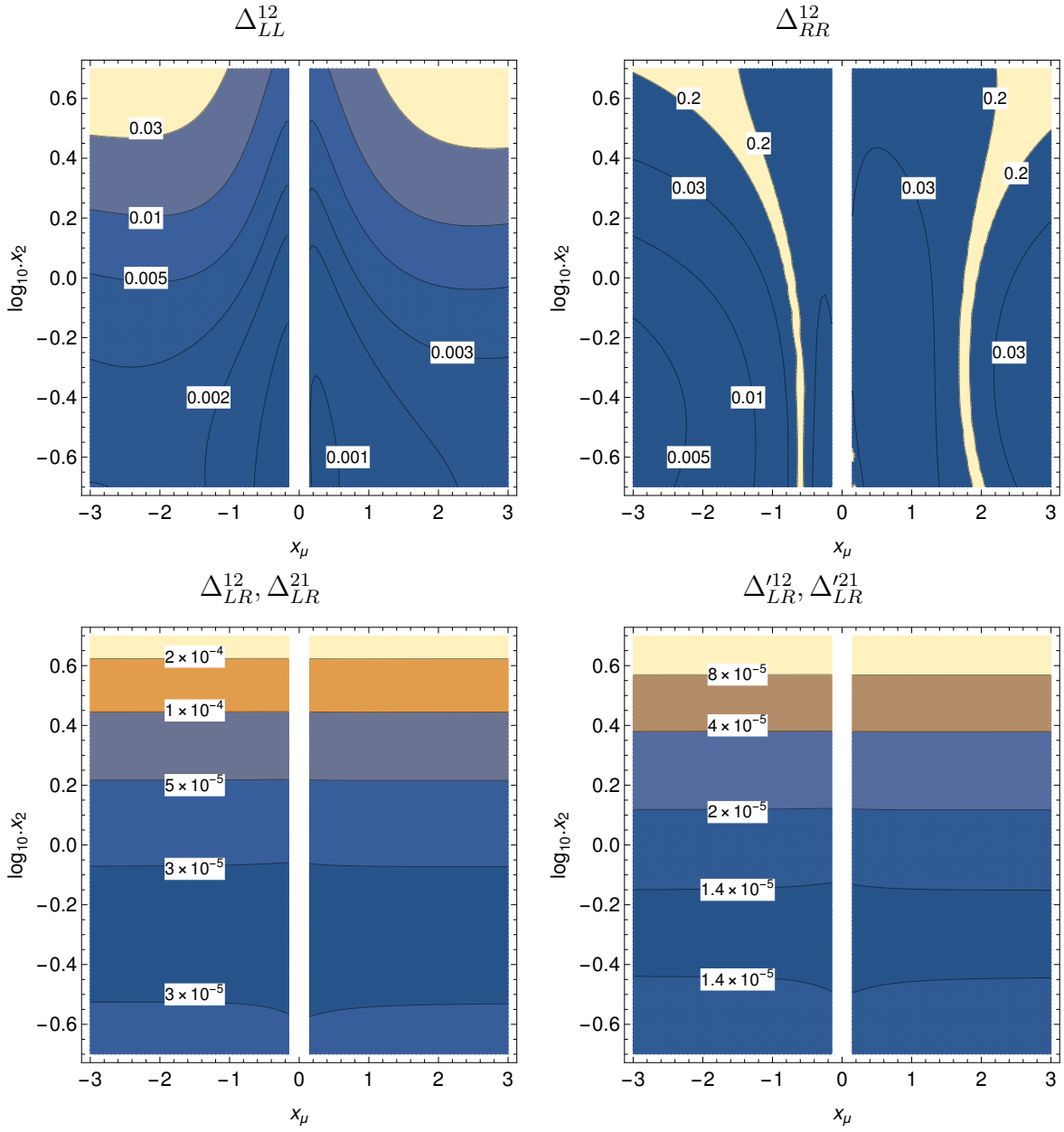

Figure 9: Upper bounds on the LFV parameters using the current experimental limit on the $\mathrm{Br}(\mu \to e\gamma)$ for degenerate slepton masses $M = 800$ GeV as a function of mass splitting between the gaugino and the μ related parameters, $x_\mu = \mu/M$, $x_2 = M_1/M = M_2/M$.

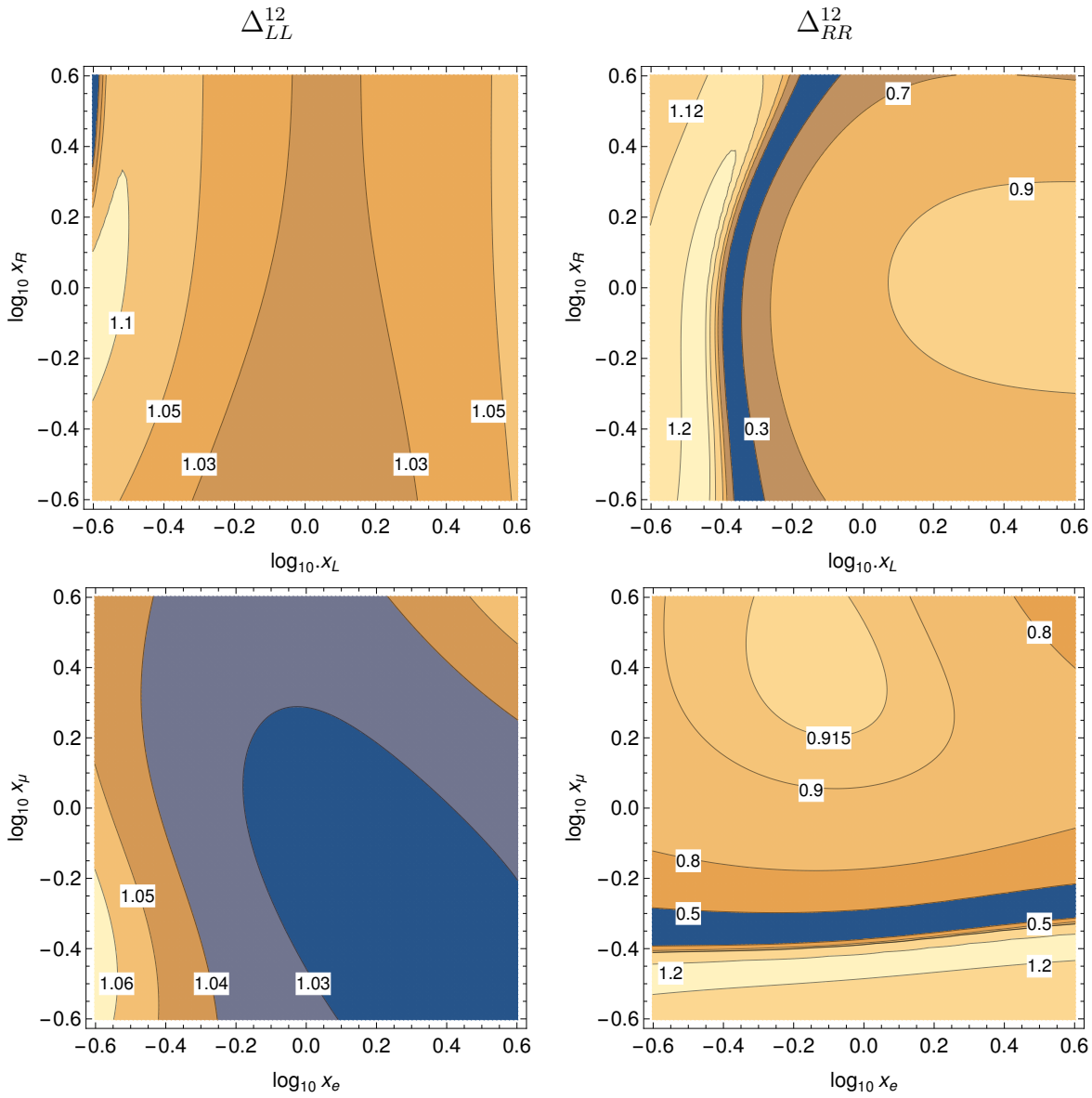

Figure 10: The ratio $R_{\ell\ell'}$ as a function of the mass splitting between left and right slepton masses (upper row) and between the selectron and smuon masses (lower row) for $M = 800$ GeV as a function of the normalised slepton masses $x_{L(R)} = m_{L(R)}/M$ and $x_{\tilde{e}(\tilde{\mu})} = m_{\tilde{e}(\tilde{\mu})}/M$.

and non-holomorphic, a photon penguin dominated scenario is always realised and $R_{\ell\ell'}$ is very close to 1.

As one can see from Fig. 10, radiative and 3-body decays are almost always closely correlated, with $R_{\ell\ell'}$ differing from 1 by a few % at most. Exceptions are only possible for parameter combinations for which $\mathrm{Br}(\ell \to \ell'\gamma)$ becomes small due to cancellations or some other type of suppression, like in scenarios with large mass splitting (compare Figs. 7 and 8). Simultaneously, $\mathrm{Br}(\ell \to 3\ell')$ is given by the more complicated expression (3.11), which in the limit of small photon penguin contribution becomes the sum of positive terms and cannot vanish. Thus, although both decays are usually strongly correlated and only

relative experimental sensitivities decide which of them has better chances to discover generic LFV effects mediated by the slepton sector, for some particular ranges of MSSM parameter searches for 3-body charged lepton decays are a safer choice, allowing to avoid blind spots appearing for such setups due to the suppression of $\ell \to \ell'\gamma$ decay rates.

5.4 Non-decoupling effects in LFV Higgs decays

LFV Higgs decays in the SM are absent at the tree level and strongly suppressed also at the loop level. Examining LFV Higgs boson decays within the MSSM is very interesting because, contrary to the other processes discussed in this paper, some contributions to the Higgs decay amplitudes proportional to the lepton Yukawa couplings or to the non-holomorphic trilinear slepton soft terms do not decouple in the limit of heavy SUSY masses and can be potentially large.

As can be seen from Tables 5, for an average SUSY mass scale of $M = 400$ GeV and the parameter setup of Eq. (5.3) the upper bounds on the flavour violating parameters from Higgs decays are much weaker than from the other processes. However, the bounds from Higgs decays on the Δ_{LL}^{IJ}, Δ_{RR}^{IJ} and on the non-holomorphic LR terms $\Delta_{LR}^{\prime IJ}$ do not scale like $1/M^2$. Thus, comparing the limits on $\Delta_{LR}^{\prime 13}$ and $\Delta_{LR}^{\prime 23}$ entries from $h \to \ell\ell'$ and $\ell \to \ell'\gamma$ decays one can check that e.g. for $\tan\beta = 20$ and

$$M_{SUSY} \gtrsim \frac{1.5}{\sqrt{|\cos(\alpha-\beta)|}}\ \text{TeV}\,, \tag{5.11}$$

the latter are becoming weaker. For $\Delta_{LR}^{\prime 12}$ the same occurs at much higher scale

$$M_{SUSY} \gtrsim \frac{220}{\sqrt{|\cos(\alpha-\beta)|}}\ \text{TeV}\,. \tag{5.12}$$

The bounds on Δ_{LL}^{IJ}, Δ_{RR}^{IJ} are obtained assuming that the flavour diagonal A_l' terms vanish, so that all non-decoupling LL and RR contributions are proportional to the Yukawa couplings (see Eq. (E.24)). In this case the Higgs decays become most constraining for slightly higher SUSY scales, again for $\tan\beta = 20$ and α angle of Eq. (5.4) bounds on Δ_{LL}^{IJ} and Δ_{RR}^{IJ} from Higgs decays become stronger than the bounds from $\ell \to \ell'\gamma$ decays for $M_{SUSY} \gtrsim 2/\sqrt{|\cos(\alpha-\beta)|}$ TeV for $\tau\mu$ transitions, $M_{SUSY} \gtrsim 3/\sqrt{|\cos(\alpha-\beta)|}$ TeV for τe transitions and $M_{SUSY} \gtrsim 200/\sqrt{|\cos(\alpha-\beta)|}$ TeV for μe transitions.

The Higgs decays in supersymmetric extensions of the SM have been already studied e.g. in [88–94]. In this Section we analyse within the general MSSM the decays of the lighter CP-even Higgs boson h. The mass eigenstates formulae for the MSSM contributions to the effective leptonic Yukawa couplings of h are given in Eqs. (2.14 – 2.16) while the relevant MI expressions are collected in Appendix E.3. The potentially largest contributions to $h \to \ell\ell'$ decays come from the effects non decoupling in the limit of large SUSY masses and proportional to non-holomorphic trilinear terms (see Eq. (E.23)). Assuming that flavour violating $A_l^{\prime IJ}$ terms are the only source of LFV and using Eqs. (3.4), (E.23) and (A.8), one can write

$$\begin{aligned} Br(h \to \ell^I \bar{\ell}^J) \;&\approx\; \frac{e^4 M_h}{8192\pi^5 c_W^4 \Gamma_h} \frac{\cos^2(\alpha-\beta)}{\cos^2\beta} \left(g(x_{\tilde{e}_{LI}}, x_{\tilde{e}_{RJ}})^2 \left|\Delta_{LR}^{\prime IJ}\right|^2 \right. \\ &+\; \left. g(x_{\tilde{e}_{LJ}}, x_{\tilde{e}_{RI}})^2 \left|\Delta_{LR}^{\prime JI}\right|^2 \right)\,, \end{aligned} \tag{5.13}$$

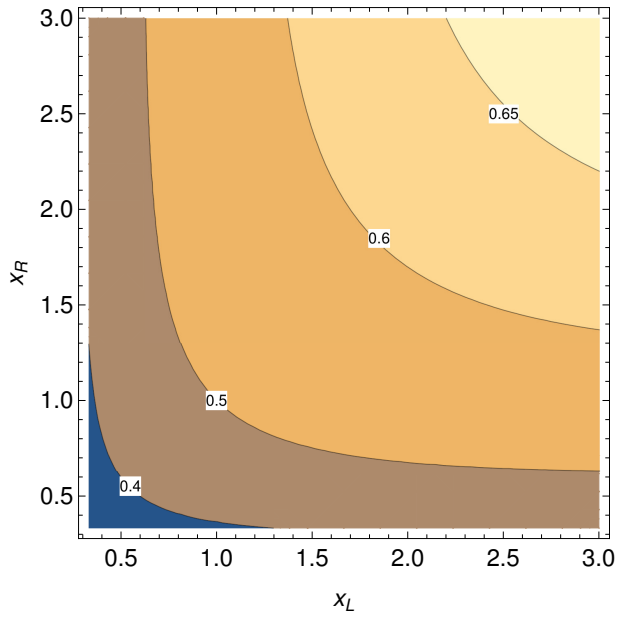

Figure 11: Dependence of function $g(x_L, x_R)$ of Eq. (5.15) on the splitting between the slepton and bino masses.

where α, β are the mixing angles in the Higgs sector (see Appendix A), the dimensionless mass ratios are

$$x_{\tilde{e}_{L(R)I}} = \frac{m_{\tilde{e}_{L(R)I}}}{|M_1|}\,, \tag{5.14}$$

and we defined

$$g(x,y) = -\sqrt{xy}\, C_0(x,y,1)\,. \tag{5.15}$$

As can be seen from of Fig. 11, for reasonable mass splittings $g(x,y) \sim \mathcal{O}(1)$ and, inserting the numerical values of known quantities, one has

$$Br(h \to \ell^I \bar{\ell}^J) \sim 2 \cdot 10^{-4}\, \frac{\cos^2(\alpha-\beta)}{\cos^2\beta} \left|\Delta_{LR}^{\prime IJ(JI)}\right|^2 . \tag{5.16}$$

Even if for large SUSY mass scale $\Delta_{LR}^{\prime IJ}$ insertions are not constrained experimentally by other LFV measurements, $Br(h \to \ell^I \bar{\ell}^J)$ cannot be arbitrarily large in the MSSM because $\Delta_{LR}^{\prime IJ}$ are constrained to $\mathcal{O}(1)$ by the vacuum stability conditions and the requirement of the absence of charge and colour breaking (CCB) minima of the scalar potential (see e.g. discussion in [95]).

The Higgs mixing angle α is subject to strong radiative corrections from the squark sector and thus from the point of view of pure leptonic sector can be treated as a free parameter. However, the allowed values of the Higgs mixing angles α, β are limited by the existing experimental constraints (see e.g. Fig. 6 in Appendix B of ref. [92]), thus also the overall prefactor $\frac{\cos^2(\alpha-\beta)}{\cos^2\beta}$ in Eq. (5.16) can be at most $\mathcal{O}(1)$. Summarising, the maximal $Br(h \to \ell^I \bar{\ell}^J)$ which can be generated with the non-holomorphic trilinear terms

is $\mathcal{O}(10^{-4})$, not much below the current experimental sensitivities collected in Table 2 (including of decoupling contributions does not change this conclusion even for a light SUSY spectrum [91, 92]). Further searches may therefore find the effects of non-holomorphic trilinear terms or provide stricter bounds on them.

Similar analysis could be done for non-decoupling contributions proportional to Δ_{LL}^{IJ} and Δ_{RR}^{IJ} parameters. However, in this case non-decoupling terms are proportional also either to the diagonal A_l' soft terms or to lepton Yukawa couplings, so the formulae become complicated and a more involved numerical analysis is required. Terms proportional to Δ_{LL}^{IJ} and Δ_{RR}^{IJ} multiplied by diagonal A_l' terms can generate similar LFV Higgs decay rates as the flavour off-diagonal non-holomorphic A_l'-terms. However, assuming that all non-holomorphic terms vanish, and including only the Yukawa suppressed contributions one has a much stricter bound $Br(h \to \ell^I \bar{\ell}^J) \lesssim 10^{-4}(Y_l^I)^2$ in the MSSM.

For a complete phenomenological analysis of LFV Higgs decays in the MSSM one would need to go beyond the one-loop analysis of this article. First, one would need to perform the matching of the MSSM on the 2HDM with generic Yukawa couplings including the resummation of the higher order chirally enhanced effects (see for example [44–46]). Then, one has to calculate the loop effects for flavour observables within this generic 2HDM [96].

6 Conclusions

New precision data in the lepton flavour sector are expected to come in the foreseeable future. In the search for beyond the SM effects, they will require precision and efficient calculations in various BSM models. In this article lepton flavour violating processes within MSSM have been calculated using the Flavour Expansion Theorem, a recently developed new technique of a purely algebraic mass-insertion expansion of the amplitudes [29]. Both flavour-violating off-diagonal terms and flavour-conserving mass-insertions are considered. The expansion in the flavour conserving off-diagonal mass terms leads to a transparent qualitative understanding of the coefficients in front of the flavour violating mass insertions (see Eq. (4.2)) in various decoupling limits. Most flavour violating one-loop amplitudes decouple as v^2/M^2 where M is one of the soft SUSY breaking mass parameters. The exception are the Higgs flavour violating decays where the amplitudes decouple as v^2/M_A^2. We find that our full MI approximation, both in flavour violating and flavour conserving off-diagonal mass terms is an excellent approximation to the calculations in the mass eigenstates basis for a very broad pattern of supersymmetric spectra, in particular for highly non-degenerate spectra. This is useful because in the MI approximation we work directly with the Lagrangian parameters and can constrain them with experimental limits.

On the physics side, the considered processes are: $\ell \to \ell'\gamma$, $\ell \to 3\ell'$, $\ell \to 2\ell'\ell''$, $h \to \ell\ell'$ as well as $\mu \to e$ conversion in nuclei. The bounds on the flavour changing parameters of the MSSM have been updated and their sensitivity to the forthcoming experimental results in different channels has been discussed. We have emphasised that, given the foreseen experimental progress, precision measurements of different processes have very different potential for the discovery of supersymmetric effects. The radiative and leptonic muon decays are likely to remain the most important source of information on supersymmetric LFV. The leptonic decays play a complementary role to the radiative ones in eliminating some "blind spots" of weakly constrained by the latter LFV mass insertions. This is

illustrated in Sections 5.2 and 5.3. Our complete analytical MI expansion facilitates the investigation of the LFV processes when the SUSY spectra are non-degenerate and finding such "blind spots" with suppressed branching ratios and regions of correlations between various processes. This is illustrated in Sections 5.2 and 5.3. The LFV Higgs decays are discussed in some detail. For the supersymmetric spectrum of order of 1 TeV, the current experimental limits on the LFV Higgs decays give several orders of magnitude weaker bounds on lepton violating MI than the radiative lepton decays. However, for the superpartner masses of several TeV Higgs decays provide stronger bounds than the latter because the bounds from Higgs decays do not scale with superpartner masses. We have also analysed the role of the so-called non-holomorphic A-terms in the flavour-violating Higgs boson decays, which can give branching ratios not much below the present experimental sensitivity.

Acknowledgements

ZF, WM, SP and JR are supported in part by the National Science Centre, Poland, under research grants DEC-2015/19/B/ST2/02848, DEC-2015/18/M/ST2/00054 and DEC-2014/15/B/ST2/02157. U.N. is supported by BMBF under grant no. 05H15VKKB1. The work of A.C. is supported by an Ambizione Grant of the Swiss National Science Foundation (PZ00P2_154834). JR would also like to thank CERN for hospitality during his visits there.

A MSSM Lagrangian and vertices

Throughout this article we use the notation of Refs. [33,34] which is very similar to SLHA2 conventions [35], up to minor differences listed in Table 6.

For completeness, we collect here the definitions of the mass and mixing matrices for the supersymmetric particles and the relevant MSSM Feynman rules. The slepton and sneutrino mass and mixing matrices are defined as:

$$Z_\nu^\dagger \left(M_{LL}^2 + \frac{M_Z^2 \cos 2\beta}{2} \hat{1} \right) Z_\nu \;=\; \mathrm{diag}\left(m_{\nu_1}^2 \dots m_{\nu_3}^2 \right) , \tag{A.1}$$

$$Z_L^\dagger \begin{pmatrix} (\mathcal{M}_L^2)_{LL} & (\mathcal{M}_L^2)_{LR} \\ (\mathcal{M}_L^2)_{LR}^\dagger & (\mathcal{M}_L^2)_{RR} \end{pmatrix} Z_L = \mathrm{diag}\left(m_{L_1}^2 \dots m_{L_6}^2 \right) , \tag{A.2}$$

$$\left(\mathcal{M}_L^2\right)_{LL} \;=\; (M_{LL}^2)^T + \frac{M_Z^2 \cos 2\beta}{2}(1 - 2c_W^2)\hat{1} + \frac{v_1^2 Y_l^2}{2} , \tag{A.3}$$

$$\left(\mathcal{M}_L^2\right)_{RR} \;=\; M_{RR}^2 - \frac{M_Z^2 \cos 2\beta}{2} s_W^2 \hat{1} + \frac{v_1^2 Y_l^2}{2} , \tag{A.4}$$

$$\left(\mathcal{M}_L^2\right)_{LR} \;=\; \frac{1}{\sqrt{2}} \left(v_2 (Y_l \mu^\star - A_l^{'}) + v_1 A_l \right) , \tag{A.5}$$

where, as usual, we use $\tan\beta = v_2/v_1$ and M_{LL}^2, M_{RR}^2, A_l, $A_l^{'}$, $Y_l = -\sqrt{2} m_l / v_1$ are 3×3 matrices in flavour space.

The neutralino and chargino mass and mixing matrices can be written down as:

$$Z_N^T \begin{pmatrix} M_1 & 0 & -\frac{e v_1}{2 c_W} & \frac{e v_2}{2 c_W} \\ 0 & M_2 & \frac{e v_1}{2 s_W} & -\frac{e v_2}{2 s_W} \\ -\frac{e v_1}{2 c_W} & \frac{e v_1}{2 s_W} & 0 & -\mu \\ \frac{e v_2}{2 c_W} & -\frac{e v_2}{2 s_W} & -\mu & 0 \end{pmatrix} Z_N \;=\; \mathrm{diag}\left(m_{\chi_1^0} \dots m_{\chi_4^0} \right) , \tag{A.6}$$

$$(Z_-)^T \begin{pmatrix} M_2 & \frac{e v_2}{\sqrt{2} s_W} \\ \frac{e v_1}{\sqrt{2} s_W} & \mu \end{pmatrix} Z_+ = \mathrm{diag}\left(m_{\chi_1}, m_{\chi_2} \right) . \tag{A.7}$$

We also use the following abbreviation for the matrix Z_R parametrizing the mixing in the CP-even Higgs sector:

$$Z_R = \begin{pmatrix} \cos\alpha & -\sin\alpha \\ \sin\alpha & \cos\alpha \end{pmatrix} . \tag{A.8}$$

Below we list the vertices used in calculations of the LFV processes expressed in terms of the mixing matrices defined above.

SLHA2 [35]	Ref. [33, 34]
$\hat{T}_U$, $\hat{T}_D$, $\hat{T}_E$	$-A_u^T$, $+A_d^T$, $+A_l^T$
$\hat{m}^2_{\tilde{Q}}$, $\hat{m}^2_{\tilde{L}}$	m_Q^2, m_L^2
$\hat{m}^2_{\tilde{u}}$, $\hat{m}^2_{\tilde{d}}$, $\hat{m}^2_{\tilde{l}}$	$(m_U^2)^T$, $(m_D^2)^T$, $(m_E^2)^T$
$\mathcal{M}^2_{\tilde{u}}$, $\mathcal{M}^2_{\tilde{d}}$	$(\mathcal{M}_U^2)^T$, $(\mathcal{M}_D^2)^T$

Table 6: Comparison of SLHA2 [35] and ref. [33, 34] conventions.

1) Lepton-slepton-neutralino and lepton-sneutrino-chargino vertices (for an *incoming* charged lepton of flavour I):

$$\begin{aligned}
V^{Iij}_{\ell\tilde{L}N,L} &= \frac{e}{\sqrt{2}s_W c_W} Z_L^{Ii}(Z_N^{1j}s_W + Z_N^{2j}c_W) + Y_l^I Z_L^{(I+3)i} Z_N^{3j}\,, \\
V^{Iij}_{\ell\tilde{L}N,R} &= \frac{-e\sqrt{2}}{c_W} Z_L^{(I+3)i} Z_N^{1j\star} + Y_l^I Z_L^{Ii} Z_N^{3j\star}\,, \\
V^{IKj}_{\ell\tilde{\nu}C,L} &= -\frac{e}{s_W} Z_+^{1j}\,, Z_\nu^{IK\star} \\
V^{IKj}_{\ell\tilde{\nu}C,R} &= -Y_l^I Z_-^{2j\star} Z_\nu^{IK\star}\,.
\end{aligned} \tag{A.9}$$

2) Z-chargino and Z-neutralino vertices:

$$\begin{aligned}
V^{ij}_{CCZ,L} &= -\frac{e}{2s_W c_W}\left(Z_+^{1i*}Z_+^{1j} + \delta^{ij}(c_W^2 - s_W^2)\right)\,, \\
V^{ij}_{CCZ,R} &= -\frac{e}{2s_W c_W}\left(Z_-^{1i}Z_-^{1j*} + \delta^{ij}(c_W^2 - s_W^2)\right)\,, \\
V^{ij}_{NNZ,L} &= -V^{ji}_{NNZ,R} = \frac{e}{2s_W c_W}\left(Z_N^{4i*}Z_N^{4j} - Z_N^{3i*}Z_N^{3j}\right)\,.
\end{aligned} \tag{A.10}$$

3) CP-even-Higgs-slepton and CP-even-Higgs-sneutrino vertices:

$$\begin{aligned}
V^{Kil}_{HLL} &= \sum_{C=1}^{3}\Bigg(\frac{e^2}{2c_W^2}\left(v_1 Z_R^{1K} - v_2 Z_R^{2K}\right)\left(\delta^{il} + \frac{1-4s_W^2}{2s_W^2} Z_L^{Ci\star} Z_L^{Cl}\right) \\
&- (Y_l^C)^2 v_1 Z_R^{1K}(Z_L^{Ci\star}Z_L^{Cl} + Z_L^{(C+3)i\star}Z_L^{(C+3)l}) \\
&- \frac{Z_R^{2K}}{\sqrt{2}}(Y_l^{C*}\mu^* Z_L^{Ci\star}Z_L^{(C+3)l} + Y_l^C \mu Z_L^{Cl} Z_L^{(C+3)i\star})\Bigg) \\
&- \frac{1}{\sqrt{2}}\sum_{C,D=1}^{3}\Big(Z_R^{1K}(A_l^{CD\star} Z_L^{Cl} Z_L^{(D+3)i\star} + A_l^{CD} Z_L^{Ci\star} Z_L^{(D+3)l}) \\
&- Z_R^{2K}(A_l'^{CD\star} Z_L^{Cl} Z_L^{(D+3)i\star} + A_l'^{CD} Z_L^{Ci\star} Z_L^{(D+3)l})\Big)\,, \\
V^{KLI}_{H\tilde{\nu}\tilde{\nu}} &= -\frac{e^2}{4s_W^2 c_W^2}(v_1 Z_R^{1K} - v_2 Z_R^{2K})\delta_{LI}\,.
\end{aligned} \tag{A.11}$$

4) CP-odd-Higgs-slepton and CP-odd-Higgs-sneutrino vertices:

$$\begin{aligned} V_{ALL}^{1il} &= \frac{i\cos\beta}{\sqrt{2}} \sum_{C,D=1}^{3} \Big((A_l^{CD*}\tan\beta + A_l^{\prime CD*} - Y_l^C \mu \delta^{CD}) Z_L^{Cj} Z_L^{(D+3)i\star} \\ &- (A_l^{CD}\tan\beta + A_l^{\prime CD} - Y_l^C \mu^* \delta^{CD}) Z_L^{Ci\star} Z_L^{(D+3)j} \Big) , \\ V_{A\tilde{\nu}\tilde{\nu}}^{1LI} &= 0 . \end{aligned} \tag{A.12}$$

5) CP-even-Higgs-neutralino and CP-even-Higgs-chargino vertices:

$$\begin{aligned} V_{NHN,L}^{iKl} &= V_{NHN,R}^{iKl\,*} = \frac{e}{2 s_W c_W} \big((Z_R^{1K} Z_N^{3l} - Z_R^{2K} Z_N^{4l})(Z_N^{1i} s_W - Z_N^{2i} c_W) \\ &+ (Z_R^{1K} Z_N^{3i} - Z_R^{2K} Z_N^{4i})(Z_N^{1l} s_W - Z_N^{2l} c_W) \big) , \\ V_{CHC,L}^{iKl} &= V_{CHC,R}^{iKl\,*} = -\frac{e}{\sqrt{2} s_W} \left(Z_R^{1K} Z_-^{2i} Z_+^{1l} + Z_R^{2K} Z_-^{1i} Z_+^{2l} \right) . \end{aligned} \tag{A.13}$$

6) CP-odd-Higgs-neutralino and CP-odd-Higgs-chargino vertices:

$$\begin{aligned} V_{NAN,L}^{i1l} &= V_{NAN,R}^{i1l\,*} = \frac{-ie^2}{4 s_W^2 c_W^2 M_Z} \big((v_2 Z_N^{3j} - v_1 Z_N^{4j})(Z_N^{1i} s_W - Z_N^{2i} c_W) \\ &+ (v_2 Z_N^{3i} - v_1 Z_N^{4i})(Z_N^{1j} s_W - Z_N^{2j} c_W) \big) , \\ V_{CAC,L}^{i1l} &= V_{CAC,R}^{i1l\,*} = \frac{ie^2}{2\sqrt{2} s_W^2 M_W} (v_2 Z_-^{2i} Z_+^{1j} + v_1 Z_-^{1i} Z_+^{2j}) . \end{aligned} \tag{A.14}$$

7) Z-slepton vertex:

$$V_{LLZ}^{ij} = \frac{e}{2 s_W c_W} \left(Z_L^{ki*} Z_L^{kj} - 2 s_W^2 \delta^{ij} \right) . \tag{A.15}$$

B Loop integrals

We define the following loop integrals for 2-point and 3-point functions with non-vanishing external momenta p and q:

$$\begin{aligned} \frac{i}{(4\pi)^2} B_0(p, m_1, m_2) &= \int \frac{d^4k}{(2\pi)^4} \frac{1}{(k^2 - m_1^2)((k-p)^2 - m_2^2)} , \\ \frac{i}{(4\pi)^2} p_\mu B_1(p, m_1, m_2) &= \int \frac{d^4k}{(2\pi)^4} \frac{k_\mu}{(k^2 - m_1^2)((k-p)^2 - m_2^2)} , \\ \frac{i}{(4\pi)^2} C_{2n}(p, q, m_1, m_2, m_3) &= \int \frac{d^4k}{(2\pi)^4} \frac{(k^2)^n}{(k^2 - m_1^2)((k+p)^2 - m_2^2)((k+p+q)^2 - m_3^2)} , \\ \frac{i}{(4\pi)^2} \left(p_\mu C_{11}(p, q, m_1, m_2, m_3) \right. &+ \left. q_\mu C_{12}(p, q, m_1, m_2, m_3) \right) \\ &= \int \frac{d^4k}{(2\pi)^4} \frac{k_\mu}{(k^2 - m_1^2)((k+p)^2 - m_2^2)((k+p+q)^2 - m_3^2)} . \end{aligned} \tag{B.1}$$

In our expanded results we need only the integrals above, their derivatives and higher point 1-loop integrals calculated at vanishing external momenta. Let us define

$$\frac{i}{(4\pi)^2} L_i^{2n}(m_1,\ldots,m_i) \;=\; \int \frac{d^4k}{(2\pi)^4} \frac{(k^2)^n}{\prod\limits_{j=1}^{i}(k^2-m_j^2)}\,. \tag{B.2}$$

In common notation $L_3^{2n} = C_{2n}, L_4^{2n} = D_{2n}, L_5^{2n} = E_{2n}$ etc.

For $i \geq 3$ one has:

$$\begin{aligned} L_i^0(m_1,\ldots,m_i) &= -\sum_{j=2}^{i} \frac{m_j^2 \log\frac{m_j^2}{m_1^2}}{\prod\limits_{k=1,k\neq j}^{i}(m_j^2-m_k^2)}\,, \\ L_i^2(m_1,\ldots,m_i) &= \sum_{j=2}^{i} \frac{m_j^4 \log\frac{m_j^2}{m_1^2}}{\prod\limits_{k=1,k\neq j}^{i}(m_j^2-m_k^2)}\,, \end{aligned} \tag{B.3}$$

(with the exception of $L_3^2 \equiv C_2$ having also an infinite part, which however is always cancelled out in flavour violating processes and is thus not given here explicitly).

To simplify our formulae, we use the relation

$$\begin{aligned} 2L_i^0(m_1,m_2,\ldots,m_i) &= L_{i+1}^2(m_1,m_1,m_2,\ldots,m_i) + L_{i+1}^2(m_1,m_2,m_2,\ldots,m_i) \\ &+ \ldots + L_{i+1}^2(m_1,\ldots,m_{i-1},m_i,m_i)\,, \end{aligned} \tag{B.4}$$

which can be obtained by differentiating with respect to λ the integral form of the homogeneity property

$$L_i^0(\lambda m_1,\ldots,\lambda m_i) \;=\; \lambda^{4-2i} L_i^0(m_1,\ldots,m_i)\,, \tag{B.5}$$

and using the relation ($k = 1,\ldots,i$)

$$\begin{aligned} m_k^2 L_{i+1}^0(m_1,\ldots,m_k,m_k,\ldots,m_i) &= L_{i+1}^2(m_1,\ldots,m_k,m_k,\ldots,m_i) \\ &- L_i^0(m_1,\ldots,m_k,\ldots,m_i)\,. \end{aligned} \tag{B.6}$$

In addition, we define the following integrals:

$$\begin{aligned} C_0'(m_1,m_2,m_3) &= \left.\frac{\partial C_0(p,q,m_1,m_2,m_3)}{\partial q^2}\right|_{p=q=0} \\ &= \frac{2m_2^2m_3^2 - m_1^2(m_2^2+m_3^2)}{2(m_1^2-m_2^2)(m_1^2-m_3^2)(m_2^2-m_3^2)^2} \\ &+ \frac{m_1^4 \log\frac{m_1^2}{m_2^2}}{2(m_1^2-m_2^2)^2(m_1^2-m_3^2)^2} + \frac{m_3^2(m_3^4-2m_1^2m_2^2+m_2^2m_3^2)\log\frac{m_3^2}{m_2^2}}{2(m_1^2-m_3^2)^2(m_2^2-m_3^2)^3}\,, \end{aligned} \tag{B.7}$$

$$C_{11}(m_1,m_2) = -\frac{m_1^2-3m_2^2}{4(m_1^2-m_2^2)^2}+\frac{m_2^4}{2(m_1^2-m_2^2)^3}\log\frac{m_2^2}{m_1^2}\,, \tag{B.8}$$

$$C_{12}(m_1,m_2) = -\frac{m_1^2+m_2^2}{2(m_1^2-m_2^2)^2}-\frac{m_1^2m_2^2}{(m_1^2-m_2^2)^3}\log\frac{m_2^2}{m_1^2}\,, \tag{B.9}$$

$$C_{23}(m_1,m_2) = -\frac{m_1^4-5m_1^2m_2^2-2m_2^4}{12(m_1^2-m_2^2)^3}+\frac{m_1^2m_2^4}{2(m_1^2-m_2^2)^4}\log\frac{m_2^2}{m_1^2}\,, \tag{B.10}$$

$$C_{01}(m_1,m_2) = \frac{7m_1^4-29m_1^2m_2^2+16m_2^4}{36(m_1^2-m_2^2)^3}+\frac{m_2^4(-3m_1^2+2m_2^2)}{6(m_1^2-m_2^2)^4}\log\frac{m_2^2}{m_1^2}\,, \tag{B.11}$$

$$C_{02}(m_1,m_2) = \frac{11m_1^4-7m_1^2m_2^2+2m_2^4}{36(m_1^2-m_2^2)^3}+\frac{m_1^6}{6(m_1^2-m_2^2)^4}\log\frac{m_2^2}{m_1^2}\,. \tag{B.12}$$

C Divided differences

The expansion of the amplitudes given in the mass eigenbasis in terms of mass insertions can be naturally expressed [29] in via of so-called divided differences of the loop functions.

In case the function has a single argument (e.g. $f(x)$) divided differences are defined recursively as:

$$\begin{aligned} f^{[0]}(x) &= f(x)\,, \\ f^{[1]}(x,y) &= \frac{f^{[0]}(x)-f^{[0]}(y)}{x-y}\,, \\ f^{[2]}(x,y,z) &= \frac{f^{[1]}(x,y)-f^{[1]}(x,z)}{y-z}\,, \\ &\dots \quad . \end{aligned} \tag{C.1}$$

As can be easily checked, a divided difference of order n is symmetric under permutation of any of its n arguments. It also has a smooth limit for degenerate arguments:

$$\lim_{\{x_0,\dots,x_m\}\to\{\xi,\dots,\xi\}} f^{[k]}(x_0,\dots,x_k) = \frac{1}{m!}\frac{\partial^m}{\partial\xi^m} f^{[k-m]}(\xi,x_{m+1}\dots,x_k)\,. \tag{C.2}$$

To compactify the formulae for functions of many arguments, we use the notation

$$f^{[k]}(x_0,\dots,x_k) \equiv f(\{x_0,\dots,x_k\})\,, \tag{C.3}$$

where the order of the divided difference is defined by the number of arguments inside curly brackets. Then, for example a divided difference of the 1st order in the 1st argument and of the 3rd order in the 2nd argument for the function of 3 variables, $g(x,y,z)$, can be written down as:

$$g(\{x_1,x_2\},\{y_1,y_2,y_3,y_4\},z)\,. \tag{C.4}$$

For the loop functions defined in Appendix B one should note that their natural arguments are squares of masses. However, we use m_i's instead of m_i^2's to compactify the notation. Thus, for loop functions we write divided differences as

$$L(m_1,\dots,\{m_i,m_i'\},\dots,m_n) = \frac{L(m_1,\dots,m_i,\dots,m_n)-L(m_1,\dots,m_i',\dots,m_n)}{m_i^2-m_i'^2}\,, \tag{C.5}$$

with squared masses in the denominator.

The notion of the divided differences is naturally encoded in the structure of 1-loop functions: a divided difference of a n-point function is a $(n+1)$-point function. Thus, for example, the scalar functions with vanishing external momenta (see [29] for the discussion of more general case) one has

$$\begin{aligned} B_0(m_1,\{m_2,m_3\}) &= B_0(\{m_1,m_2\},m_3) = C_0(m_1,m_2,m_3) \\ B_0(m_1,\{m_2,m_3,m_4\}) &= C_0(m_1,m_2,\{m_3,m_4\}) = D_0(m_1,m_2,m_3,m_4) \\ &\dots \end{aligned} \tag{C.6}$$

We use such relations extensively to find cancellations between various terms and to identify the lowest non-vanishing order of mass insertion expansion for a given process.

D Box diagrams in the mass eigenstates basis

There are four types of box diagrams with four external leptons involving slepton (sneutrinos) and neutralinos (charginos) in the loop, displayed in Fig. 12. Both chargino-sneutrino and neutralino-slepton pairs contribute to diagrams A) and B), while only neutralinos (Majorana fermions) can be exchanged in the "crossed" diagrams C) and D).

Using whenever necessary Fierz identities, the amplitudes describing each of the diagrams $N = A, B, C, D$ can be brought into the form

$$iA_N^{JIKL} = i \sum_{Q=V,S,T} B_{N\,QXY}^{JIKL} [\bar{u}(p_J)\Gamma_Q P_X u(p_I)][\bar{u}(p_K)\Gamma_Q P_Y v(p_L)] \tag{D.1}$$

with $\Gamma_V = \gamma^\mu$, $\Gamma_S = 1$ and $\Gamma_T = \sigma_{\mu\nu}$. Note that for Γ_T only the case $X = Y$ is non vanishing. Assuming that the generic couplings for an incoming lepton ℓ^I - an incoming scalar particle S_k and an outgoing fermion f_i takes the form

$$iV_{\ell Sf}^{Iki} = i(A_{\ell Sf}^{Iki} P_L + B_{\ell Sf}^{Iki} P_R)\,, \tag{D.2}$$

the contribution from diagram A) in Fig. 12) to the Wilson coefficients B_{QXY} can be written down as:

$$\begin{aligned}
(4\pi)^2 B_{A\,VLL}^{JIKL} &= \frac{1}{4} A_{\ell Sf}^{Iki} A_{\ell Sf}^{Jli*} A_{\ell Sf}^{Kkj*} A_{\ell Sf}^{Llj} D_2\,, \\
(4\pi)^2 B_{A\,VRR}^{JIKL} &= \frac{1}{4} B_{\ell Sf}^{Iki} B_{\ell Sf}^{Jli*} B_{\ell Sf}^{Kkj*} B_{\ell Sf}^{Llj} D_2\,, \\
(4\pi)^2 B_{A\,VLR}^{JIKL} &= \frac{1}{4} A_{\ell Sf}^{Iki} A_{\ell Sf}^{Jli*} B_{\ell Sf}^{Kkj*} B_{\ell Sf}^{Llj} D_2\,, \\
(4\pi)^2 B_{A\,VRL}^{JIKL} &= \frac{1}{4} B_{\ell Sf}^{Iki} B_{\ell Sf}^{Jli*} A_{\ell Sf}^{Kkj*} A_{\ell Sf}^{Llj} D_2\,, \\
(4\pi)^2 B_{A\,SLL}^{JIKL} &= A_{\ell Sf}^{Iki} B_{\ell Sf}^{Jli*} B_{\ell Sf}^{Kkj*} A_{\ell Sf}^{Llj} m_{f_i} m_{f_j} D_0\,, \\
(4\pi)^2 B_{A\,SRR}^{JIKL} &= B_{\ell Sf}^{Iki} A_{\ell Sf}^{Jli*} A_{\ell Sf}^{Kkj*} B_{\ell Sf}^{Llj} m_{f_i} m_{f_j} D_0\,, \\
(4\pi)^2 B_{A\,SLR}^{JIKL} &= A_{\ell Sf}^{Iki} B_{\ell Sf}^{Jli*} A_{\ell Sf}^{Kkj*} B_{\ell Sf}^{Llj} m_{f_i} m_{f_j} D_0\,, \\
(4\pi)^2 B_{A\,SRL}^{JIKL} &= B_{\ell Sf}^{Iki} A_{\ell Sf}^{Jli*} B_{\ell Sf}^{Kkj*} A_{\ell Sf}^{Llj} m_{f_i} m_{f_j} D_0\,, \\
(4\pi)^2 B_{A\,TL}^{JIKL} &= 0\,, \\
(4\pi)^2 B_{A\,TR}^{JIKL} &= 0\,.
\end{aligned} \tag{D.3}$$

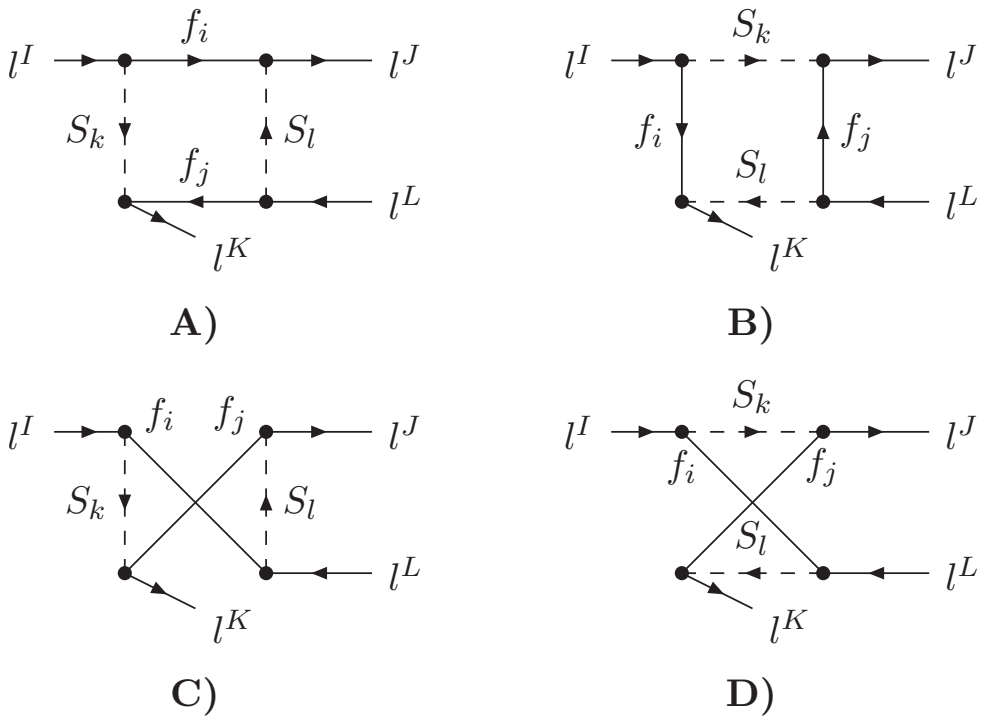

Figure 12: MSSM box diagrams with 4 external charged leptons

where D_0, D_2 above are the abbreviations for 4-point loop functions with respective mass arguments, $D_0 = D_0(m_{f_i}, m_{f_j}, m_{S_k}, m_{S_l}), D_2 = D_2(m_{f_i}, m_{f_j}, m_{S_k}, m_{S_l})$ (see Appendix B).

Using the same notation, the contributions from diagram B), C), D) are:

$$
\begin{aligned}
(4\pi)^2 B^{JIKL}_{B\,VLL} &= \frac{1}{4} A^{Iki}_{\ell Sf} A^{Jkj*}_{\ell Sf} A^{Kli*}_{\ell Sf} A^{Llj}_{\ell Sf} D_2 \,, \\
(4\pi)^2 B^{JIKL}_{B\,VRR} &= \frac{1}{4} B^{Iki}_{\ell Sf} B^{Jkj*}_{\ell Sf} B^{Kli*}_{\ell Sf} B^{Llj}_{\ell Sf} D_2 \,, \\
(4\pi)^2 B^{JIKL}_{B\,VLR} &= -\frac{1}{2} A^{Iki}_{\ell Sf} A^{Jkj*}_{\ell Sf} B^{Kli*}_{\ell Sf} B^{Llj}_{\ell Sf} m_{f_i} m_{f_j} D_0 \,, \\
(4\pi)^2 B^{JIKL}_{B\,VRL} &= -\frac{1}{2} B^{Iki}_{\ell Sf} B^{Jkj*}_{\ell Sf} A^{Kli*}_{\ell Sf} A^{Llj}_{\ell Sf} m_{f_i} m_{f_j} D_0 \,, \\
(4\pi)^2 B^{JIKL}_{B\,SLL} &= -\frac{1}{2} A^{Iki}_{\ell Sf} B^{Jkj*}_{\ell Sf} B^{Kli*}_{\ell Sf} A^{Llj}_{\ell Sf} m_{f_i} m_{f_j} D_0 \,, \\
(4\pi)^2 B^{JIKL}_{B\,SRR} &= -\frac{1}{2} B^{Iki}_{\ell Sf} A^{Jkj*}_{\ell Sf} A^{Kli*}_{\ell Sf} B^{Llj}_{\ell Sf} m_{f_i} m_{f_j} D_0 \,, \\
(4\pi)^2 B^{JIKL}_{B\,SLR} &= -\frac{1}{2} A^{Iki}_{\ell Sf} B^{Jkj*}_{\ell Sf} A^{Kli*}_{\ell Sf} B^{Llj}_{\ell Sf} D_2 \,, \\
(4\pi)^2 B^{JIKL}_{B\,SRL} &= -\frac{1}{2} B^{Iki}_{\ell Sf} A^{Jkj*}_{\ell Sf} B^{Kli*}_{\ell Sf} A^{Llj}_{\ell Sf} D_2 \,, \\
(4\pi)^2 B^{JIKL}_{B\,TL} &= -\frac{1}{8} A^{Iki}_{\ell Sf} B^{Jkj*}_{\ell Sf} B^{Kli*}_{\ell Sf} A^{Llj}_{\ell Sf} m_{f_i} m_{f_j} D_0 \,, \\
(4\pi)^2 B^{JIKL}_{B\,TR} &= -\frac{1}{8} B^{Iki}_{\ell Sf} A^{Jkj*}_{\ell Sf} A^{Kli*}_{\ell Sf} B^{Llj}_{\ell Sf} m_{f_i} m_{f_j} D_0 \,,
\end{aligned}
\tag{D.4}
$$

$$
\begin{aligned}
(4\pi)^2 B^{JIKL}_{C\,VLL} &= \frac{1}{2} A^{Iki}_{\ell Sf} A^{Lli}_{\ell Sf} A^{Jlj*}_{\ell Sf} A^{Kkj*}_{\ell Sf} m_{f_i} m_{f_j} D_0 \,, \\
(4\pi)^2 B^{JIKL}_{C\,VRR} &= \frac{1}{2} B^{Iki}_{\ell Sf} B^{Lli}_{\ell Sf} B^{Jlj*}_{\ell Sf} B^{Kkj*}_{\ell Sf} m_{f_i} m_{f_j} D_0 \,, \\
(4\pi)^2 B^{JIKL}_{C\,VLR} &= \frac{1}{4} B^{Iki}_{\ell Sf} A^{Lli}_{\ell Sf} B^{Jlj*}_{\ell Sf} A^{Kkj*}_{\ell Sf} D_2 \,, \\
(4\pi)^2 B^{JIKL}_{C\,VRL} &= \frac{1}{4} A^{Iki}_{\ell Sf} B^{Lli}_{\ell Sf} A^{Jlj*}_{\ell Sf} B^{Kkj*}_{\ell Sf} D_2 \,, \\
(4\pi)^2 B^{JIKL}_{C\,SLL} &= -\frac{1}{2} A^{Iki}_{\ell Sf} A^{Lli}_{\ell Sf} B^{Jlj*}_{\ell Sf} B^{Kkj*}_{\ell Sf} m_{f_i} m_{f_j} D_0 \,, \\
(4\pi)^2 B^{JIKL}_{C\,SRR} &= -\frac{1}{2} B^{Iki}_{\ell Sf} B^{Lli}_{\ell Sf} A^{Jlj*}_{\ell Sf} A^{Kkj*}_{\ell Sf} m_{f_i} m_{f_j} D_0 \,, \\
(4\pi)^2 B^{JIKL}_{C\,SLR} &= \frac{1}{2} B^{Iki}_{\ell Sf} A^{Lli}_{\ell Sf} A^{Jlj*}_{\ell Sf} B^{Kkj*}_{\ell Sf} D_2 \,, \\
(4\pi)^2 B^{JIKL}_{C\,SRL} &= \frac{1}{2} A^{Iki}_{\ell Sf} B^{Lli}_{\ell Sf} B^{Jlj*}_{\ell Sf} A^{Kkj*}_{\ell Sf} D_2 \,, \\
(4\pi)^2 B^{JIKL}_{C\,TL} &= \frac{1}{8} A^{Iki}_{\ell Sf} A^{Lli}_{\ell Sf} B^{Jlj*}_{\ell Sf} B^{Kkj*}_{\ell Sf} m_{f_i} m_{f_j} D_0 \,, \\
(4\pi)^2 B^{JIKL}_{C\,TR} &= \frac{1}{8} B^{Iki}_{\ell Sf} B^{Lli}_{\ell Sf} A^{Jlj*}_{\ell Sf} A^{Kkj*}_{\ell Sf} m_{f_i} m_{f_j} D_0 \,,
\end{aligned}
\tag{D.5}
$$

$$
\begin{aligned}
(4\pi)^2 B^{JIKL}_{D\,VLL} &= \frac{1}{2} A^{Iki}_{\ell Sf} A^{Lli}_{\ell Sf} A^{Jkj*}_{\ell Sf} A^{Klj*}_{\ell Sf} m_{f_i} m_{f_j} D_0 \,, \\
(4\pi)^2 B^{JIKL}_{D\,VRR} &= \frac{1}{2} B^{Iki}_{\ell Sf} B^{Lli}_{\ell Sf} B^{Jkj*}_{\ell Sf} B^{Klj*}_{\ell Sf} m_{f_i} m_{f_j} D_0 \,, \\
(4\pi)^2 B^{JIKL}_{D\,VLR} &= -\frac{1}{4} B^{Iki}_{\ell Sf} A^{Lli}_{\ell Sf} B^{Jkj*}_{\ell Sf} A^{Klj*}_{\ell Sf} D_2 \,, \\
(4\pi)^2 B^{JIKL}_{D\,VRL} &= -\frac{1}{4} A^{Iki}_{\ell Sf} B^{Lli}_{\ell Sf} A^{Jkj*}_{\ell Sf} B^{Klj*}_{\ell Sf} D_2 \,, \\
(4\pi)^2 B^{JIKL}_{D\,SLL} &= -\frac{1}{2} A^{Iki}_{\ell Sf} A^{Lli}_{\ell Sf} B^{Jkj*}_{\ell Sf} B^{Klj*}_{\ell Sf} m_{f_i} m_{f_j} D_0 \,, \\
(4\pi)^2 B^{JIKL}_{D\,SRR} &= -\frac{1}{2} B^{Iki}_{\ell Sf} B^{Lli}_{\ell Sf} A^{Jkj*}_{\ell Sf} A^{Klj*}_{\ell Sf} m_{f_i} m_{f_j} D_0 \,, \\
(4\pi)^2 B^{JIKL}_{D\,SLR} &= -\frac{1}{2} B^{Iki}_{\ell Sf} A^{Lli}_{\ell Sf} A^{Jkj*}_{\ell Sf} B^{Klj*}_{\ell Sf} D_2 \,, \\
(4\pi)^2 B^{JIKL}_{D\,SRL} &= -\frac{1}{2} A^{Iki}_{\ell Sf} B^{Lli}_{\ell Sf} B^{Jkj*}_{\ell Sf} A^{Klj*}_{\ell Sf} D_2 \,, \\
(4\pi)^2 B^{JIKL}_{D\,TL} &= \frac{1}{8} A^{Iki}_{\ell Sf} A^{Lli}_{\ell Sf} B^{Jkj*}_{\ell Sf} B^{Klj*}_{\ell Sf} m_{f_i} m_{f_j} D_0 \,, \\
(4\pi)^2 B^{JIKL}_{D\,TR} &= \frac{1}{8} B^{Iki}_{\ell Sf} B^{Lli}_{\ell Sf} A^{Jkj*}_{\ell Sf} A^{Klj*}_{\ell Sf} m_{f_i} m_{f_j} D_0 \,,
\end{aligned}
\tag{D.6}
$$

To obtain the actual MSSM contributions to the 4-lepton operators, one should add terms from eqs. (D.3,D.4) with replacements $f \to C, S \to \tilde{\nu}, A_{\ell Sf} \to V_{\ell\tilde{\nu}C,L}, B_{\ell Sf} \to V_{\ell\tilde{\nu}C,R}$ and $f \to N, S \to \tilde{L}, A_{\ell Sf} \to V_{\ell\tilde{L}N,L}, B_{\ell Sf} \to V_{\ell\tilde{L}N,R}$ (summing over repeated indices of loop particles) and terms from eqs. (D.5,D.6), substituting there only $f \to N, S \to \tilde{L}, A_{\ell Sf} \to V_{\ell\tilde{L}N,L}, B_{\ell Sf} \to V_{\ell\tilde{L}N,R}$.

The contributions to 2-quark 2-lepton operators can be obtained from diagrams A) and C) by replacing ℓ_K and ℓ_L with q_K and q_L as defined in Eq. (2.28). Therefore, the expressions for $B_{q\,QXY}$ can be obtained replacing vertices of leptons ℓ^K and ℓ^L by the relevant quark-squark vertices. Such vertices are not listed in Appendix A but can be found in Refs. [33, 34]. The explicit form of $\ell\ell dd$ box amplitudes can be also found in Appendix A.3 of Ref. [97].

E Effective lepton couplings in the leading MI order

We list below the MI expanded expressions for the leptonic penguin and box diagram amplitudes. For penguins we follow the decomposition of Eq. (4.2), with F_{XY} denoting functions of flavour diagonal SUSY parameters multiplying the respective slepton mass insertions:

$$\begin{aligned} F_X^{IJ} &= \frac{1}{(4\pi)^2}\left(F_X^{IJ}{}_{LL}\,\Delta_{LL}^{IJ} + F_X^{IJ}{}_{RR}\,\Delta_{RR}^{JI}\right. \\ &+ \left. F_X^{IJ}{}_{ALR}\,\Delta_{LR}^{JI} + F_X^{IJ}{}_{BLR}\,\Delta_{LR}^{IJ*} + F_X^{\prime IJ}{}_{ALR}\,\Delta_{LR}^{\prime JI} + F_X^{\prime IJ}{}_{BLR}\,\Delta_{LR}^{\prime IJ*}\right) . \end{aligned} \tag{E.1}$$

To compactify the notation, we also introduce the abbreviation

$$\bar{M}_{XY}^{IJ} = \sqrt{\left(M_{XX}^2\right)^{II}\left(M_{YY}^2\right)^{JJ}} \tag{E.2}$$

where $X, Y = L$ or R.

E.1 Lepton-photon vertex

E.1.1 Tensor (magnetic) couplings

After performing MI expansion, one can see that terms coming from $F_{\gamma A}$ in Eq. (2.4) are always suppressed by the powers of lepton Yukawa couplings or lepton masses, and may add to or cancel terms generated from $F_{\gamma LB}, F_{\gamma RB}$. Thus, in the expressions below we give the sum of both types of contributions.

The chargino contributions contain only terms proportional to LL slepton mass insertions (see Appendix C for the notation of divided differences and curly brackets around the function arguments)

$$\begin{aligned} \left(F_{\gamma\ LL}\right)_C^{JI} &= \frac{e^2 v_1 Y_L^J}{2\sqrt{2}s_W^2}\bar{M}_{LL}^{IJ}\left(C_{11}(|M_2|, \{m_{\tilde{\nu}_I}, m_{\tilde{\nu}_J}\})\right. \\ &+ C_{11}(|\mu|, \{m_{\tilde{\nu}_I}, m_{\tilde{\nu}_J}\}) - C_{23}(|M_2|, \{m_{\tilde{\nu}_I}, m_{\tilde{\nu}_J}\}) \\ &+ \left.\left(|\mu|^2 + |M_2|^2 + 2\mu^* M_2^* \tan\beta\right) C_{11}(\{|\mu|, |M_2|\}, \{m_{\tilde{\nu}_I}, m_{\tilde{\nu}_J}\})\right) \end{aligned} \tag{E.3}$$

The non-vanishing neutralino contributions are:

$$
\begin{aligned}
(F_{\gamma\ LL})_N^{JI} &= \frac{e^2}{2c_W^2}\bar{M}_{LL}^{IJ}\left(M_1^\star C_{12}(\{m_{\tilde{e}_{LI}},m_{\tilde{e}_{LJ}},m_{\tilde{e}_{RJ}}\},|M_1|)\left(M_{LR}^2\right)_{JJ}\right.\\
&- \frac{v_1}{2\sqrt{2}}Y_L^J\left(\frac{c_W^2}{s_W^2}(C_{12}(\{m_{\tilde{e}_{LI}},m_{\tilde{e}_{LJ}}\},|\mu|)-C_{23}(\{m_{\tilde{e}_{LI}},m_{\tilde{e}_{LJ}}\},|M_2|))\right.\\
&- C_{12}(\{m_{\tilde{e}_{LI}},m_{\tilde{e}_{LJ}}\},|\mu|)-C_{23}(\{m_{\tilde{e}_{LI}},m_{\tilde{e}_{LJ}}\},|M_1|)\\
&+ \left(|M_2|^2+\mu^\star M_2^\star\tan\beta\right)\frac{c_W^2}{s_W^2}C_{12}(\{m_{\tilde{e}_{LI}},m_{\tilde{e}_{LJ}}\},\{|\mu|,|M_2|\})\\
&- \left.\left.\left(|M_1|^2+\mu^\star M_1^\star\tan\beta\right)C_{12}(\{m_{\tilde{e}_{LJ}},m_{\tilde{e}_{LI}}\},\{|\mu|,|M_1|\})\right)\right) \qquad \text{(E.4)}\\
(F_{\gamma\ RR})_N^{JI} &= \frac{e^2}{2c_W^2}\bar{M}_{RR}^{IJ}\left(M_1^\star C_{12}\left(\{m_{\tilde{e}_{LI}},m_{\tilde{e}_{RI}},m_{\tilde{e}_{RJ}}\},|M_1|\right)\left(M_{LR}^2\right)_{II}\right.\\
&- \frac{v_1}{\sqrt{2}}Y_L^I\left(C_{12}\left(\{m_{\tilde{e}_{RI}},m_{\tilde{e}_{RJ}}\},|\mu|\right)-2C_{23}(\{m_{\tilde{e}_{RI}},m_{\tilde{e}_{RJ}}\},|M_1|)\right.\\
&+ \left.\left.\left(|M_1|^2+\mu^\star M_1^\star\tan\beta\right)C_{12}(\{m_{\tilde{e}_{RI}},m_{\tilde{e}_{RJ}}\},\{\mu,|M_1|\})\right)\right)\\
(F_{\gamma\ ALR})_N^{JI} &= -\frac{v_1}{v_2}\left(F'_{\gamma\ ALR}\right)_N^{JI} = \frac{e^2 v_1}{2\sqrt{2}c_W^2}\sqrt{\bar{M}_{LR}^{IJ}}\,M_1^\star C_{12}(\{m_{\tilde{e}_{LI}},m_{\tilde{e}_{RJ}}\},|M_1|)
\end{aligned}
$$

E.1.2 Vector couplings

Loop functions C_{01} and C_{02} appearing in Eq. (2.6) scale with the inverse of the squared SUSY scale M^2. Thus, only LL and RR terms contribute to the MI expanded expressions at the v^2/M^2 order, as LR mass insertions always come with additional v/M powers. The non-vanishing chargino and neutralino contributions are:

$$
(V_{\gamma L\ LL})_C^{JI} = \frac{e^2}{s_W^2}\bar{M}_{LL}^{IJ}\,C_{01}(|M_2|,\{m_{\tilde{\nu}_I},m_{\tilde{\nu}_J}\}) \qquad \text{(E.5)}
$$

$$
\begin{aligned}
(V_{\gamma L\ LL})_N^{JI} &= -\frac{e^2}{2s_W^2c_W^2}\bar{M}_{LL}^{IJ}\left(c_W^2C_{02}(|M_2|,\{m_{\tilde{e}_{LI}},m_{\tilde{e}_{LJ}}\})+s_W^2C_{02}(|M_1|,\{m_{\tilde{e}_{LI}},m_{\tilde{e}_{LJ}}\})\right.\\
(V_{\gamma R\ RR})_N^{JI} &= -\frac{2e^2}{c_W^2}\bar{M}_{RR}^{IJ}\,C_{02}(|M_1|,\{m_{\tilde{e}_{RI}},m_{\tilde{e}_{RJ}}\}) \qquad \text{(E.6)}
\end{aligned}
$$

E.2 Lepton-Z^0 vertex

The leading v^2/M_{SUSY}^2 terms in the effective $Z\bar{\ell}^I\ell^J$ vertex defined in Eq. (2.7), expanded to the 1st order in LFV mass insertions, depend on divided differences of scalar C_0 and C_2 3-point functions. They can be expressed as higher point 1-loop functions (see Appendices B and C). We give here the expressions using explicitly scalar 4-, 5- and 6-point functions D, E and F.

The only non-negligible chargino contribution to $Z\ell\ell'$ vertex read:

$$\begin{aligned}(F_{ZL\ LL})^{JI}_C &= -\frac{e^5}{4s_W^5 c_W}\bar{M}^{IJ}_{LL}\Big(v_2^2\, D_0(|M_2|,|\mu|,m_{\tilde{\nu}^I},m_{\tilde{\nu}^J}) \\ &+ (v_1^2-v_2^2)E_2(|M_2|,|M_2|,|\mu|,m_{\tilde{\nu}^I},m_{\tilde{\nu}^J}) \\ &+ \frac{1}{2}\left|v_2M_2+v_1\mu^*\right|^2 F_2(|M_2|,|M_2|,|\mu|,|\mu|,m_{\tilde{\nu}^I},m_{\tilde{\nu}^J})\Big) \end{aligned} \tag{E.7}$$

Neutralino contributions have a more complicated form. They can be written down as:

$$\begin{aligned}(F_{ZL\ LL})^{JI}_N &= \frac{e^3\sqrt{2}}{16s_W^3c_W^3}\bar{M}^{IJ}_{LL}\,(X^{JI}_{ZNL4}+X^{JI}_{ZNL5}+X^{IJ*}_{ZNL5}) \\ (F_{ZR\ LL})^{JI}_N &= \frac{e^3\sqrt{2}}{8s_Wc_W^3}\bar{M}^{IJ}_{LL}\,(X^{IJ}_{ZNR4}+X^{JI}_{ZNR5}+X^{IJ*}_{ZNR5}) \end{aligned} \tag{E.8}$$

$$\begin{aligned}(F_{ZL\ RR})^{JI}_N &= \frac{e^3\sqrt{2}}{16s_W^3c_W^3}\bar{M}^{IJ}_{RR}\,(X^{JI}_{ZNL2}+X^{JI}_{ZNL3}+X^{IJ*}_{ZNL3}) \\ (F_{ZR\ RR})^{JI}_N &= \frac{e^3\sqrt{2}}{8s_Wc_W^3}\bar{M}^{IJ}_{RR}\,(X^{JI}_{ZNR2}+X^{JI}_{ZNR3}+X^{IJ*}_{ZNR3}) \end{aligned} \tag{E.9}$$

$$\begin{aligned}(F_{ZL\ ALR})^{JI}_N &= (F_{ZL\ BLR})^{IJ*}_N = -\frac{v_1}{v_2}(F'_{ZL\ ALR})^{JI}_N = -\frac{v_1}{v_2}(F_{ZL\ BLR})^{IJ*}_N \\ &= \frac{e^3v_1}{16s_W^3c_W^3}\sqrt{\bar{M}^{IJ}_{LR}}\,X^{JI}_{ZNL1} \\ (F_{ZR\ ALR})^{JI}_N &= (F_{ZR\ BLR})^{IJ*}_N = -\frac{v_1}{v_2}(F'_{ZR\ ALR})^{JI}_N = -\frac{v_1}{v_2}(F_{ZR\ BLR})^{IJ*}_N \\ &= \frac{e^3v_1}{4s_Wc_W^3}\sqrt{\bar{M}^{IJ}_{LR}}\,X^{JI}_{ZNR1} \end{aligned} \tag{E.10}$$

where we defined

$$\begin{aligned}X^{JI}_{ZNL1} &= \sqrt{2}(s_W^2E_2(|M_1|,m_{\tilde{e}_{LJ}},m_{\tilde{e}_{LI}},m_{\tilde{e}_{RJ}},m_{\tilde{e}_{RJ}}) \\ &+ c_W^2E_2(|M_2|,m_{\tilde{e}_{LJ}},m_{\tilde{e}_{LI}},m_{\tilde{e}_{RJ}},m_{\tilde{e}_{RJ}}))(M^2_{LR})^*_{JJ} \\ &+ Y_l^J\left(2v_1(M_1^*s_W^2D_0(|M_1|,|\mu|,m_{\tilde{e}_{LI}},m_{\tilde{e}_{RJ}}) - c_W^2M_2^*D_0(|M_2|,|\mu|,m_{\tilde{e}_{LI}},m_{\tilde{e}_{RJ}})\right) \\ &- s_W^2(v_1M_1^*+v_2\mu)(E_2(|M_1|,|\mu|,m_{\tilde{e}_{LI}},m_{\tilde{e}_{RJ}},m_{\tilde{e}_{RJ}}) \\ &+ E_2(|M_1|,|\mu|,|\mu|,m_{\tilde{e}_{LI}},m_{\tilde{e}_{RJ}})) \\ &+ c_W^2(v_1M_2^*+v_2\mu)(E_2(|M_2|,|\mu|,m_{\tilde{e}_{LI}},m_{\tilde{e}_{RJ}},m_{\tilde{e}_{RJ}}) \\ &+ E_2(|M_2|,|\mu|,|\mu|,m_{\tilde{e}_{LI}},m_{\tilde{e}_{RJ}}))) \end{aligned} \tag{E.11}$$

$$\begin{aligned}X^{JI}_{ZNL2} &= \sqrt{2}(M^2_{LR})^*_{JJ}(M^2_{LR})_{II}(s_W^2(F_2(|M_1|,m_{\tilde{e}_{LJ}},m_{\tilde{e}_{LI}},m_{\tilde{e}_{RJ}},m_{\tilde{e}_{RJ}},m_{\tilde{e}_{RI}}) \\ &+ F_2(|M_1|,m_{\tilde{e}_{LJ}},m_{\tilde{e}_{LI}},m_{\tilde{e}_{RJ}},m_{\tilde{e}_{RI}},m_{\tilde{e}_{RI}})) \\ &+ c_W^2(F_2(|M_2|,m_{\tilde{e}_{LJ}},m_{\tilde{e}_{LI}},m_{\tilde{e}_{RJ}},m_{\tilde{e}_{RJ}},m_{\tilde{e}_{RI}}) \\ &+ F_2(|M_2|,m_{\tilde{e}_{LJ}},m_{\tilde{e}_{LI}},m_{\tilde{e}_{RJ}},m_{\tilde{e}_{RI}},m_{\tilde{e}_{RI}}))) \end{aligned} \tag{E.12}$$

$$
\begin{aligned}
X^{JI}_{ZNL3} &= Y_l^{I*}(M^2_{LR})^*_{JJ}\left(2v_1(M_1^* s_W^2 E_0(|M_1|,|\mu|,m_{\tilde{e}_{LJ}},m_{\tilde{e}_{RJ}},m_{\tilde{e}_{RI}})\right.\\
&- c_W^2 M_2^* E_0(|M_2|,|\mu|,m_{\tilde{e}_{LJ}},m_{\tilde{e}_{RJ}},m_{\tilde{e}_{RI}}))\\
&- s_W^2(v_1M_1^*+v_2\mu)(F_2(|M_1|,|\mu|,m_{\tilde{e}_{LJ}},m_{\tilde{e}_{RJ}},m_{\tilde{e}_{RJ}},m_{\tilde{e}_{RI}})\\
&+ F_2(|M_1|,|\mu|,m_{\tilde{e}_{LJ}},m_{\tilde{e}_{RJ}},m_{\tilde{e}_{RI}},m_{\tilde{e}_{RI}})+F_2(|M_1|,|\mu|,|\mu|,m_{\tilde{e}_{LJ}},m_{\tilde{e}_{RJ}},m_{\tilde{e}_{RI}}))\\
&+ c_W^2(v_1M_2^*+v_2\mu)(F_2(|M_2|,|\mu|,m_{\tilde{e}_{LJ}},m_{\tilde{e}_{RJ}},m_{\tilde{e}_{RJ}},m_{\tilde{e}_{RI}})\\
&+ \left.F_2(|M_2|,|\mu|,m_{\tilde{e}_{LJ}},m_{\tilde{e}_{RJ}},m_{\tilde{e}_{RI}},m_{\tilde{e}_{RI}})+F_2(|M_2|,|\mu|,|\mu|,m_{\tilde{e}_{LJ}},m_{\tilde{e}_{RJ}},m_{\tilde{e}_{RI}})\right)
\end{aligned}
\tag{E.13}
$$

$$
\begin{aligned}
X^{JI}_{ZNL4} &= \frac{e^2(v_1^2-v_2^2)}{\sqrt{2}s_W^2c_W^2}\left(s_W^4 D_0(|M_1|,|\mu|,m_{\tilde{e}_{LJ}},m_{\tilde{e}_{LI}})+c_W^4 D_0(|M_2|,|\mu|,m_{\tilde{e}_{LJ}},m_{\tilde{e}_{LI}})\right.\\
&+ 2s_W^2c_W^2\,\mathrm{Re}\,(M_1M_2^*)E_0(|M_1|,|M_2|,|\mu|,m_{\tilde{e}_{LJ}},m_{\tilde{e}_{LI}})\\
&- s_W^4(E_2(|M_1|,|M_1|,|\mu|,m_{\tilde{e}_{LJ}},m_{\tilde{e}_{LI}})+E_2(|M_1|,|\mu|,|\mu|,m_{\tilde{e}_{LJ}},m_{\tilde{e}_{LI}}))\\
&- c_W^4(E_2(|M_2|,|M_2|,|\mu|,m_{\tilde{e}_{LJ}},m_{\tilde{e}_{LI}})+E_2(|M_2|,|\mu|,|\mu|,m_{\tilde{e}_{LJ}},m_{\tilde{e}_{LI}}))\\
&+ 2s_W^2c_W^2E_2(|M_1|,|M_2|,|\mu|,m_{\tilde{e}_{LJ}},m_{\tilde{e}_{LI}})\\
&+ \frac{1}{2}s_W^4(|\mu|^2-|M_1|^2)F_2(|M_1|,|M_1|,|\mu|,|\mu|,m_{\tilde{e}_{LJ}},m_{\tilde{e}_{LI}})\\
&+ \frac{1}{2}c_W^4(|\mu|^2-|M_2|^2)F_2(|M_2|,|M_2|,|\mu|,|\mu|,m_{\tilde{e}_{LJ}},m_{\tilde{e}_{LI}})\\
&+ \left.s_W^2c_W^2(|\mu|^2-\mathrm{Re}\,(M_1M_2^*))F_2(|M_1|,|M_2|,|\mu|,|\mu|,m_{\tilde{e}_{LJ}},m_{\tilde{e}_{LI}})\right)
\end{aligned}
\tag{E.14}
$$

$$
\begin{aligned}
X^{JI}_{ZNL5} &= Y_l^{I*}(M^2_{LR})^*_{II}\left(2v_1(s_W^2M_1^*E_0(|M_1|,|\mu|,m_{\tilde{e}_{LJ}},m_{\tilde{e}_{LI}},m_{\tilde{e}_{RI}})\right.\\
&- c_W^2M_2^*E_0(|M_2|,|\mu|,m_{\tilde{e}_{LJ}},m_{\tilde{e}_{LI}},m_{\tilde{e}_{RI}}))\\
&- s_W^2(v_1M_1^*+v_2\mu)(F_2(|M_1|,|\mu|,m_{\tilde{e}_{LJ}},m_{\tilde{e}_{LI}},m_{\tilde{e}_{RI}},m_{\tilde{e}_{RI}})\\
&+ F_2(|M_1|,|\mu|,|\mu|,m_{\tilde{e}_{LJ}},m_{\tilde{e}_{LI}},m_{\tilde{e}_{RI}}))\\
&+ c_W^2(v_1M_2^*+v_2\mu)(F_2(|M_2|,|\mu|,m_{\tilde{e}_{LJ}},m_{\tilde{e}_{LI}},m_{\tilde{e}_{RI}},m_{\tilde{e}_{RI}})\\
&+ F_2(|M_2|,|\mu|,|\mu|,m_{\tilde{e}_{LJ}},m_{\tilde{e}_{LI}},m_{\tilde{e}_{RI}})))\\
&+ \sqrt{2}\left(s_W^2F_2(|M_1|,m_{\tilde{e}_{LJ}},m_{\tilde{e}_{LI}},m_{\tilde{e}_{LI}},m_{\tilde{e}_{RI}},m_{\tilde{e}_{RI}})\right.\\
&+ \left.c_W^2F_2(|M_2|,m_{\tilde{e}_{LJ}},m_{\tilde{e}_{LI}},m_{\tilde{e}_{LI}},m_{\tilde{e}_{RI}},m_{\tilde{e}_{RI}})\right)\left|(M^2_{LR})_{II}\right|^2
\end{aligned}
\tag{E.15}
$$

$$
\begin{aligned}
X^{JI}_{ZNR1} &= Y_l^I\left(2v_1M_1^*D_0(|M_1|,|\mu|,m_{\tilde{e}_{LI}},m_{\tilde{e}_{RJ}})\right.\\
&- (v_1M_1^*+v_2\mu)(E_2(|M_1|,|\mu|,m_{\tilde{e}_{LI}},m_{\tilde{e}_{LI}},m_{\tilde{e}_{RJ}})\\
&+ \left.E_2(|M_1|,|\mu|,|\mu|,m_{\tilde{e}_{LI}},m_{\tilde{e}_{RJ}}))\right)\\
&- 2\sqrt{2}\,E_2(|M_1|,m_{\tilde{e}_{LI}},m_{\tilde{e}_{LI}},m_{\tilde{e}_{RJ}},m_{\tilde{e}_{RI}})(M^2_{LR})^*_{II}
\end{aligned}
\tag{E.16}
$$

$$
\begin{aligned}
X^{JI}_{ZNR2} &= \frac{\sqrt{2}e^2(v_1^2-v_2^2)}{c_W^2}\left(|M_1|^2E_0(|M_1|,|\mu|,|\mu|,m_{\tilde{e}_{RJ}},m_{\tilde{e}_{RI}})\right.\\
&+ E_2(|M_1|,|M_1|,|\mu|,m_{\tilde{e}_{RJ}},m_{\tilde{e}_{RI}})\\
&- \frac{1}{2}(|M_1|^2-|\mu|^2)(F_2(|M_1|,|\mu|,|\mu|,m_{\tilde{e}_{RJ}},m_{\tilde{e}_{RJ}},m_{\tilde{e}_{RI}})\\
&+ F_2(|M_1|,|\mu|,|\mu|,m_{\tilde{e}_{RJ}},m_{\tilde{e}_{RI}},m_{\tilde{e}_{RI}})\\
&+ \left.2F_2(|M_1|,|\mu|,|\mu|,|\mu|,m_{\tilde{e}_{RJ}},m_{\tilde{e}_{RI}}))\right)
\end{aligned}
\tag{E.17}
$$

$$
\begin{aligned}
X^{JI}_{ZNR3} &= Y^I_l (M^2_{LR})_{II} \, (2 v_1 M_1^* E_0(|M_1|, |\mu|, m_{\tilde{e}_{LI}}, m_{\tilde{e}_{RJ}}, m_{\tilde{e}_{RI}}) \\
&- (v_1 M_1^* + v_2 \mu)(F_2(|M_1|, |\mu|, m_{\tilde{e}_{LI}}, m_{\tilde{e}_{LI}}, m_{\tilde{e}_{RJ}}, m_{\tilde{e}_{RI}}) \\
&+ F_2(|M_1|, |\mu|, |\mu|, m_{\tilde{e}_{LI}}, m_{\tilde{e}_{RJ}}, m_{\tilde{e}_{RI}}))) \\
&- 2\sqrt{2}\, F_2(|M_1|, m_{\tilde{e}_{LI}}, m_{\tilde{e}_{LI}}, m_{\tilde{e}_{RJ}}, m_{\tilde{e}_{RI}}, m_{\tilde{e}_{RI}}) \left|(M^2_{LR})_{II}\right|^2
\end{aligned} \tag{E.18}
$$

$$
\begin{aligned}
X^{JI}_{ZNR4} &= -2\sqrt{2}\, (F_2(|M_1|, m_{\tilde{e}_{LJ}}, m_{\tilde{e}_{LJ}}, m_{\tilde{e}_{LI}}, m_{\tilde{e}_{RJ}}, m_{\tilde{e}_{RI}}) \\
&+ F_2(|M_1|, m_{\tilde{e}_{LJ}}, m_{\tilde{e}_{LI}}, m_{\tilde{e}_{LI}}, m_{\tilde{e}_{RJ}}, m_{\tilde{e}_{RI}}))(M^2_{LR})_{JJ} (M^2_{LR})^*_{II}
\end{aligned} \tag{E.19}
$$

$$
\begin{aligned}
X^{JI}_{ZNR5} &= -Y^I_l (M^2_{LR})_{JJ} \, (2\mu v_2 E_0(|M_1|, |\mu|, m_{\tilde{e}_{LJ}}, m_{\tilde{e}_{LI}}, m_{\tilde{e}_{RJ}}) \\
&- (v_1 M_1^* + v_2 \mu)(F_2(|M_1|, |M_1|, |\mu|, m_{\tilde{e}_{LJ}}, m_{\tilde{e}_{LI}}, m_{\tilde{e}_{RJ}}) \\
&+ F_2(|M_1|, |\mu|, m_{\tilde{e}_{LJ}}, m_{\tilde{e}_{LI}}, m_{\tilde{e}_{RJ}}, m_{\tilde{e}_{RJ}})))
\end{aligned} \tag{E.20}
$$

E.3 CP-even Higgs-lepton vertex

The dominant MI terms in the effective CP-even Higgs - lepton couplings (see Eq. (2.13)) can be split into four classes,

$$
F^{IJK}_h = \frac{1}{(4\pi)^2} \left(F^{IJK}_{hnd} + F^{IJK}_{hY} + F^{IJK}_{hdec} + F^{IJK}_{hm} \right) \, , \tag{E.21}
$$

defined as (below we give the sum of neutralino and chargino contributions, the latter appearing only as single term depending on sneutrino masses in eq. (E.24) and follow notation of Eq. (4.2)):

1. Contributions proportional to non-holomorphic A'_l trilinear terms, non-decoupling for $M_{SUSY} \gg v$[9]:

$$
F^{IJK}_{hnd\ ALR} = \frac{e^2 (v_1 Z^{2K}_R - v_2 Z^{1K}_R)}{\sqrt{2} c^2_W v_1} \sqrt{\bar{M}^{IJ}_{LR}}\, M_1^\star \, C_0(|M_1|, m_{\tilde{e}_{LI}}, m_{\tilde{e}_{RJ}}) \tag{E.22}
$$

$$
\begin{aligned}
F^{IJK}_{hnd\ LL} &= \frac{e^2 (v_1 Z^{2K}_R - v_2 Z^{1K}_R)}{\sqrt{2} c^2_W v_1} \bar{M}^{IJ}_{LL}\, M_1^\star D_0(|M_1|, m_{\tilde{e}_{LI}}, m_{\tilde{e}_{LJ}}, m_{\tilde{e}_{RJ}}) A'^{JJ}_L \\
F^{IJK}_{hnd\ RR} &= \frac{e^2 (v_1 Z^{2K}_R - v_2 Z^{1K}_R)}{\sqrt{2} c^2_W v_1} \bar{M}^{IJ}_{RR}\, M_1^\star \, D_0(|M_1|, m_{\tilde{e}_{LI}}, m_{\tilde{e}_{RI}}, m_{\tilde{e}_{RJ}}) A'^{II}_L
\end{aligned} \tag{E.23}
$$

2. Contributions suppressed by the lepton Yukawa couplings, also non-decoupling for $M_{SUSY} \gg v$:

$$
\begin{aligned}
F^{IJK}_{hY\ LL} &= -\frac{e^2}{2\sqrt{2} v_1 c^2_W s^2_W} \left(v_1 Z^{2K}_R - v_2 Z^{1K}_R \right) \left(s^2_W M_1^\star \mu^\star (D_0(|M_1|, |\mu|, m_{\tilde{e}_{LI}}, m_{\tilde{e}_{LJ}}) \right. \\
&+ 2 D_0(|M_1|, m_{\tilde{e}_{LI}}, m_{\tilde{e}_{LJ}}, m_{\tilde{e}_{RJ}})) - c^2_W M_2^\star \mu^\star (D_0(|M_2|, |\mu|, m_{\tilde{e}_{LI}}, m_{\tilde{e}_{LJ}}) \\
&+ \left. 2 D_0(|M_2|, |\mu|, m_{\tilde{\nu}_I}, m_{\tilde{\nu}_J})) \right) \bar{M}^{IJ}_{LL}\, Y^J_L \\
F^{IJK}_{hY\ RR} &= -\frac{e^2}{\sqrt{2} v_1 c^2_W} \left(v_1 Z^{2K}_R - v_2 Z^{1K}_R \right) M_1^\star \mu^\star (D_0(|M_1|, m_{\tilde{e}_{LI}}, m_{\tilde{e}_{RI}}, m_{\tilde{e}_{RJ}}) \\
&- D_0(|M_1|, |\mu|, m_{\tilde{e}_{RI}}, m_{\tilde{e}_{RJ}})) \, \bar{M}^{IJ}_{RR}\, Y^I_L
\end{aligned} \tag{E.24}
$$

[9] For comparison with commonly used notation of the Higgs mixing angles, note that $(v_1 Z^{2K}_R - v_2 Z^{1K}_R)/v_1 = \begin{cases} \sin(\alpha-\beta)/\cos\beta & \text{for} \quad K=1 \\ \cos(\alpha-\beta)/\cos\beta & \text{for} \quad K=2 \end{cases}$.

3. Contributions decoupling as v^2/M^2_{SUSY}. We neglect here terms proportional to Δ_{LL}, Δ_{RR}, Δ'_{LR} as they are dominated by non-decoupling contributions listed in points 1) and 2). Only the terms proportional to Δ^{IJ}_{LR} and Δ^{JI*}_{RL} are generated starting at order v^2/M^2_{SUSY}. To simplify the expressions, below we also neglect terms additionally suppressed by lepton Yukawa couplings (this approximation becomes inaccurate for large μ and $\tan\beta \geq 30$, when the diagonal LR elements of the slepton mass matrix proportional to μY_l become important).

$$
\begin{aligned}
F^{IJK}_{hdec\ ALR} &= \Bigg(\frac{e^4}{4v_1\sqrt{2}c^4_W s^2_W} \big((v_1 Z^{1K}_R - v_2 Z^{2K}_R) M^*_1 (2s^2_W D_0(|M_1|, m_{\tilde{e}_{LI}}, m_{\tilde{e}_{RJ}}, m_{\tilde{e}_{RJ}}) \\
&- (2s^2_W - 1) D_0(|M_1|, m_{\tilde{e}_{LI}}, m_{\tilde{e}_{LI}}, m_{\tilde{e}_{RJ}})) \\
&+ 2(v_1 Z^{1K}_R + v_2 Z^{2K}_R)(c^2_W (M^*_1 + M^*_2) E_2(|M_1|, |M_2|, |\mu|, m_{\tilde{e}_{LI}}, m_{\tilde{e}_{RJ}}) \\
&- 2s^2_W M^*_1 E_2(|M_1|, |M_1|, |\mu|, m_{\tilde{e}_{LI}}, m_{\tilde{e}_{RJ}})) \\
&+ 2(v_2 Z^{1K}_R + v_1 Z^{2K}_R) \big(M^*_1 \mu^* (c^2_W M^*_2 E_0(|M_1|, |M_2|, |\mu|, m_{\tilde{e}_{LI}}, m_{\tilde{e}_{RJ}}) \\
&- s^2_W M^*_1 E_0(|M_1|, |M_1|, |\mu|, m_{\tilde{e}_{LI}}, m_{\tilde{e}_{RJ}})) \\
&+ \mu (c^2_W E_2(|M_1|, |M_2|, |\mu|, m_{\tilde{e}_{LI}}, m_{\tilde{e}_{RJ}}) \\
&- s^2_W E_2(|M_1|, |M_1|, |\mu|, m_{\tilde{e}_{LI}}, m_{\tilde{e}_{RJ}})))\big) \\
&- \frac{e^2 v_1^2}{\sqrt{2}c^2_W} Z^{1K}_R M^*_1 \Big(\left|A^{II}_l\right|^2 E_0(|M_1|, m_{\tilde{e}_{LI}}, m_{\tilde{e}_{LI}}, m_{\tilde{e}_{RJ}}, m_{\tilde{e}_{RI}}) \\
&+ \left|A^{JJ}_l\right|^2 E_0(|M_1|, m_{\tilde{e}_{LJ}}, m_{\tilde{e}_{LI}}, m_{\tilde{e}_{RJ}}, m_{\tilde{e}_{RJ}}) \Big) \Bigg) \sqrt{\bar{M}^{IJ}_{LR}} \\
F^{IJK}_{hdec\ BLR} &= -\frac{e^2 v_1^2}{\sqrt{2}c^2_W} Z^{1K}_R M^*_1 E_0(|M_1|, m_{\tilde{e}_{LJ}}, m_{\tilde{e}_{LI}}, m_{\tilde{e}_{RJ}}, m_{\tilde{e}_{RI}}) A^{II}_l A^{JJ}_l \sqrt{\bar{M}^{JI}_{LR}}
\end{aligned}
\tag{E.25}
$$

4. Contributions decoupling as $M^2_{h(H)}/M^2_{SUSY}$,

$$
F^{IJK}_{hm\ ALR} = \frac{e^2 M_{H^K_0}}{\sqrt{2}c^2_W} Z^{1K}_R M^*_1 C'_0(|M_1|, m_{\tilde{e}_{RJ}}, m_{\tilde{e}_{LI}}) \sqrt{\bar{M}^{IJ}_{LR}} \tag{E.26}
$$

where by C'_0 we denote the derivative of C_0 over the external Higgs mass, $C'_0 = \frac{\partial C_0}{\partial M^2_h}$ (see Eq. (B.7)).

E.4 CP-odd Higgs-lepton vertex

For the processes considered in this article, the contribution from the LFV CP-odd Higgs-lepton vertex can become important only in the case of the three body charged lepton decays and only in the limit of $M_{SUSY} \gg v$, when photon, Z^0 and box contributions decouple. Thus, we give here only the dominant non-decoupling terms for this vertex.

$$
F^{IJ}_A = \frac{1}{(4\pi)^2} \left(F^{IJ}_{And} + F^{IJ}_{AY} \right) . \tag{E.27}
$$

As for CP-odd Higgs vertices, we give the sum of the neutralino and chargino contributions, the latter appearing only as single term depending on sneutrino masses in Eq. (E.30):

1. Contributions proportional to non-holomorphic A'_l terms:

$$F^{IJ}_{And\ ALR} = -\frac{ie^2}{\sqrt{2}c_W^2\cos\beta}\sqrt{\bar{M}^{IJ}_{LR}}\,M_1^\star\,C_0(|M_1|,m_{\tilde{e}_{LI}},m_{\tilde{e}_{RJ}}) \quad \text{(E.28)}$$

$$F^{IJ}_{And\ LL} = -\frac{ie^2}{\sqrt{2}c_W^2\cos\beta}\,\bar{M}^{IJ}_{LL}\,M_1^\star D_0(|M_1|,m_{\tilde{e}_{LI}},m_{\tilde{e}_{LJ}},m_{\tilde{e}_{RJ}})A'^{JJ}_L$$

$$F^{IJ}_{And\ RR} = -\frac{ie^2}{\sqrt{2}c_W^2\cos\beta}\,\bar{M}^{IJ}_{RR}\,M_1^\star\,D_0(|M_1|,m_{\tilde{e}_{LI}},m_{\tilde{e}_{RI}},m_{\tilde{e}_{RJ}})A'^{II}_L \quad \text{(E.29)}$$

2. Contributions suppressed by lepton Yukawa couplings:

$$\begin{aligned}
F^{IJ}_{AY\ LL} &= \frac{ie^2}{2\sqrt{2}c_W^2 s_W^2\cos\beta}\left(s_W^2 M_1^\star\mu^\star(D_0(|M_1|,|\mu|,m_{\tilde{e}_{LI}},m_{\tilde{e}_{LJ}})\right.\\
&+ 2D_0(|M_1|,m_{\tilde{e}_{LI}},m_{\tilde{e}_{LJ}},m_{\tilde{e}_{RJ}})) - c_W^2 M_2^\star\mu^\star(D_0(|M_2|,|\mu|,m_{\tilde{e}_{LI}},m_{\tilde{e}_{LJ}})\\
&+ \left.2D_0(|M_2|,|\mu|,m_{\tilde{\nu}_I},m_{\tilde{\nu}_J}))\right)\ \bar{M}^{IJ}_{LL}\,Y^J_L\\
F^{IJ}_{AY\ RR} &= \frac{ie^2}{\sqrt{2}c_W^2\cos\beta}M_1^\star\mu^\star(D_0(|M_1|,m_{\tilde{e}_{LI}},m_{\tilde{e}_{RI}},m_{\tilde{e}_{RJ}})\\
&- D_0(|M_1|,|\mu|,m_{\tilde{e}_{RI}},m_{\tilde{e}_{RJ}}))\ \bar{M}^{IJ}_{RR}\,Y^I_L
\end{aligned} \quad \text{(E.30)}$$

E.5 4-lepton box diagrams

All genuine box diagram contributions listed in eqs. (D.3–D.6) have negative mass dimension and without any cancellations explicitly decouple like v^2/M^2_{SUSY}. Thus, it is sufficient to expand them only in the lowest order in chargino and neutralino mass insertions. Also the LR slepton mass insertions are always associated with additional factors of v/M_{SUSY}. Thus in the leading v^2/M^2_{SUSY} order only LL and RR slepton mass insertion can contribute to formulae for box diagrams.

Expressions listed below are valid only for $\Delta L = 1$ processes, i.e. excluding combinations of indices $I = J, K = L$ or $I = K, J = L$ - for these one would also take into account flavour conserving diagrams. As mentioned in Sec. 3.3, we do not consider MI expanded expressions for exotic $\Delta L = 2$ processes.

The chargino diagrams contribute significantly only to the B_{VLL}, all other contributions are at least double Yukawa suppressed and very small. The B_{VLL} term is:

$$\begin{aligned}
(4\pi)^2 B^{JIKL}_{VLLC} &= \frac{e^4}{4s_W^4}\left(E_2(|M_2|,|M_2|,m_{\tilde{\nu}_I},m_{\tilde{\nu}_J},m_{\tilde{\nu}_K})\left(\delta^{KL}\Delta^{JI}_{LL}\bar{M}^{IJ}_{LL}+\delta^{JL}\Delta^{KI}_{LL}\bar{M}^{IK}_{LL}\right)\right.\\
&+ \left.E_2(|M_2|,|M_2|,m_{\tilde{\nu}_J},m_{\tilde{\nu}_K},m_{\tilde{\nu}_L})\left(\delta^{IK}\Delta^{JL}_{LL}\bar{M}^{JL}_{LL}+\delta^{IJ}\Delta^{KL}_{LL}\bar{M}^{KL}_{LL}\right)\right)
\end{aligned} \quad \text{(E.31)}$$

Contributions arising from neutralino box diagrams, both normal and crossed added together, are listed below in Eqs. (E.32-E.37). We do not give here formulae for the neutralino contributions to B_{SLL}, B_{SRR}, B_{TL} and B_{TR}, as they are also double Yukawa suppressed and small.

$$
\begin{aligned}
(4\pi)^2 B_{VLLN}^{JIKL} &= \frac{e^4}{16 s_W^4 c_W^4}\Big(\big(\delta^{KL}\Delta_{LL}^{JI}\bar{M}_{LL}^{IJ} + \delta^{IK}\Delta_{LL}^{JL}\bar{M}_{LL}^{JL}\big)\,(3c_W^4 E_2(|M_2|,|M_2|,m_{\tilde{e}_{LI}},m_{\tilde{e}_{LJ}},m_{\tilde{e}_{LL}}) \\
&+ 3s_W^4 E_2(|M_1|,|M_1|,m_{\tilde{e}_{LI}},m_{\tilde{e}_{LJ}},m_{\tilde{e}_{LL}}) \\
&- 2c_W^4 D_0(|M_2|,m_{\tilde{e}_{LI}},m_{\tilde{e}_{LJ}},m_{\tilde{e}_{LL}}) - 2s_W^4 D_0(|M_1|,m_{\tilde{e}_{LI}},m_{\tilde{e}_{LJ}},m_{\tilde{e}_{LL}}) \\
&+ 4s_W^2 c_W^2\,\mathrm{Re}\,(M_1 M_2^*) E_0(|M_1|,|M_2|,m_{\tilde{e}_{LI}},m_{\tilde{e}_{LJ}},m_{\tilde{e}_{LL}}) \\
&+ 2s_W^2 c_W^2 E_2(|M_1|,|M_2|,m_{\tilde{e}_{LI}},m_{\tilde{e}_{LJ}},m_{\tilde{e}_{LL}})) \\
&+ \big(\delta^{JL}\Delta_{LL}^{KI}\bar{M}_{LL}^{IK} + \delta^{IJ}\Delta_{LL}^{KL}\bar{M}_{LL}^{KL}\big)\,(3c_W^4 E_2(|M_2|,|M_2|,m_{\tilde{e}_{LI}},m_{\tilde{e}_{LK}},m_{\tilde{e}_{LL}}) \\
&+ 3s_W^4 E_2(|M_1|,|M_1|,m_{\tilde{e}_{LI}},m_{\tilde{e}_{LK}},m_{\tilde{e}_{LL}}) \\
&- 2c_W^4 D_0(|M_2|,m_{\tilde{e}_{LI}},m_{\tilde{e}_{LK}},m_{\tilde{e}_{LL}}) - 2s_W^4 D_0(|M_1|,m_{\tilde{e}_{LI}},m_{\tilde{e}_{LK}},m_{\tilde{e}_{LL}}) \\
&+ 4s_W^2 c_W^2\,\mathrm{Re}\,(M_1 M_2^*) E_0(|M_1|,|M_2|,m_{\tilde{e}_{LI}},m_{\tilde{e}_{LK}},m_{\tilde{e}_{LL}}) \\
&+ 2s_W^2 c_W^2 E_2(|M_1|,|M_2|,m_{\tilde{e}_{LI}},m_{\tilde{e}_{LK}},m_{\tilde{e}_{LL}}))\Big) \qquad \text{(E.32)}
\end{aligned}
$$

$$
\begin{aligned}
(4\pi)^2 B_{VRRN}^{JIKL} &= -\frac{e^4}{c_W^4}\Big(\big(\delta^{KL}\Delta_{RR}^{IJ}\bar{M}_{RR}^{IJ} + \delta^{IK}\Delta_{RR}^{LJ}\bar{M}_{RR}^{JL}\big)\,(2D_0(|M_1|,m_{\tilde{e}_{RI}},m_{\tilde{e}_{RJ}},m_{\tilde{e}_{RL}}) \\
&- 3E_2(|M_1|,|M_1|,m_{\tilde{e}_{RI}},m_{\tilde{e}_{RJ}},m_{\tilde{e}_{RL}})) \\
&+ \big(\delta^{JL}\Delta_{RR}^{IK}\bar{M}_{RR}^{IK} + .\delta^{IJ}\Delta_{RR}^{LK}\bar{M}_{RR}^{KL}\big)\,(2D_0(|M_1|,m_{\tilde{e}_{RI}},m_{\tilde{e}_{RK}},m_{\tilde{e}_{RL}}) \\
&- 3E_2(|M_1|,|M_1|,m_{\tilde{e}_{RI}},m_{\tilde{e}_{RK}},m_{\tilde{e}_{RL}}))) \qquad \text{(E.33)}
\end{aligned}
$$

$$
\begin{aligned}
(4\pi)^2 B_{VLRN}^{JIKL} &= -\frac{e^4}{4c_W^4}(\delta^{KL}\Delta_{LL}^{JI}\bar{M}_{LL}^{IJ}(2D_0(|M_1|,m_{\tilde{e}_{LI}},m_{\tilde{e}_{LJ}},m_{\tilde{e}_{RL}}) \\
&- 3E_2(|M_1|,|M_1|,m_{\tilde{e}_{LI}},m_{\tilde{e}_{LJ}},m_{\tilde{e}_{RL}})) \\
&+ \delta^{IJ}\Delta_{RR}^{LK}\bar{M}_{RR}^{KL}(2D_0(|M_1|,m_{\tilde{e}_{LI}},m_{\tilde{e}_{RK}},m_{\tilde{e}_{RL}}) \\
&- 3E_0(|M_1|,|M_1|,m_{\tilde{e}_{LI}},m_{\tilde{e}_{RK}},m_{\tilde{e}_{RL}})) \qquad \text{(E.34)}
\end{aligned}
$$

$$
\begin{aligned}
(4\pi)^2 B_{VRLN}^{JIKL} &= -\frac{e^4}{4c_W^4}(\delta^{KL}\Delta_{RR}^{IJ}\bar{M}_{RR}^{IJ}(2D_0(|M_1|,m_{\tilde{e}_{RI}},m_{\tilde{e}_{RJ}},m_{\tilde{e}_{LL}}) \\
&- 3E_2(|M_1|,|M_1|,m_{\tilde{e}_{RI}},m_{\tilde{e}_{RJ}},m_{\tilde{e}_{LL}})) \\
&+ \delta^{IJ}\Delta_{LL}^{KL}\bar{M}_{LL}^{KL}(2D_0(|M_1|,m_{\tilde{e}_{RI}},m_{\tilde{e}_{LK}},m_{\tilde{e}_{LL}}) \\
&- 3E_0(|M_1|,|M_1|,m_{\tilde{e}_{RI}},m_{\tilde{e}_{LK}},m_{\tilde{e}_{LL}})) \qquad \text{(E.35)}
\end{aligned}
$$

$$
\begin{aligned}
(4\pi)^2 B_{SLRN}^{JIKL} &= \frac{e^4}{2c_W^4}(\delta^{JL}\Delta_{LL}^{KI}\bar{M}_{LL}^{IK}(2D_0(|M_1|,m_{\tilde{e}_{LI}},m_{\tilde{e}_{LK}},m_{\tilde{e}_{RL}}) \\
&- 3E_2(|M_1|,|M_1|,m_{\tilde{e}_{LI}},m_{\tilde{e}_{LK}},m_{\tilde{e}_{RL}})) \\
&+ \delta^{IK}\Delta_{RR}^{LJ}\bar{M}_{RR}^{LJ}(2D_0(|M_1|,m_{\tilde{e}_{LI}},m_{\tilde{e}_{RJ}},m_{\tilde{e}_{RL}}) \\
&- 3E_2(|M_1|,|M_1|,m_{\tilde{e}_{LI}},m_{\tilde{e}_{RJ}},m_{\tilde{e}_{RL}}))) \qquad \text{(E.36)}
\end{aligned}
$$

$$
\begin{aligned}
(4\pi)^2 B_{SRLN}^{JIKL} &= \frac{e^4}{2c_W^4}(\delta^{JL}\Delta_{RR}^{IK}\bar{M}_{RR}^{IK}(2D_0(|M_1|,m_{\tilde{e}_{RI}},m_{\tilde{e}_{RK}},m_{\tilde{e}_{LL}}) \\
&- 3E_2(|M_1|,|M_1|,m_{\tilde{e}_{RI}},m_{\tilde{e}_{RK}},m_{\tilde{e}_{LL}})) \\
&+ \delta^{IK}\Delta_{LL}^{JL}\bar{M}_{LL}^{LJ}(2D_0(|M_1|,m_{\tilde{e}_{RI}},m_{\tilde{e}_{LJ}},m_{\tilde{e}_{LL}}) \\
&- 3E_2(|M_1|,|M_1|,m_{\tilde{e}_{RI}},m_{\tilde{e}_{LJ}},m_{\tilde{e}_{LL}}))) \qquad \text{(E.37)}
\end{aligned}
$$

References

[1] ATLAS collaboration, G. Aad et al., *Observation of a new particle in the search for the Standard Model Higgs boson with the ATLAS detector at the LHC*, *Phys. Lett.* **B716** (2012) 1–29, [1207.7214].

[2] CMS collaboration, S. Chatrchyan et al., *Observation of a new boson at a mass of 125 GeV with the CMS experiment at the LHC*, *Phys. Lett.* **B716** (2012) 30–61, [1207.7235].

[3] F. Borzumati and A. Masiero, *Large Muon and electron Number Violations in Supergravity Theories*, *Phys. Rev. Lett.* **57** (1986) 961.

[4] J. A. Casas and A. Ibarra, *Oscillating neutrinos and $\mu \to e\gamma$*, *Nucl. Phys.* **B618** (2001) 171–204, [hep-ph/0103065].

[5] I. Masina and C. A. Savoy, *Sleptonarium: Constraints on the CP and flavor pattern of scalar lepton masses*, *Nucl. Phys.* **B661** (2003) 365–393, [hep-ph/0211283].

[6] A. Brignole and A. Rossi, *Anatomy and phenomenology of mu-tau lepton flavor violation in the MSSM*, *Nucl. Phys.* **B701** (2004) 3–53, [hep-ph/0404211].

[7] P. Paradisi, *Constraints on SUSY lepton flavor violation by rare processes*, *JHEP* **10** (2005) 006, [hep-ph/0505046].

[8] T. Fukuyama, A. Ilakovac and T. Kikuchi, *Lepton flavor violating leptonic/semileptonic decays of charged leptons in the minimal supersymmetric standard model*, *Eur. Phys. J.* **C56** (2008) 125–146, [hep-ph/0506295].

[9] P. Paradisi, *Higgs-mediated $\tau \to \mu$ and $\tau \to e$ transitions in II Higgs doublet model and supersymmetry*, *JHEP* **02** (2006) 050, [hep-ph/0508054].

[10] A. Dedes, S. Rimmer and J. Rosiek, *Neutrino masses in the lepton number violating MSSM*, *JHEP* **08** (2006) 005, [hep-ph/0603225].

[11] A. Dedes, H. E. Haber and J. Rosiek, *Seesaw mechanism in the sneutrino sector and its consequences*, *JHEP* **11** (2007) 059, [0707.3718].

[12] S. Antusch and S. F. King, *Lepton Flavour Violation in the Constrained MSSM with Constrained Sequential Dominance*, *Phys. Lett.* **B659** (2008) 640–650, [0709.0666].

[13] E. Arganda, M. J. Herrero and J. Portoles, *Lepton flavour violating semileptonic tau decays in constrained MSSM-seesaw scenarios*, *JHEP* **06** (2008) 079, [0803.2039].

[14] A. Ilakovac and A. Pilaftsis, *Supersymmetric Lepton Flavour Violation in Low-Scale Seesaw Models*, *Phys. Rev.* **D80** (2009) 091902, [0904.2381].

[15] L. Calibbi, J. Jones-Perez, A. Masiero, J.-h. Park, W. Porod and O. Vives, *FCNC and CP Violation Observables in a SU(3)-flavoured MSSM*, *Nucl. Phys.* **B831** (2010) 26–71, [0907.4069].

[16] W. Altmannshofer, A. J. Buras, S. Gori, P. Paradisi and D. M. Straub, *Anatomy and Phenomenology of FCNC and CPV Effects in SUSY Theories*, *Nucl. Phys.* **B830** (2010) 17–94, [0909.1333].

[17] L. Calibbi, A. Faccia, A. Masiero and S. K. Vempati, *Lepton flavour violation from SUSY-GUTs: Where do we stand for MEG, PRISM/PRIME and a super flavour factory*, *Phys. Rev.* **D74** (2006) 116002, [hep-ph/0605139].

[18] L. Calibbi, M. Frigerio, S. Lavignac and A. Romanino, *Flavour violation in supersymmetric SO(10) unification with a type II seesaw mechanism*, *JHEP* **12** (2009) 057, [0910.0377].

[19] J. Hisano, M. Nagai, P. Paradisi and Y. Shimizu, *Waiting for $\mu \to e\gamma$ from the MEG experiment*, *JHEP* **12** (2009) 030, [0904.2080].

[20] J. Girrbach, S. Mertens, U. Nierste and S. Wiesenfeldt, *Lepton flavour violation in the MSSM*, *JHEP* **05** (2010) 026, [0910.2663].

[21] C. Biggio and L. Calibbi, *Phenomenology of SUSY SU(5) with type I+III seesaw*, *JHEP* **10** (2010) 037, [1007.3750].

[22] J. N. Esteves, J. C. Romao, M. Hirsch, F. Staub and W. Porod, *Supersymmetric type-III seesaw: lepton flavour violating decays and dark matter*, *Phys. Rev.* **D83** (2011) 013003, [1010.6000].

[23] A. Ilakovac, A. Pilaftsis and L. Popov, *Charged lepton flavor violation in supersymmetric low-scale seesaw models*, *Phys. Rev.* **D87** (2013) 053014, [1212.5939].

[24] T. Goto, Y. Okada, T. Shindou, M. Tanaka and R. Watanabe, *Lepton flavor violation in the supersymmetric seesaw model after the LHC 8 TeV run*, *Phys. Rev.* **D91** (2015) 033007, [1412.2530].

[25] A. Abada, M. E. Krauss, W. Porod, F. Staub, A. Vicente and C. Weiland, *Lepton flavor violation in low-scale seesaw models: SUSY and non-SUSY contributions*, *JHEP* **11** (2014) 048, [1408.0138].

[26] A. Vicente, *Lepton flavor violation beyond the MSSM*, *Adv. High Energy Phys.* **2015** (2015) 686572, [1503.08622].

[27] C. Bonilla, M. E. Krauss, T. Opferkuch and W. Porod, *Perspectives for Detecting Lepton Flavour Violation in Left-Right Symmetric Models*, *JHEP* **03** (2017) 027, [1611.07025].

[28] L. Calibbi and G. Signorelli, *Charged Lepton Flavour Violation: An Experimental and Theoretical Introduction*, *Riv. Nuovo Cim.* **41** (2018) 1, [1709.00294].

[29] A. Dedes, M. Paraskevas, J. Rosiek, K. Suxho and K. Tamvakis, *Mass Insertions vs. Mass Eigenstates calculations in Flavour Physics*, *JHEP* **06** (2015) 151, [1504.00960].

[30] J. Rosiek, *MassToMI —A Mathematica package for an automatic Mass Insertion expansion*, *Comput. Phys. Commun.* **201** (2016) 144–158, [1509.05030].

[31] F. Gabbiani, E. Gabrielli, A. Masiero and L. Silvestrini, *A Complete analysis of FCNC and CP constraints in general SUSY extensions of the standard model*, *Nucl. Phys.* **B477** (1996) 321–352, [hep-ph/9604387].

[32] M. Misiak, S. Pokorski and J. Rosiek, *Supersymmetry and FCNC effects*, *Adv. Ser. Direct. High Energy Phys.* **15** (1998) 795–828, [hep-ph/9703442].

[33] J. Rosiek, *Complete Set of Feynman Rules for the Minimal Supersymmetric Extension of the Standard Model*, *Phys. Rev.* **D41** (1990) 3464.

[34] J. Rosiek, *Complete set of Feynman rules for the MSSM: Erratum*, hep-ph/9511250.

[35] B. C. Allanach et al., *SUSY Les Houches Accord 2*, *Comput. Phys. Commun.* **180** (2009) 8–25, [0801.0045].

[36] S. M. Barr and A. Zee, *Electric Dipole Moment of the Electron and of the Neutron*, *Phys. Rev. Lett.* **65** (1990) 21–24.

[37] D. Chang, W. S. Hou and W.-Y. Keung, *Two loop contributions of flavor changing neutral Higgs bosons to $\mu \to e\gamma$*, *Phys. Rev.* **D48** (1993) 217–224, [hep-ph/9302267].

[38] J. Hisano, M. Nagai and P. Paradisi, *New Two-loop Contributions to Hadronic EDMs in the MSSM*, *Phys. Lett.* **B642** (2006) 510–517, [hep-ph/0606322].

[39] M. Jung and A. Pich, *Electric Dipole Moments in Two-Higgs-Doublet Models*, *JHEP* **04** (2014) 076, [1308.6283].

[40] T. Abe, J. Hisano, T. Kitahara and K. Tobioka, *Gauge invariant Barr-Zee type contributions to fermionic EDMs in the two-Higgs doublet models*, *JHEP* **01** (2014) 106, [1311.4704].

[41] V. Ilisie, *New Barr-Zee contributions to $(\mathbf{g}-\mathbf{2})_\mu$ in two-Higgs-doublet models*, *JHEP* **04** (2015) 077, [1502.04199].

[42] A. Crivellin, J. Heeck and P. Stoffer, *A perturbed lepton-specific two-Higgs-doublet model facing experimental hints for physics beyond the Standard Model*, *Phys. Rev. Lett.* **116** (2016) 081801, [1507.07567].

[43] A. J. Buras, P. H. Chankowski, J. Rosiek and L. Slawianowska, *$\Delta M_{d,s}, B^0 d, s \to \mu^+\mu^-$ and $B \to X_s\gamma$ in supersymmetry at large* $\tan\beta$, *Nucl. Phys.* **B659** (2003) 3, [hep-ph/0210145].

[44] A. Crivellin, *Effective Higgs Vertices in the generic MSSM*, *Phys. Rev.* **D83** (2011) 056001, [1012.4840].

[45] A. Crivellin, L. Hofer and J. Rosiek, *Complete resummation of chirally-enhanced loop-effects in the MSSM with non-minimal sources of flavor-violation*, *JHEP* **07** (2011) 017, [1103.4272].

[46] A. Crivellin and C. Greub, *Two-loop supersymmetric QCD corrections to Higgs-quark-quark couplings in the generic MSSM*, *Phys. Rev.* **D87** (2013) 015013, [1210.7453].

[47] L. J. Hall, R. Rattazzi and U. Sarid, *The Top quark mass in supersymmetric SO(10) unification*, *Phys. Rev.* **D50** (1994) 7048–7065, [hep-ph/9306309].

[48] M. Carena, M. Olechowski, S. Pokorski and C. E. M. Wagner, *Electroweak symmetry breaking and bottom - top Yukawa unification*, *Nucl. Phys.* **B426** (1994) 269–300, [hep-ph/9402253].

[49] M. Carena, D. Garcia, U. Nierste and C. E. M. Wagner, *Effective Lagrangian for the $\bar{t}bH^+$ interaction in the MSSM and charged Higgs phenomenology*, *Nucl. Phys.* **B577** (2000) 88–120, [hep-ph/9912516].

[50] C. Bobeth, T. Ewerth, F. Kruger and J. Urban, *Analysis of neutral Higgs boson contributions to the decays $\bar{B}(s) \to \ell^+\ell^-$ and $\bar{B} \to K\ell^+\ell^-$*, *Phys. Rev.* **D64** (2001) 074014, [hep-ph/0104284].

[51] K. S. Babu and C. F. Kolda, *Higgs mediated $B^0 \to \mu^+\mu^-$ in minimal supersymmetry*, *Phys. Rev. Lett.* **84** (2000) 228–231, [hep-ph/9909476].

[52] G. Isidori and A. Retico, *Scalar flavor changing neutral currents in the large tan beta limit*, *JHEP* **11** (2001) 001, [hep-ph/0110121].

[53] A. Dedes and A. Pilaftsis, *Resummed effective Lagrangian for Higgs mediated FCNC interactions in the CP violating MSSM*, *Phys. Rev.* **D67** (2003) 015012, [hep-ph/0209306].

[54] L. Hofer, U. Nierste and D. Scherer, *Resummation of tan-beta-enhanced supersymmetric loop corrections beyond the decoupling limit*, *JHEP* **10** (2009) 081, [0907.5408].

[55] D. Noth and M. Spira, *Supersymmetric Higgs Yukawa Couplings to Bottom Quarks at next-to-next-to-leading Order*, *JHEP* **06** (2011) 084, [1001.1935].

[56] J. Rosiek, P. Chankowski, A. Dedes, S. Jager and P. Tanedo, *SUSY_FLAVOR: A Computational Tool for FCNC and CP-violating Processes in the MSSM*, *Comput. Phys. Commun.* **181** (2010) 2180–2205, [1003.4260].

[57] A. Crivellin, J. Rosiek, P. H. Chankowski, A. Dedes, S. Jaeger and P. Tanedo, *SUSY_FLAVOR v2: A Computational tool for FCNC and CP-violating processes in the MSSM*, *Comput. Phys. Commun.* **184** (2013) 1004–1032, [1203.5023].

[58] J. Rosiek, *SUSY_ FLAVOR v2.5: a computational tool for FCNC and CP-violating processes in the MSSM*, *Comput. Phys. Commun.* **188** (2015) 208–210, [1410.0606].

[59] Particle Data Group collaboration, K. A. Olive et al., *Review of Particle Physics*, *Chin. Phys.* **C38** (2014) 090001.

[60] S. A. R. Ellis and A. Pierce, *Impact of Future Lepton Flavor Violation Measurements in the Minimal Supersymmetric Standard Model*, *Phys. Rev.* **D94** (2016) 015014, [1604.01419].

[61] R. Kitano, M. Koike and Y. Okada, *Detailed calculation of lepton flavor violating muon electron conversion rate for various nuclei*, *Phys. Rev.* **D66** (2002) 096002, [hep-ph/0203110].

[62] A. Crivellin, S. Davidson, G. M. Pruna and A. Signer, *Renormalisation-group improved analysis of $\mu \to e$ processes in a systematic effective-field-theory approach*, *JHEP* **05** (2017) 117, [1702.03020].

[63] M. A. Shifman, A. I. Vainshtein and V. I. Zakharov, *Remarks on Higgs Boson Interactions with Nucleons*, *Phys. Lett.* **78B** (1978) 443–446.

[64] V. Cirigliano, R. Kitano, Y. Okada and P. Tuzon, *On the model discriminating power of mu —¿ e conversion in nuclei*, *Phys. Rev.* **D80** (2009) 013002, [0904.0957].

[65] A. Crivellin, M. Hoferichter and M. Procura, *Accurate evaluation of hadronic uncertainties in spin-independent WIMP-nucleon scattering: Disentangling two- and three-flavor effects*, *Phys. Rev.* **D89** (2014) 054021, [1312.4951].

[66] A. Crivellin, M. Hoferichter and M. Procura, *Improved predictions for $\mu \to e$ conversion in nuclei and Higgs-induced lepton flavor violation*, *Phys. Rev.* **D89** (2014) 093024, [1404.7134].

[67] M. Hoferichter, J. Ruiz de Elvira, B. Kubis and U.-G. Meißner, *High-Precision Determination of the Pion-Nucleon σ Term from Roy-Steiner Equations*, *Phys. Rev. Lett.* **115** (2015) 092301, [1506.04142].

[68] P. Junnarkar and A. Walker-Loud, *Scalar strange content of the nucleon from lattice QCD*, *Phys. Rev.* **D87** (2013) 114510, [1301.1114].

[69] A. Czarnecki, W. J. Marciano and K. Melnikov, *Coherent muon electron conversion in muonic atoms*, *AIP Conf. Proc.* **435** (1998) 409–418, [hep-ph/9801218].

[70] T. Suzuki, D. F. Measday and J. P. Roalsvig, *Total Nuclear Capture Rates for Negative Muons*, *Phys. Rev.* **C35** (1987) 2212.

[71] J. Rosiek, *General Mass Insertion Expansion in Flavor Physics*, in *5th Large Hadron Collider Physics Conference (LHCP 2017) Shanghai, China, May 15-20, 2017*, 2017, 1708.06818, http://inspirehep.net/record/1618354/files/arXiv:1708.06818.pdf.

[72] BaBar collaboration, B. Aubert et al., *Searches for Lepton Flavor Violation in the Decays $\tau^\pm \to e^\pm\gamma$ and $\tau^\pm \to \mu^\pm\gamma$*, *Phys. Rev. Lett.* **104** (2010) 021802, [0908.2381].

[73] Belle, Belle-II collaboration, K. Hayasaka, *Results and prospects on lepton flavor violation at Belle/Belle II*, *J. Phys. Conf. Ser.* **408** (2013) 012069.

[74] Belle collaboration, K. Hayasaka et al., *New Search for $\tau \to \mu\gamma$ and $\tau \to e\gamma$ Decays at Belle*, *Phys. Lett.* **B666** (2008) 16–22, [0705.0650].

[75] MEG collaboration, J. Adam et al., *New constraint on the existence of the $\mu^+ \to e^+\gamma$ decay*, *Phys. Rev. Lett.* **110** (2013) 201801, [1303.0754].

[76] A. M. Baldini et al., *MEG Upgrade Proposal*, 1301.7225.

[77] ATLAS collaboration, G. Aad et al., *Search for the lepton flavor violating decay $Z \to e\mu$ in pp collisions at $\sqrt{s} = 8$ TeV with the ATLAS detector*, *Phys. Rev.* **D90** (2014) 072010, [1408.5774].

[78] DELPHI collaboration, P. Abreu et al., *Search for lepton flavor number violating Z_0 decays*, *Z. Phys.* **C73** (1997) 243–251.

[79] SINDRUM collaboration, U. Bellgardt et al., *Search for the Decay $\mu^+ \to e^+e^+e^-$*, *Nucl. Phys.* **B299** (1988) 1–6.

[80] A. Blondel et al., *Research Proposal for an Experiment to Search for the Decay $\mu \to eee$*, 1301.6113.

[81] Mu3e collaboration, N. Berger, *The Mu3e Experiment*, *Nucl. Phys. Proc. Suppl.* **248-250** (2014) 35–40.

[82] K. Hayasaka et al., *Search for Lepton Flavor Violating Tau Decays into Three Leptons with 719 Million Produced Tau+Tau- Pairs*, *Phys. Lett.* **B687** (2010) 139–143, [1001.3221].

[83] CMS collaboration, C. Collaboration, *Search for lepton flavour violating decays of the Higgs boson to $\mu\tau$ and $e\tau$ in proton-proton collisions at $\sqrt{s} = 13$ TeV*, .

[84] CMS collaboration, C. Collaboration, *Search for lepton-flavour-violating decays of the Higgs boson to etau and emu at sqrt(s)=8 TeV*, .

[85] SINDRUM II collaboration, W. H. Bertl et al., *A Search for muon to electron conversion in muonic gold*, *Eur. Phys. J.* **C47** (2006) 337–346.

[86] Mu2e collaboration, R. J. Abrams et al., *Mu2e Conceptual Design Report*, 1211.7019.

[87] T. Appelquist and J. Carazzone, *Infrared Singularities and Massive Fields*, *Phys. Rev.* **D11** (1975) 2856.

[88] A. Azatov, S. Chang, N. Craig and J. Galloway, *Higgs fits preference for suppressed down-type couplings: Implications for supersymmetry*, *Phys. Rev.* **D86** (2012) 075033, [1206.1058].

[89] C. Petersson, A. Romagnoni and R. Torre, *Liberating Higgs couplings in supersymmetry*, *Phys. Rev.* **D87** (2013) 013008, [1211.2114].

[90] A. Bartl, H. Eberl, E. Ginina, K. Hidaka and W. Majerotto, $h^0 \to c\bar{c}$ *as a test case for quark flavor violation in the MSSM*, *Phys. Rev.* **D91** (2015) 015007, [1411.2840].

[91] M. Arana-Catania, E. Arganda and M. J. Herrero, *Non-decoupling SUSY in LFV Higgs decays: a window to new physics at the LHC*, *JHEP* **09** (2013) 160, [1304.3371].

[92] D. Aloni, Y. Nir and E. Stamou, *Large BR($h \to \tau\mu$) in the MSSM?*, *JHEP* **04** (2016) 162, [1511.00979].

[93] G. Barenboim, C. Bosch, J. S. Lee, M. L. López-Ibáñez and O. Vives, *Flavor-changing Higgs boson decays into bottom and strange quarks in supersymmetric models*, *Phys. Rev.* **D92** (2015) 095017, [1507.08304].

[94] M. E. Gomez, S. Heinemeyer and M. Rehman, *Lepton flavor violating Higgs Boson Decays in Supersymmetric High Scale Seesaw Models*, 1703.02229.

[95] A. Dedes, M. Paraskevas, J. Rosiek, K. Suxho and K. Tamvakis, *Rare Top-quark Decays to Higgs boson in MSSM*, *JHEP* **11** (2014) 137, [1409.6546].

[96] A. Crivellin, A. Kokulu and C. Greub, *Flavor-phenomenology of two-Higgs-doublet models with generic Yukawa structure*, *Phys. Rev.* **D87** (2013) 094031, [1303.5877].

[97] A. Dedes, J. Rosiek and P. Tanedo, *Complete One-Loop MSSM Predictions for* $B \to \ell\ell'$ *at the Tevatron and LHC*, *Phys. Rev.* **D79** (2009) 055006, [0812.4320].